

Lek. Michał Lanckoroński

Przydatność badania metodą rezonansu magnetycznego całego ciała w diagnostyce
wybranych chorób reumatycznych wieku rozwojowego

Rozprawa na stopień doktora nauk medycznych i nauk o zdrowiu w dyscyplinie nauki
medyczne

Promotor: prof. dr hab. n. med. Iwona Sudoł-Szopińska

Zakład Radiologii, Narodowy Instytut Geriatrii, Reumatologii i Rehabilitacji, ul. Spartańska,
02-673 Warszawa

Obrona rozprawy doktorskiej przed Radą Naukową Narodowego Instytutu Geriatrii,
Reumatologii i Rehabilitacji

Warszawa 2024



Podziękowanie

Dziękuję Pani Profesor dr hab. n. med. Iwonie Sudoł-Szopińskiej za nieustanne wsparcie i zaufanie.

Rozprawę dedykuję moim Bliskim.

Wykaz publikacji stanowiących rozprawę doktorską

Niniejsza rozprawa doktorska została oparta na cyklu trzech publikacji, o łącznym wskaźniku IF 7,2 i 340 punktach MNiSW, powstałych na podstawie zgromadzonego materiału badawczego i międzynarodowej współpracy naukowej:

1. Michał Lanckoroński, Piotr Gietka, Małgorzata Mańczak, Iwona Sudoł-Szopińska. Whole-Body MRI at Initial Presentation of Chronic Recurrent Multifocal Osteomyelitis, Juvenile Idiopathic Arthritis, Their Overlapping Syndrome, and Non-Specific Arthropathy. *Journal of Clinical Medicine* 2024; 13, 998. doi.org/10.3390/jcm13040998

IF 3,0 Pkt. MNiSW 140

2. Chianca Vito, Michał Lanckoroński, Marco Curti, Majid Chalian, Iwona Sudoł-Szopińska, Chiara Giraud, Filippo Del Grande. Whole-Body Magnetic Resonance Imaging in Rheumatology. *Radiologic Clinics of North America*, 2024;62:865-876. S0033838924000216. <https://doi.org/10.1016/j.rcl.2024.02.008>

IF 2,1 Pkt. MNiSW 100

3. Sudoł-Szopińska Iwona, Michał Lanckoroński, Torsten Diekhoff, Damjana Ključevšek, Filippo Del Grande, Andrea Doria. Update on MRI in Rheumatic Diseases. *Radiologic Clinics of North America*, 2024;62:821-836. S003383892400040X. <https://doi.org/10.1016/j.rcl.2024.03.003>

IF 2,1 Pkt. MNiSW 100

Spis treści

1.	Wykaz stosowanych skrótów.....	strona 5
2.	Streszczenie w języku polskim.....	strona 6
3.	Streszczenie w języku angielskim.....	strona 8
4.	Wstęp.....	strona 10
5.	Cel pracy.....	strona 11
6.	Materiał i metody.....	strona 11
7.	Podsumowanie i wnioski.....	strona 15
8.	Przedstawienie cyklu opublikowanych prac.....	strona 19
9.	Spis rycin i tabel.....	strona 65
10.	Decyzja Komisji Bioetycznej.....	strona 69
11.	Oświadczenia współautorów publikacji.....	strona 71
12.	Piśmiennictwo.....	strona 76

1. Wykaz stosowanych skrótów

- CRMO - Chronic Recurrent Multifocal Osteomyelitis (Przewlekłe Nawracające Wielogniskowe Zapalenie Kości i Szpiku)
- CNO - Chronic Nonbacterial Osteomyelitis (Przewlekłe Niebakteryjne Zapalenie Kości i Szpiku)
- ERA – Enthesitis - Related Arthritis (Zapalenie Stawów Związane z Zapaleniem Przyczepów Ścięgnistych)
- ESSR - European Society of Musculoskeletal Radiology (Europejskie Towarzystwo Radiologii Mięśniowo-Szkieletowej)
- JIA – Juvenile Idiopathic Arthritis (Młodzieńcze Idiopatyczne Zapalenie Stawów)
- MIZS - Młodzieńcze Idiopatyczne Zapalenie Stawów
- MR – Rezonans Magnetyczny
- MRI – Magnetic Resonance Imaging (obrazowanie metodą rezonansu magnetycznego)
- NA- Nonspecific Arthropathy (Niespecyficzna Artropatia)
- NIGRiR – Narodowy Instytut Geriatrii, Reumatologii i Rehabilitacji
- OS – Overlapping Syndrome – Zespół Nakładania
- SAPHO – Synovitis, Acne, Pustulosis, Hyperostosis, Osteoporosis (Zapalenie błony maziowej, Trądzik, Krostkowica, Hiperostoza i Osteoporoza)
- SpA – Spondyloarthropatia
- STIR - Short Tau Inversion Recovery
- T - Tesla
- TIRM - Turbo Inversion Recovery Magnitude
- WB-MRI – Whole-Body Magnetic Resonance Imaging – Rezonans magnetyczny całego ciała

2. Streszczenie w języku polskim

Rezonans magnetyczny całego ciała (Whole-Body Magnetic Resonance Imaging, WB-MRI) jest podstawową metodą obrazową pozwalającą na kompleksową ocenę układu ruchu [1], bez użycia promieniowania jonizującego i w stosunkowo krótkim czasie, co jest szczególnie istotne w diagnostyce dzieci i młodzieży z chorobami reumatycznymi. Dzięki szerokiemu polu obrazowania oraz wysokiej rozdzielczości liniowej i przestrzennej, umożliwia rozpoznawanie patologii o charakterze wielogniskowym, zajmujących różne układy i narządy [1], stanowiąc cenne uzupełnienie badania klinicznego [2].

Dwa najczęstsze zastosowania WB-MRI u pacjentów w wieku rozwojowym to przewlekłe nawracające wielogniskowe zapalenie kości i szpiku (Chronic Recurrent Multifocal Osteomyelitis, CRMO), obecnie częściej określane jako przewlekłe niebakteryjne zapalenie kości i szpiku (Chronic Nonbacterial Osteomyelitis, CNO) oraz młodzieńcze idiopatyczne zapalenie stawów (MIZS; Juvenile Idiopathic Arthritis, JIA) [1,3]. Kolejnymi wskazaniami do WB-MRI, wg badania ankietowego przeprowadzonego przez Podkomitet ds. Zapaleń Stawów przy Europejskim Towarzystwie Radiologii Mięśniowo-Szkieletowej (European Society of Musculoskeletal Radiology, ESSR), są choroby nerwowo-mięśniowe i zespoły nakładania (overlapping syndromes), w przebiegu których u danego chorego występują minimum 2 choroby reumatyczne i charakterystyczne dla nich markery serologiczne. Przykładem zespołu nakładania jest współistnienie CRMO z MIZS [3].

O ile w chorobach nerwowo-mięśniowych obraz kliniczny jest typowy i udowodniono kliniczną przydatność WB-MRI [1,4,5], tak w CRMO i MIZS, tym samym w zespole nakładania tych dwóch chorób (OS), obraz kliniczny oraz wyniki badań laboratoryjnych nie są specyficzne i WB-MRI może pomóc w ich rozpoznaniu i różnicowaniu [6].

W świetle problemów diagnostycznych związanych z rozpoznaniem wyżej wymienionych jednostek, przeprowadzono retrospektywne badanie w dużym ośrodku reumatologii dziecięcej w celu określenia i porównania charakteru, liczby i lokalizacji zmian w WB-MRI u pacjentów z CRMO, MIZS i OS. Do grupy badanej włączono również pacjentów z niespecyficzną artropatią (Nonspecific Arthropathy, NA), tj. z dolegliwościami mięśniowo-szkieletowymi, u których wykluczono jakąkolwiek chorobę zakaźną. Występująca głównie u dziewcząt, NA staje się coraz większym globalnym problemem diagnostycznym i terapeutycznym [7-10]. Zgłaszane objawy to głównie ból, w tym ból wzrostowy, ból związany z zespołami nadmiernej ruchomości stawów, ból psychogeny, neuropatyczny, czy kompleksowy zespół bólu regionalnego [11-14].

W cyklu publikacji pod wspólnym tytułem: "Przydatność badania metodą rezonansu magnetycznego całego ciała w diagnostyce wybranych chorób reumatycznych wieku rozwojowego" znalazły się trzy recenzowane prace, w tym jedna oryginalna, przedstawiająca wyniki badań własnych [15] oraz dwie publikacje pogładowe, powstałe w ramach międzynarodowej współpracy naukowej, omawiające technikę WB-MRI i jej zastosowanie w diagnostyce chorób reumatycznych [16,17]. Łączny wskaźnik Impact Factor powyższego cyklu wynosi 7,2, zaś łączna wartość punktów MNiSW 340.

Retrospektywne, jednośrodkowe badanie własne (Publikacja nr 1) przeprowadzono na aparacie MR Avanto o natężeniu pola 1,5 Tesli (T) z wykorzystaniem dedykowanych wielokanałowych cewek powierzchniowych [15]. Do badania włączono 173 pacjentów

pediatrycznych z następującymi ostatecznymi rozpoznaniem: CRMO u 26 pacjentów (15,0%), MIZS u 51 (29,5%), OS u 8 (4,6%) i NA u 88 (50,9%).

Przeprowadzone badania wykazały, że najczęstszą nieprawidłowością w badanej grupie w WB-MRI był obrzęk szpiku kostnego (Bone Marrow Edema, BME). BME stwierdzono u wszystkich pacjentów z CRMO, u 88% chorych z OS, 55% z MIZS i 11% z NA. We wszystkich porównywanych jednostkach BME najczęściej lokalizował się w kończynach dolnych.

Wysięk obserwowano u 62,5% dzieci z OS i 52,9% z MIZS; w CRMO i NA wysięk występował sporadycznie. Zapalenie przyczepów ścięgnistych (enthesitis) stwierdzono u 7,8% pacjentów z MIZS i u 3,8% z CRMO, zaś zapalenie mięśni u 12,5% pacjentów z OS i u 3,9% z MIZS.

Badanie wykazało ponadto, że najczęstszym wskazaniem do wykonania WB-MRI w naszym ośrodku było MIZS, podczas gdy w innych badaniach dominowali pacjenci z CRMO. Zaprezentowana grupa pacjentów z MIZS jest najliczniejsza spośród prezentowanych w literaturze w kontekście zastosowania WB-MRI.

W badaniu własnym po raz pierwszy oceniono obraz zmian w WB-MRI u dzieci i młodzieży z zespołem nakładania CRMO i MIZS.

Pionierska również jest przeprowadzona analiza zmian widocznych w WB-MRI u pacjentów z niespecyficzną artropatią.

Uzupełnieniem powyższych badań są dwie międzynarodowe prace poglądowe, opublikowane w recenzowanych czasopismach (Publikacje 2 i 3) [16,17].

Omówiono w nich technikę badania WB-MRI, zwracając, m.in., uwagę na brak standaryzacji badania wynikający z mnogości protokołów i sekwencji stosowanych w różnych ośrodkach. Przedstawiono zalety WB-MRI w diagnostyce chorób tkanki łącznej, spondyloartropatii (SpA), a także w CRMO i SAPHO, na etapie wczesnej diagnostyki oraz monitorowania leczenia.

3. Streszczenie w języku angielskim

Whole-body magnetic resonance imaging (WB-MRI) is now considered central to defining total inflammatory burden in juveniles with arthritis [1], providing additional information to clinical findings [2]. The technique lends itself well to pathologies that are diffuse, multifocal or affect different organ systems, providing excellent anatomical definition through high soft-tissue contrast and spatial resolution [1].

The two most common WB-MRI applications in children and adolescents are Chronic Recurrent Multifocal Osteomyelitis (CRMO), also known as chronic Nonbacterial Osteomyelitis (CNO), and Juvenile Idiopathic Arthritis (JIA) [1,3]. Other entities recognized by the European Society of Musculoskeletal Radiology (ESSR) arthritis subcommittee survey that investigated the current role of WB-MRI for rheumatic inflammatory diseases are: neuromuscular diseases and overlapping syndromes, including CRMO and JIA overlapping syndrome (OS) [3]. Whereas in neuromuscular diseases the clinical presentation is typical and applicability of WB-MRI has been proven [1,4,5], in CRMO and JIA, thus in course of their comorbidity, both clinical picture and laboratory data are not specific and WB-MRI may help in their diagnosis [6].

In light of the diagnostic problems associated with the recognition of the abovementioned entities, a retrospective study within a single large pediatric rheumatology referral center was carried out to determine and compare the type, number and initial distribution of lesions in the WB-MRI in patients with CRMO, JIA, and OS. Also, Non-specific Arthropathy (NA) was included in the cohort. This group comprised juveniles with non-specific musculoskeletal complaints in whom any inflammatory disease had been diagnosed. Occurring mainly in girls, NA is becoming a growing global diagnostic and therapeutic problem [7-10]. The symptoms reported are mainly pain, including growth pain, pain associated with joint hypermobility syndromes, psychogenic pain, neuropathic pain, and complex regional pain syndrome [11-14].

In the series of publications under the common title: "Usefulness of whole-body magnetic resonance imaging in the diagnosis of selected rheumatic diseases of the developmental age", three peer-reviewed papers were included, including an original paper presenting the results of own research and two review publications created as part of an international collaboration, discussing the WB-MRI technique and its use in the diagnosis of rheumatic diseases in children and adults. The total Impact Factor of the above series is 7.2 and the total MNiSW points value is 340.

The retrospective single center study (Publication No 1) was performed on an Avanto 1.5 Tesla (T) MRI scanner with a dedicated multichannel surface coil system. A total of 173 pediatric patients were included with the following final diagnoses: CRMO in 26 (15.0%), JIA in 51 (29.5%), OS in 8 (4.6%), and NA in 88 (50.9%) [15].

Results showed that bone marrow edema (BME) was the most common abnormality, being seen in 100% patients with CRMO, 88% with OS, 55% with JIA, and 11% with NA. The bones of the lower extremities were the most affected in all compared entities.

Effusion was seen in 62.5% children with OS, and in 52.9% with JIA, whereas in CRMO and NA the exudate was sporadic. Enthesitis was found in 7.8% of patients with JIA and 3.8% with CRMO, and myositis was seen in 12.5% of patients with OS and in 3.9% with JIA.

The study further showed that the most common indication for WB-MRI in our centre was JIA, while in other centers CRMO is the leading entity. At the same time, the group of patients with

JIA we studied is the largest presented in the literature to date in the context of the use of WB-MRI.

In addition, our study is the first to evaluate WB-MRI lesions in children with CRMO and JIA overlapping syndrome.

Also pioneering is the study of changes seen on WB-MRI in children and adolescents with non-specific musculoskeletal (NA) complaints.

The above studies are complemented by two international review papers published in peer-reviewed journals (Publications 2 and 3) [16,17].

They discuss the WB-MRI technique, drawing attention, among other things, to the lack of standardization of the study resulting from the multiplicity of protocols and sequences used in different centers. The advantages of WB-MRI in the diagnosis of connective tissue diseases, spondyloarthropathies (SpAs), as well as in CRMO and SAPHO, in early diagnosis and treatment monitoring, were presented.

4. Wstęp

Rezonans magnetyczny całego ciała (WB-MRI) jest podstawową metodą obrazową pozwalającą na kompleksową ocenę układu ruchu [1], bez użycia promieniowania jonizującego i w stosunkowo krótkim czasie, co jest szczególnie istotne w diagnostyce dzieci i młodzieży z chorobami reumatycznymi. Dzięki szerokiemu polu obrazowania oraz wysokiej rozdzielczości liniowej i przestrzennej, umożliwia rozpoznanie patologii o charakterze wieloogniskowym, zajmujących różne układy i narządy [1], stanowiąc cenne uzupełnienie badania klinicznego [2].

Dwa najczęstsze zastosowania WB-MRI u dzieci i młodzieży to Przewlekłe Nawracające Wieloogniskowe Zapalenie Kości i Szpiku (CRMO), obecnie określane częściej jako Przewlekłe Niebakteryjne Zapalenie Kości i Szpiku (CNO) oraz Młodzieńcze Idiopatyczne Zapalenie Stawów (MIZS) [1,3]. Kolejnymi częstymi wskazaniami do WB-MRI, wg badania ankietowego przeprowadzonego wśród ośrodków radiologicznych przez Podkomitet ds. Zapaleń Stawów przy Europejskim Towarzystwie Radiologii Mięśniowo-Szkieletowej (ESSR), są choroby nerwowo-mięśniowe i zespoły nakładania (OS), gdzie u jednego chorego występują minimum 2 choroby reumatyczne i charakterystyczne dla nich markery serologiczne. Przykładem zespołu nakładania jest współistnienie CRMO z MIZS [3]. O ile w chorobach nerwowo-mięśniowych obraz kliniczny jest typowy i udowodniono kliniczną przydatność WB-MRI [1,4,5], tak w CRMO i MIZS, tym samym w zespole ich nakładania, zarówno obraz kliniczny jak i dane laboratoryjne nie są specyficzne, a WB-MRI może pomóc w ich rozpoznaniu [6].

Przy rosnącej liczbie publikacji na temat zastosowania WB-MRI w CRMO, liczba doniesień na temat WB-MRI w MIZS jest znikoma i żadna praca, według analizy dostępnego piśmiennictwa, nie została poświęcona zespołowi nakładania CRMO i MIZS [1,18-22]. Nie zidentyfikowano także doniesień nt. wykorzystania WB-MRI w diagnostyce niespecyficznego artropatii (NA), która staje się coraz większym problemem na całym świecie, zaś WB-MRI może mieć szczególne znaczenie w diagnostyce niespecyficznego dolegliwości ze strony układu ruchu u dzieci i młodzieży charakteryzujących tę jednostkę [7-14].

CRMO jest niebakteryjnym zapaleniem kości o niejasnej etiologii, charakteryzującym się nawracającymi epizodami bólu kości i ograniczonym zakresem ruchu przez ponad 6 miesięcy [1,18,21,23-25]. Występuje z reguły u dziewcząt, z częstością 0,4/100 000 osób [1,23]. CRMO jest chorobą trudną do rozpoznania ze względu na utajony charakter i niespecyficzne objawy oraz problematyczną w leczeniu, m.in. z uwagi na trudności w określeniu aktywności choroby [20]. Badanie fizykalne i tradycyjne markery stanu zapalnego nie są czułymi wskaźnikami do diagnozowania i monitorowania postępu choroby czy skuteczności leczenia [20]. Obecnie złotym standardem obrazowania CRMO jest WB-MRI, zwłaszcza na wstępie diagnostyki [20]. WB-MRI umożliwia wykrywanie zmian, w tym klinicznie bezobjawowych. Zmiany chorobowe w postaci ognisk (obszarów) obrzęku szpiku kostnego (BME), odzwierciedlających jego zapalenie, są typowo wieloogniskowe i obustronnie symetryczne (do 75% przypadków) i najczęściej zlokalizowane w okolicy okołostawowej, z reguły w przynasadach kości długich (do 90% przypadków) [1,19]. Do innych charakterystycznych dla CRMO zmian należą: zajęcie obojczyka, żuchwy, zapalenie mięśni, zapalenie powięzi, zapalenie błony maziowej i wysięk w stawach, zapalenie entez [1,26,27].

MIZS jest najczęstszą chorobą reumatyczną wieku rozwojowego; zapadalność wynosi od 2 do 20 na 100 000 osób [18,21,28]. Zapalenie Stawów Związane z Zapaleniem Przyczepów Ścięgnistych (Enthesitis-Related Arthritis, ERA) jest młodzieńczym zapaleniem stawów

kręgosłupa, które zajmuje głównie stawy obwodowe i przyczepy ścięgna, w surowicy pacjentów występuje antygen HLA-B27 [1]. Stanowi 20% przypadków MIZS, dotyczy częściej chłopców, a średni wiek w momencie rozpoznania wynosi 12 lat [1]. Najwcześniej zajęte są stawy kończyn dolnych, następnie stawy krzyżowo-biodrowe i kręgosłup [1]. Charakterystyczne wyniki badań obrazowych w początkowej fazie choroby to zapalenie przyczepów ścięgniastych ze współistniejącym BME i otaczającym obrzękiem tkanek miękkich, a także zapalenie błony maziowej stawów [1,22].

Zespół nakładania CRMO z MIZS (OS) jest stwierdzany u około 30-80% pacjentów z CRMO, u których rozwija się zapalenie stawów [19,21]. Rozpoznanie OS opiera się na obecności wielu obszarów BME (odpowiadających CRMO) oraz zapalenia entez, zapalenia błony maziowej stawów obwodowych i kręgosłupa (typowych dla MIZS) [18]. WB-MRI ma istotne znaczenie w diagnostyce OS, w tym w rozpoznawaniu niemych klinicznie obszarów BME w CRMO [29,30]. Brak specyficznych objawów klinicznych jest głównym powodem opóźnień diagnostycznych, w efekcie czego pacjenci nie otrzymują optymalnego leczenia, co prowadzi do progresji choroby [18].

Niespecyficzna artropatia (NA) dotyczy pacjentów nieletnich z dolegliwościami mięśniowo-szkieletowymi, u których wykluczono jakąkolwiek chorobę zapalną. Występuje głównie u dziewcząt i staje się coraz większym globalnym problemem diagnostycznym i terapeutycznym [7-10]. Zgłaszane objawy to głównie ból, w tym ból wzrostowy, ból związany z zespołami hipermobilności stawów, ból psychogeny, neuropatyczny i zespół złożonego bólu regionalnego [11-14]. WB-MRI umożliwia wykluczenie innych schorzeń i przybliżenie do rozpoznania tej coraz częstszej jednostki.

5. Cel pracy

W świetle problemów diagnostycznych związanych z rozpoznawaniem i różnicowaniem wyżej wymienionych jednostek, przeprowadzono retrospektywne badanie jednośrodkowe w celu określenia i porównania charakteru, liczby i lokalizacji zmian w WB-MRI u pacjentów diagnozowanych pierwszorazowo z CRMO, MIZS, OS i NA.

6. Materiał i metody

6.1. Pacjenci

Retrospektywne badanie przeprowadzono w największym w Polsce ośrodku referencyjnym reumatologii dziecięcej w Narodowym Instytucie Geriatrii, Reumatologii i Rehabilitacji (NIGRiR) w Warszawie. Badanie zostało przeprowadzone zgodnie z Deklaracją Helsińską i zostało zatwierdzone przez lokalną komisję bioetyczną (nr KBT-3/1/2018) (Rozdział 10). Rodzice/opiekunowie prawni wszystkich pacjentów wyrazili świadomą zgodę na udział w badaniu.

Badanie oparto na analizie badań WB-MRI dostępnych w szpitalnej bazie danych z okresu 5 lat, od stycznia 2017 roku do grudnia 2022 roku.

W tym okresie zidentyfikowano 173 pacjentów pediatrycznych z ostatecznym rozpoznaniem 4 jednostek chorobowych, tj.: 26 pacjentów (15,0%) z CRMO, 51 pacjentów (29,5%) z MIZS, 8 pacjentów (4,6%) z OS i 88 pacjentów (50,9%) z NA.

Analizowano tylko wstępne badania WB-MRI tych chorych.

Pacjenci byli kierowani na badanie WB-MRI przez reumatologów dziecięcych Kliniki i Polikliniki Reumatologii Wieków Rozwojowych NIGRiR. Wszyscy spełniali kryteria włączenia, tj. kryteria Boston dla CRMO [31] i kryteria EULAR dla MIZS [32]. Zespół nakładania tych jednostek (OS) rozpoznawano głównie na podstawie objawów klinicznych. Zgłaszane dolegliwości we wszystkich tych chorobach obejmowały: ból stawów lub ograniczenie zakresu ruchu w stawach lub obrzęk stawów, utrzymujące się przez ponad sześć tygodni [27,32-35]. NA rozpoznawano wówczas, gdy pacjent nie spełniał kryteriów diagnostycznych CRMO, MIZS lub innej układowej choroby tkanki łącznej [36-38]. W tej grupie mieścili się także chorzy z różnymi dolegliwościami mięśniowo-szkieletowymi niezwiązanymi z procesem zapalnym (ból wzrostowy, ból związany z zespołami hiper mobilności stawów, ból łuszczykowy lub neuropatyczne).

Zebrane w stworzonej na potrzeby pracy bazie danych informacje kliniczne i obrazowe obejmowały: dane demograficzne, ostateczną diagnozę oraz informacje o liczbie stawów z wyszczególnieniem zajętych tkanek układu ruchu (kości i tkanki miękkie, w tym stawy, mięśnie, entezy).

6.2. Protokół badania WB-MRI

Badanie WB-MRI wykonano na aparacie model Avanto firmy Siemens o natężeniu pola magnetycznego 1,5 T. Badanie przeprowadzono zgodnie z protokołem „WB-MRI” obowiązującym w Zakładzie Radiologii NIGRiR stosowanym do oceny chorób reumatycznych, z systemem dedykowanych cewek powierzchniowych wielokanałowych (Siemens Total Imaging Matrix; Siemens Healthcare, Erlangen, Niemcy).

Pacjenci byli ułożeni do badania na plecach z rękami ułożonymi wzdłuż ciała, a całe ciało było pokryte cewkami. Do badania wykorzystano cewki powierzchniowe do badania głowy, szyi, kręgosłupa, ciała i kończyn dolnych, w tym: ośmiokanałową cewkę matrycową do badania głowy, ośmiokanałową cewkę matrycową do badania szyi, osiemnastokanałową cewkę matrycową do badania kręgosłupa, dwie sześciokanałowe cewki matrycowe „body matrix” i szesnastokanałową cewkę matrycową do badania kończyn dolnych. Badanie wykonano przy swobodnym oddechu, w płaszczyźnie czołowej i strzałkowej. Uzyskane obrazy poszczególnych części ciała nakładające się na siebie w ok. 25%, zostały połączone przy użyciu dostępnego pakietu oprogramowania (Siemens Composing; Siemens, Erlangen, Niemcy) w celu utworzenia pojedynczego obrazu całego ciała. Całkowity czas badania wynosił od 30 do 40 minut, w zależności od wzrostu danego pacjenta.

Protokół obrazowania został przedstawiony w Tabeli nr 1 i obejmował obrazy uzyskane w sekwencji TIRM (Turbo Inversion Recovery Magnitude) w płaszczyźnie czołowej i strzałkowej. Nie podawano dożylnego środka kontrastowego ani środków antyperystaltycznych.

Tabela 1. Protokół badania MR.

TIRM	TR (ms)	TE (ms)	S	FOV (mm)	PO (%)	PED	ST (mm)	Matryca	AT
Przekroje czołowe	5500	42	5	500x500	60	Od prawej	5/ 1,5 przerwa	384x384	3:30 / 1 S
Przekroje strzałkowe	4590	41	5	500x500	20	Od głowy	5/ 1,5 przerwa	226x320	3:00 /1 S

TIRM- Turbo Inversions Recovery Magnitude; TR- Repetition Time, czas repetycji; TE- Echo Time, czas echa; S-Slab; FOV- Field of view, pole widzenia, PO-Phase Oversampling; Kodowanie w kierunku fazy; PED- Phase Encode Direction, Kierunek fazowania/kodowania fazy; ST-Slice Thickness, grubość warstwy; AT- Acquisition Time, czas akwizycji.

6.3. Kryteria oceny WB-MRI

WB-MRI oceniano pod kątem charakteru, liczby i lokalizacji zmian zapalnych w 4 analizowanych grupach pacjentów z CRMO, MIZS, OS i UA. Obrazy zostały ocenione przez dwóch radiologów (ML, IS-S) z 5 i 15-letnim doświadczeniem w obrazowaniu układu mięśniowo-szkieletowego, bez znajomości danych klinicznych i laboratoryjnych. Ostateczna diagnoza została ustalona w drodze konsensusu.

Spośród zmian, które można uwidocznic w badaniu WB-MRI w młodzieńczych artropatiach, analizowano następujące nieprawidłowości: BME, wysięk stawowy, zapalenie mięśni oraz zapalenie przyczepów ścięgniowych.

BME jest widoczny w obrazach TIRM jako obszar wysokiego sygnału szpiku kostnego. Zmiany zapalne w tkankach miękkich, takie jak wysięk w stawie, zapalenie mięśni, zapalenie przyczepów ścięgniowych, są identyfikowane jako obszary o wysokim sygnale.

W pracy określano liczbę i lokalizację nieprawidłowych zmian, z uwzględnieniem ich występowania jedno- albo obustronnego. W kościach długich analizowano dodatkowo występowanie BME w trzonie kości, w bliższej i dalszej nasadzie lub przynasadzie.

6.4. Badania własne na tle aktualnych zastosowań WB-MRI w reumatologii dziecięcej.

Badania własne zostały uzupełnione dwoma artykułami przeglądowymi opublikowanymi w recenzowanych czasopiśmie w ramach współpracy międzynarodowej.

Pierwszy artykuł zatytułowany: „Whole - Body Magnetic Resonance Imaging in Rheumatology” (Publikacja nr 2), omawia technikę obrazowania WB-MRI, w tym zalety nowoczesnych skanerów i cewek stosowanych w WB-MRI [16]. W publikacji zwrócono uwagę na mnogość protokołów badań WB-MRI i stosowanych sekwencji, w tym sekwencję STIR (rekomendowaną przez Podkomitet ds. Zapaleń Stawów przy ESSR) [39], sekwencję Dixon (z uwagi na jednorodną saturację tkanki tłuszczowej) [40,41], oraz DWI (Diffusion Weighted Imaging), pozwalającą na uzyskiwanie informacji jakościowych i ilościowych [42-

44]. Omówiono wskazania do WB-MRI oraz zmiany zapalne widoczne w poszczególnych chorobach reumatycznych.

W przypadku młodzieńczych spondyloartropatii, WB-MRI pozwala na rozpoznanie BME, zapalenia w stawach, pochewkach ścięgniastych, zapalenia przyczepów ścięgniastych i kaletek [45,46]. Jest wykonywane na etapie wczesnej diagnostyki oraz jest skutecznym narzędziem do monitorowania przebiegu choroby i skuteczności leczenia.

W reumatoidalnym zapaleniu stawów WB-MRI jest szczególnie przydatny w wykrywaniu zapalenia błony maziowej i zajęcia kręgosłupa szyjnego oraz odgrywa kluczową rolę w ocenie odpowiedzi na leczenie [16].

W twardzinie układowej, jednej z najcięższych układowych chorób reumatologicznych o najwyższym wskaźniku śmiertelności [47], WB-MRI wykazuje zmiany wielogniskowe i często symetryczne, w tym najczęściej: pogrubienie tkanki podskórnej i powięzi, zapalenie błony maziowej stawów, ich pokontrastowe wzmocnienie w aktywnym stadium zapalnym, oraz BME. Nierzadko stwierdzany jest intensywny obrzęk mięśni odzwierciedlający ich zapalenie, obejmujący głównie proksymalne części kończyn dolnych [48]. W stadium przewlekłym obserwuje się włóknienie zapalnie zmienionych tkanek. WB-MRI jest pomocne w monitorowaniu skuteczności leczenia immunosupresyjnego [49].

W polimialgii reumatycznej głównymi zmianami w WB-MRI są: zapalenie kaletki podbarkowo-podnaramiennej, wysięk w stawie łopatkowo-ramiennym i biodrowym, zapalenie ścięgien i torebek stawowych [50]. WB-MRI odgrywa rolę w ocenie odpowiedzi na leczenie glikokortykosterydami [51].

W idiopatycznych miopatiach zapalnych, takich jak zapalenie skórno-mięśniowe, w tym typu młodzieńczego, WB-MRI jest metodą z wyboru do rozpoznawania zapalenia mięśni i identyfikacji mięśni optymalnych pod kątem wykonania biopsji. Widoczne są również cechy zajęcia innych narządów, w tym: śródmiąższowe choroby płuc, zmiany skórne, zajęcie stawów [52]. W infekcyjnym zapaleniu mięśni WB-MRI może wykazać obrzęk mięśni oraz zbiorniki płynu, w tym ropnie.

W zespole antysyntetazowym WB-MRI jest przydatny do oceny zajęcia mięśni i struktur pozamięśniowych oraz do monitorowania choroby. Jest pomocny w diagnostyce różnicowej, zwłaszcza różnicowaniu z reumatoidalnym zapaleniem stawów w początkowym stadium choroby [53].

W zespole SAPHO, WB-MRI pozwala na wczesną diagnozę poprzez rozpoznanie charakterystycznych cech wielogniskowego zapalenia kości w typowych lokalizacjach [54].

W przypadku wielogniskowej martwicy kości, WB-MRI umożliwia ocenę wszystkich potencjalnych miejsc martwicy w czasie jednej akwizycji [55]. Jest to złoty standard w diagnostyce i obserwacji tego schorzenia [55].

W drugiej publikacji poglądowej pt.: „Update on MRI in Rheumatic Diseases” (Publikacja nr 3) przedstawiono przegląd zastosowań WB-MRI u dorosłych i dzieci w oparciu o aktualne publikacje [17]. Potwierdzono, że WB-MRI jest coraz częściej wykorzystywany w diagnostyce chorób reumatycznych, umożliwiając ocenę rozległości i aktywności chorób o charakterze wielostawowym, zajmujących szpik kostny, stawy, entezy oraz mięśnie całego

ciała w czasie jednego badania. Ze względu na wysoką rozdzielczość kontrastową badanych tkanek, WB-MRI wykrywa wczesne zmiany zapalne i stanowi obiektywne narzędzie do oceny rozległości i aktywności choroby [18].

W publikacji przybliżono wyniki badania ankietowego ESSR przeprowadzonego wśród radiologów z różnych ośrodków europejskich przez Girauda i wsp. [13], w którym zidentyfikowano najczęstsze wskazania kliniczne do WB-MRI. Należą do nich: idiopatyczne zapalenia mięśni (Idiopathic Inflammatory Myositis, IMM), takie jak zapalenie skórno-mięśniowe, w tym postać młodzieńcza oraz zapalenie wielomięśniowe, CRMO (CNO), zespoły nakładania (jak CRMO z MIZS), oraz MIZS [3]. Określenie w WB-MRI lokalizacji i rodzaju zmian zapalnych typowych dla określonej jednostki chorobowej, pozwala na identyfikację osób z predyspozycjami genetycznymi do rozwoju danej choroby, co wpływa na planowane leczenie i długoterminową obserwację [18]. Nie leczone albo niewłaściwie leczone, choroby reumatyczne mogą prowadzić do deformacji kości, co ma wpływ na jakość życia.

Podkreślono jednocześnie konieczność ostrożnej interpretacji zmian widocznych w WB-MRI i ich korelacji z obrazem klinicznym, zwłaszcza obszarów wysokiego sygnału szpiku kostnego u dzieci, który jest często obserwowany i może mieć charakter fizjologiczny / rozwojowy [56,57].

7. Podsumowanie i wnioski

Stały postęp w zakresie technologii MR, opracowywane nowe protokoły badań, nowe sekwencje, wreszcie doskonalone definicje oraz metody oceny zmian patologicznych, wpływają na optymalizację diagnostyki i monitorowania stanu zajętych tkanek ze wzrastającą czułością i swoistością [3,58]. Jest to szczególnie istotne w reumatologii, gdzie zarówno obraz kliniczny, jak i dane laboratoryjne nie są specyficzne dla wielu jednostek chorobowych i WB-MRI może pomóc w ich diagnostyce różnicowej [6]. Przykładem są CRMO i MIZS, należące do najczęstszych wskazań nieonkologicznych w pediatrii do WB-MRI [1]. Obydwie choroby wykazują podobieństwa kliniczne, co więcej możliwe jest ich jednoczesne występowanie u jednego pacjenta (OS), jak również ewolucja jednej choroby w drugą [27].

Na podstawie badań własnych sformułowano następujące wnioski:

- I. WB-MRI pozwala na rozpoznanie zmian zapalnych, takich jak BME, wysięk stawowy, zapalenie przyczepów ścięgniastych oraz zapalenie mięśni u pacjentów z chorobami reumatycznymi wieku rozwojowego wraz z oceną liczby zmian i ich lokalizacji, co ma znaczenie w ich diagnostyce różnicowej.

II. W odniesieniu do liczby zmian:

1. W CRMO zarejestrowano łącznie 263 zmiany, od 1 (u 3 pacjentów) do 33 (u 1 pacjenta);
2. W MIZS zarejestrowano łącznie 296 zmian; liczba zmian wahała się od 0 (u 14 pacjentów) do 31 zmian (u 1 pacjenta);
3. W OS zarejestrowano łącznie 82 zmiany; liczba zmian wahała się od 0 (u 1 pacjenta) do 22 (u 1 pacjenta);
4. W NA zarejestrowano łącznie 56 zmian; liczba zmian wahała się od 0 (u 78 pacjentów) do 21 (u 1 pacjenta).

III. W odniesieniu do charakteru zmian:

1. BME było najczęstszą nieprawidłowością, obserwowaną u wszystkich pacjentów z CRMO, u 88% z OS, 55% z MIZS i 11% z NA. We wszystkich jednostkach BME najczęściej stwierdzano w obrębie kończyn dolnych (Tabela 2).
2. Wysięk był kolejną częstą zmianą w OS (62,5% pacjentów) i MIZS (52,9% pacjentów), podczas gdy w CRMO i NA występował sporadycznie (Tabela 3).
3. Zapalenie mięśni stwierdzono tylko u pacjentów z OS i MIZS (odpowiednio u 12,5% i 3,9%), a zapalenie przyczepów ścięgniętych (enthesitis) tylko w MIZS i CRMO (odpowiednio u 7,8% i 3,8% badanych).
4. Ze względu na artefakty i ograniczenia badania ocena niektórych stawów obwodowych była problematyczna: dłonie i łokcie w materiale własnym nie były dobrze zobrazowane u 10 dzieci (37%) z CRMO, u 10 (20%) z MIZSA, u 4 (50%) z OS i u 21 (23,9%) pacjentów z NA.

Tabela 2. Lokalizacja obrzęku szpiku kostnego w analizowanych jednostkach chorobowych.

Lokalizacja obrzęku szpiku kostnego	CRMO l=26		MIZS l=51		OS l=8		NA l=88	
	Jednostr.	Obustr.	Jednostr.	Obustr.	Jednostr.	Obustr.	Jednostr.	Obustr.
Żuchwa	4 (15,4 %)	0	0	0	0	0	0	0
Łopátka, SMO, SBO	1 (3,8 %)	1 (3,8 %)	1 (2,0 %)	0	0	0	0	0
Obojczyk	2 (7,7 %)	1 (3,8 %)	0	1 (2,0 %)	0	0	0	0
Kość ramienna	3 (11,5 %)	1 (3,8 %)	2 (3,9 %)	0	0	1 (12,5 %)	0	0
Kość łokciowa	0	1 (3,8 %)	0	1 (2,0 %)	0	0	0	0
Kość promieniowa	2 (7,7 %)	1 (3,8 %)	0	2 (3,9 %)	0	0	0	0
Ręka, nadgarstek	0	2 (7,7 %)	0	0	0	0	0	0
Miednica	2 (7,7 %)	1 (3,8 %)	4 (7,8 %)	5 (9,8 %)		1 (12,5 %)		
Rzepka	1 (3,8 %)	1 (3,8 %)	1 (2,0 %)	0	0	0	0	0
Kość udowa	3 (11,5 %)	10 (38,5 %)	6 (11,8 %)	12 (23,5 %)	2 (25,0 %)	3 (37,5 %)	1 (1,1 %)	1 (1,1 %)
Kość piszczelowa	4 (15,4 %)	12 (46,2 %)	1 (2,0 %)	6 (11,8 %)	2 (25,0 %)	2 (25,0 %)	4 (4,4 %)	0
Strzałka	3 (11,5 %)	1 (3,8 %)	1 (2,0 %)	1 (2,0 %)	0	0	1 (1,1 %)	0
Kość skokowa	4 (15,4 %)	5 (19,2 %)	5 (9,8 %)	6 (11,8 %)	0	3 (37,5 %)	2 (2,2 %)	3 (3,3 %)
Kość piętowa	5 (19,2 %)	3 (11,5 %)	1 (2,0 %)	6 (11,8 %)	1 (12,5 %)	2 (25,0 %)	1 (1,1 %)	2 (2,2 %)
Kości stępu	3 (11,5 %)	4 (15,4 %)	3 (5,9 %)	7 (13,7 %)	0	2 (25,0 %)	1 (1,1 %)	1 (1,1 %)
Kości śródstopia	4 (15,4 %)	2 (7,7 %)	0	1 (2,0 %)	0	0	2 (2,2 %)	2 (2,2 %)
Palce stóp	0	1 (3,8 %)	0	0	0	0	1 (1,1 %)	1 (1,1 %)

SMO- staw mostkowo-obojczykowy; SBO- staw barkowo-obojczykowy, CRMO- Chronic Recurrent Multifocal Osteomyelitis; MIZS- Młodzieńcze Idiopatyczne Zapalenie Stawów; OS-Overlapping Syndrome (Zespół nakładania); NA – Nonspecific Arthropathy (Niespecyficzna artropatia); Jednostr. – jednostronne; Obustr. – Obustronne.

Tabela 3. Wysięki w poszczególnych stawach w analizowanych jednostkach chorobowych.

Lokalizacja wysięku	CRMO l=26		MIZS l=51		OS l=8		NA l=88	
	Jednostr.	Obustr.	Jednostr.	Obustr.	Jednostr.	Obustr.	Jednostr.	Obustr.
Staw ramienny	0	0	5 (9,8 %)	0	1 (12,5 %)	0	0	0
Staw łokciowy	0	0	1 (2,0 %)	1 (2,0 %)	1 (12,5 %)	1 (12,5 %)	1 (1,1 %)	0
Stawy nadgarstka	0	0	1 (2,0 %)	0	0	0	1 (1,1 %)	0
Staw krzyżowo-biodrowy	0	0	1 (2,0 %)	0	0	0	0	0
Staw biodrowy	0	0	4 (7,8 %)	8 (15,7 %)	1 (12,5 %)	3 (37,5 %)	0	0
Staw kolanowy	0	2 (7,7 %)	9 (17,6 %)	8 (15,7 %)	0	1 (12,5 %)	1 (1,1 %)	0
Staw skokowy	0	1 (3,8 %)	3 (5,9 %)	3 (5,9 %)	1(12,5 %)	1(12,5 %)	1 (1,1 %)	0
Staw stopy	0	0	1 (2,0 %)	0	1(12,5 %)	1(12,5 %)	0	0
Spojenie łonowe	0	0	1 (2,0 %)	0	1(12,5 %)	0	0	0

IV. Badania własne na tle wyników innych autorów:

1. Zasadniczym elementem wyróżniającym własny materiał jest duża liczba chorych z MIZS (51 pacjentów), u których wykonano WB-MRI. Jest to najliczniejsza grupa spośród prezentowanych w literaturze.
2. W badaniach własnych po raz pierwszy dokonano analizy zmian zapalnych widocznych w WB-MRI w MIZS. Podstawową nieprawidłowością był BME (55% chorych), stwierdzany najczęściej obustronnie w kości udowej i śródstopiu. Wysięki w stawach stwierdzono u 52,9% pacjentów. Zapalenie entez występowało jedynie u 7,8% badanych, mimo że w publikacjach innych autorów odsetek ten sięgał 60-80% [45,59,60]. Należy to prawdopodobnie tłumaczyć krótkim wywiadem chorobowym analizowanej grupy własnej (oceniano tylko pierwszorazowe badania WB-MRI). Zapalenie mięśni stwierdzono u 3,9% dzieci z MIZS. Należy podkreślić, że zapalenie mięśni jest sporadycznie analizowane w kontekście MIZS, mimo że należy do obrazu chorobowego podtypu układowego MIZS lub może być powikłaniem leczenia biologicznego tej choroby [29].
3. W przypadku CRMO, badania własne potwierdziły predylekcję choroby do określonych okolic anatomicznych, w szczególności przynasad kończyn dolnych oraz ich wieloogniskowy charakter [20,21,26,62,63]. W przeciwieństwie do wielu innych publikacji wskazujących na częste zajęcie kości miednicy [21,24,61-64] i kręgosłupa [4,19,21], w materiale własnym miednica była zajęta tylko u trojga dzieci (11,5%), a kręgosłup jedynie u czterech pacjentów (15,4%). U wszystkich badanych występował BME, wysięk i zapalenie entez obserwowano sporadycznie, nie stwierdzono przypadków zapalenia mięśni.

4. Praca własna jest pierwszą analizą częstości i charakteru zmian w WB-MRI w przebiegu zespołu nakładania CRMO i MIZS. Najczęstszą nieprawidłowością był BME (88% badanych), następnie wysięk (62,5% chorych) i zapalenie mięśni (12,5%), nie stwierdzono przypadków zapalenia przyczepów ścięgniastych.
5. W badaniach własnych po raz pierwszy dokonano analizy zmian w WB-MRI u dzieci i młodzieży z niespecyficzną artropatią (NA). Badanie MR odgrywa ważną rolę w szerokiej diagnostyce różnicowej w tej grupie pacjentów [65]. Podobnie jak w poprzednio opisanych chorobach, w materiale własnym obejmującym 88 pacjentów dominował BME w kończynach dolnych (11% chorych). Wysięki były sporadyczne, nie stwierdzono przypadków zapalenia mięśni ani zapalenia przyczepów ścięgniastych.

8. Przedstawienie cyklu opublikowanych prac

Publikacja nr 1.

Whole-Body MRI at Initial Presentation of Chronic Recurrent Multifocal Osteomyelitis, Juvenile Idiopathic Arthritis, Their Overlapping Syndrome, and Non-Specific Arthropathy.

Michał Lanckoroński, Piotr Gietka Małgorzata Mańczak, Iwona Sudoł-Szopińska.
Journal of Clinical Medicine 2024; 13, 998. doi.org/10.3390/jcm13040998

Article

Whole-Body MRI at Initial Presentation of Chronic Recurrent Multifocal Osteomyelitis, Juvenile Idiopathic Arthritis, Their Overlapping Syndrome, and Non-Specific Arthropathy

Michał Lanckoroński ^{1,*}, Piotr Gietka ², Małgorzata Mańczak ³ and Iwona Sudol-Szopińska ^{1,*}

¹ Department of Radiology, National Institute of Geriatrics, Rheumatology and Rehabilitation, 1 Spartańska Street, 02-637 Warsaw, Poland

² Clinic of Paediatric Rheumatology, National Institute of Geriatrics, Rheumatology and Rehabilitation, 1 Spartańska Street, 02-637 Warsaw, Poland; piotr.gietka@spartanska.pl

³ Department of Gerontology, Public Health and Didactics, National Institute of Geriatrics, Rheumatology and Rehabilitation in Warsaw, 1 Spartańska Street, 02-637 Warsaw, Poland; malgorzata.manczak@spartanska.pl

* Correspondence: michal.lanckoronski@spartanska.pl (M.L.); iwona.sudol-szopinska@spartanska.pl (I.S.-S.)

Abstract: (1) **Background:** Whole-body magnetic resonance imaging (WB-MRI) is central to defining total inflammatory burden in juveniles with arthritis. Our aim was to determine and compare the initial distribution of lesions in the WB-MRI in patients with chronic recurrent multifocal osteomyelitis (CRMO), juvenile idiopathic arthritis (JIA), their overlapping syndrome (OS), and with Non-specific Arthropathy (NA). (2) **Methods:** This retrospective single center study was performed on an Avanto 1.5-T MRI scanner with a dedicated multichannel surface coil system. A total of 173 pediatric patients were included with the following final diagnoses: CRMO (15.0%), JIA (29.5%), OS (4.6%), and NA (50.9%). (3) **Results:** Bone marrow edema (BME) was the most common abnormality, being seen in 100% patients with CRMO, 88% with OS, 55% with JIA, and 11% with NA. The bones of the lower extremities were the most affected in all compared entities. Effusion was seen in 62.5% children with OS, and in 52.9% with JIA, and in CRMO and NA, the exudate was sporadic. Enthesitis was found in 7.8% of patients with JIA and 3.8% with CRMO, and myositis was seen in 12.5% of patients with OS and in 3.9% with JIA. (4) **Conclusions:** The most frequent indication for WB-MRI in our center was JIA. The most common pathology in all rheumatic entities was BME, followed by effusion mainly seen in OS and JIA. Entesitis and myositis were less common; no case was observed in NA.

Keywords: whole-body magnetic resonance imaging; chronic recurrent multifocal osteomyelitis; juvenile idiopathic arthritis; overlapping syndrome



Citation: Lanckoroński, M.; Gietka, P.; Mańczak, M.; Sudol-Szopińska, I. Whole-Body MRI at Initial Presentation of Chronic Recurrent Multifocal Osteomyelitis, Juvenile Idiopathic Arthritis, Their Overlapping Syndrome, and Non-Specific Arthropathy. *J. Clin. Med.* **2024**, *13*, 998. <https://doi.org/10.3390/jcm13040998>

Academic Editor: Santos Castañeda

Received: 5 January 2024

Revised: 2 February 2024

Accepted: 7 February 2024

Published: 9 February 2024



Copyright: © 2024 by the authors. Licensee MDPI, Basel, Switzerland. This article is an open access article distributed under the terms and conditions of the Creative Commons Attribution (CC BY) license (<https://creativecommons.org/licenses/by/4.0/>).

1. Introduction

Whole-body magnetic resonance imaging (WB-MRI) is now considered central to defining total inflammatory burden in juveniles with arthritis [1], providing additional information to clinical findings [2]. The technique lends itself well to pathologies that are diffuse, multifocal or affect different organ systems, providing excellent anatomical definition through high soft-tissue contrast and spatial resolution [1].

The two most common WB-MRI applications in children and adolescents are chronic recurrent multifocal osteomyelitis (CRMO) and juvenile idiopathic arthritis (JIA) [1,3]. Other entities recognized by the ESSR arthritis subcommittee survey that investigated the current role of WB-MRI for rheumatic inflammatory diseases are neuromuscular diseases and overlapping syndromes [3]. Whereas in neuromuscular diseases, the clinical presentation is typical and clinical applicability of WB-MRI has been proven [1,4,5], in CRMO and JIA, both clinical picture and laboratory data are not specific and WB-MRI may help in their diagnosis [6].

With an increasing number of publications on the use of WB-MRI of the CRMO, the number of reports on WBMRI in JIA is negligible, and no work, to our knowledge, has been dedicated to JIA and CRMO overlapping syndrome (OS) [1,7–11].

CRMO, also referred to by the alternative name chronic nonbacterial osteomyelitis (CNO), is a non-bacterial autoinflammatory osteitis of unclear etiology characterized by recurrent episodes of bone pain and a restricted range of movement for more than 6 months [1,7,10,12–14]. More common in females, it has an incidence of 0.4/100,000 [1,12]. CRMO is challenging to physicians because of its occult nature and the difficulty of assessing disease activity [9]. Physical examination and traditional inflammatory markers are not sensitive metrics to diagnose and to monitor disease progression [9]. The current gold standard imaging modality is WB-MRI, especially at the initial evaluation [9]. It facilitates the detection of lesions, including those that are clinically silent. Multifocal and bilaterally symmetrical in 75% of cases, focal bone marrow edema (BME) lesions in long bones are characteristically perimetaphyseal, and in one study in up to 90% of cases [1,8]. Other CRMO imaging features can include clavicular osteitis, juxtaphyseal nodules, periosteal edema, myositis, fasciitis, synovitis, enthesitis, and joint effusions [1,15,16].

JIA represents the most common rheumatic disease in childhood, with an incidence and a prevalence varying from 2 to 20 cases and from 16 to 150 cases per 100,000 persons, respectively [7,10,17]. Juvenile spondyloarthritis is a subgroup of JIA with sacroiliitis and spondylitis [11,18]. Enthesitis-related arthritis (ERA) is an HLA-B27-positive juvenile spondyloarthritis that primarily affects peripheral joints and entheses [1]. Accounting for 20% of JIA, this condition affects more boys than girls, with a mean age at diagnosis of 11.7 years [1]. Lower-extremity joints are involved earliest; followed by the sacroiliac joints and the spine [1]. Characteristic imaging findings at the initial presentation are enthesitis with BME and surrounding soft-tissue swelling and edema, as well as synovitis [1,11].

Regarding OS, approximately 30–80% of CRMO patients develop arthritis including spondyloarthritis [8,10]. Commonly, the diagnosis of OS is based on the presence of multiple sites of BME, enthesitis, synovitis of peripheral and axial joints [7]. WB-MRI can confirm or exclude clinically suspected cases or diagnose occult CRMO overlapping cases [19,20] in which the diagnosis is often delayed due to the lack of specific symptoms, and consequently, the patients do not receive optimal treatment until later in the disease, which results in disease progression [7].

In light of the diagnostic problems associated with the recognition of the above-mentioned entities, we carried out a retrospective study within a single large pediatric rheumatology referral center to determine and compare the initial distribution of lesions in the WB-MRI in patients with CRMO, JIA, and OS. Also, non-specific Arthropathy (NA) was included in our cohort. This group comprised juveniles with non-specific musculoskeletal complaints in whom any inflammatory disease had been diagnosed. Occurring mainly in girls, NA is becoming a growing global diagnostic and therapeutic problem [21–24]. The symptoms reported are mainly pain, including growth pain, pain associated with joint hypermobility syndromes, psychogenic pain, neuropathic pain, and complex regional pain syndrome [25–28].

2. Materials and Methods

2.1. Patients

This retrospective single center study was undertaken at the largest referral center for pediatric rheumatology. It was performed in accordance with the Declaration of Helsinki and was approved by the local ethics committee (No KBT-3/1/2018). Parents of all patients gave informed consent to take part in the study.

Our study was based on the analysis of WB-MRI data available in the hospital database from a period of 5 years from January 2017 to December 2022.

In this timeframe, 173 pediatric patients were identified, with final diagnosis of 4 entities, including 26 (15.0%) patients with CRMO, 51 (29.5%) with JIA, 8 (4.6%) with OS, and 88 (50.9%) with NA.

Only initial WB-MRI studies were analyzed.

Children were referred for WB-MRI by pediatric rheumatologists. All included patients met the inclusion of Boston criteria for CRMO [29] and EULAR criteria for JIA [30]. OS was clinically suspected mainly on the basis of clinical symptoms. Reported complaints in all these diseases included joint pain, restricted range of movement, and/or joint swelling, persisting for more than six weeks [16,30–33]. NA was diagnosed when they did not meet the diagnostic criteria of a specific clinical subtype of JIA or other systemic connective tissue disease [34–36]. This diagnosis also includes various musculoskeletal complaints unrelated to the inflammatory process, such as growing pains, pains associated with joint hypermobility syndromes, psoriatic pains, or neuropathic pains. According to a number of journal entries, these non-specific symptoms are observed more frequently in girls than in boys [37–39].

Collected clinical data retrieved from our electronic database included demographics, information on affected bones and soft tissues (such as joints, entheses, and muscles), and the final diagnosis.

2.2. MRI Protocol and Interpretation of Imaging Features

WB-MRI scans were performed on an Avanto 1.5-T MRI scanner with a “WB-MRI” institutional protocol used for the evaluation of rheumatic diseases with a dedicated multichannel surface coil system (Siemens Total Imaging Matrix; Siemens Healthcare, Erlangen, Germany).

Patients were placed supine with arms down by the sides, and the whole body was covered with coils to allow for contiguous scanning. Integrated head, neck, spine, body, and peripheral angiography surface coils were utilized, including the following: eight-channel (CH) head matrix coil, eight-CH cervical matrix coil, eighteen-CH spine coil, two six-CH body matrix coils, and sixteen-CH peripheral angiography (bilateral peripheral MR angiography) matrix coil.

Images were acquired at multiple stations with the patient free-breathing. Sequential imaging at each station along the z-axis was first acquitted in coronal plane, followed by sagittal using the step-wise acquisition. These stations were stitched together—reconstructed using the vendor-specific software package (Siemens Composing; Siemens, Erlangen, Germany) to form a single large field of view (FOV) whole-body image.

Stations on whole-body sequences overlapped 25–30% to improve quality of the final whole-body image.

A total of 4–5 stations (depending upon the patient’ height) were required for whole-body imaging for each patient.

Total scanning time ranged between 30 and 40 min, depending upon the height and compliance of each patient.

The imaging protocol is outlined in Table 1 and includes TIRM (Turbo Inversion Recovery Magnitude) sequence acquired in coronal and sagittal whole body (Table 1). Gadolinium and antiperistaltic agents were not administered. Sedation was deemed unnecessary.

Table 1. Whole-body MRI sequence protocol.

TIRM Sequence	TR (ms)	TE (ms)	Stacks	FOV	Phase Oversampling	Phase Encode Direction	Slice Thickness	Matrix	Time of Acquisition (mins)
coronal whole body	5500	42	5	500 mm per stack	60%	right to left	5 mm, 1.5 mm gap	384 × 384	3:30 per stack
sagittal whole body	4590	41	5	500 mm per stack	20%	head to foot	5 mm, 1.5 mm gap	226 × 320	3:00 per stack

TIRM—Turbo Inversion Recovery Magnitude; TR—Repetition Time; TE—Echo Time; FOV—Field of View.

2.3. Imaging Evaluation Criteria

WB-MRI was evaluated with the aim of identifying lesions in 4 analyzed groups of patients with CRMO, JIA, OS, and UA.

The images were evaluated by two radiologists (ML, IS-S) with 5 and 15 years of experience in musculoskeletal imaging, blinded to clinical and laboratory data. The final diagnosis was established by consensus.

Among the many lesions that can be visualized on WB-MRI in juvenile arthropathies, the following lesions were recorded: (1) BME; (2) joint effusion; (3) myositis; and (4) enthesitis.

BME was defined as increased bone marrow signal on coronal and sagittal TIRM images. In long bones, BME in proximal and distal epiphysis and metaphysis was specified.

Soft tissue lesions, such as joint effusion, myositis, enthesitis were specified as high signal areas; in enthesitis, BME in the bony part of the enthesis may have been visible.

2.4. Statistical Analysis

A database with demographic data and with lesions for each patient was created. The only continuous variable was the patients' age. It was not normally distributed, and therefore, the age comparison in the analyzed groups was performed using the Kruskal–Wallis test. The gender distribution in the study groups was compared using the chi-square test.

The database recorded lesions in very detailed locations and divided into left and right sides. The database initially contained 174 variables describing the location of lesions. Then, the lesions were grouped into less detailed groups; e.g., all bones of the hand and wrist were described with the variable: hand and wrist. Symmetry of lesions was defined as a bilateral involvement of evaluated tissues (bones, joints, entheses, or muscles). Unilateral lesions were recorded as well. Then, the percentage frequency of lesions (bilaterally and unilaterally) in the 4 analyzed groups of children was calculated. Number of patients with at least 1 lesion at proximal and distal metaphyses and epiphyses were also analyzed.

3. Results

3.1. Demographic Data

Over a period of 5 years from January 2017 to December 2022, WB-MRI was performed in 173 pediatric patients with final diagnosis of four entities, including 26 (15.0%) patients with CRMO, 51 (29.5%) with JIA, 8 (4.6%) with OS, and 88 (50.9%) with NA. There were no differences in the age of patients in the study groups ($p = 0.678$), but there were differences in gender distribution ($p = 0.022$). Demographic data are presented in Table 2.

Table 2. Demographic data of the following included patients: CRMO: chronic recurrent multifocal osteomyelitis; JIA: juvenile idiopathic arthritis; OS: JIA and CRMO overlapping syndrome; NA: Non-specific Arthropathy.

	CRMO <i>n</i> = 26	JIA <i>n</i> = 51	OS <i>n</i> = 8	NA <i>n</i> = 88
age	13.5 (10–15)	13 (11–15)	12.5 (10.5–15)	14 (11–16)
gender (boys)	14 (54%)	18 (35%)	4 (50%)	21 (24%)

3.2. Imaging Findings in Patients with CRMO, JIA, OS, and NA

In all patients, WB-MRI was assessed for possible active and chronic inflammatory changes in terms of BME, joint effusion, enthesitis, myositis, bursitis, and others. Overall, in WB-MRI STIR sequences, the following information was recorded:

1. In CRMO, a total of 263 lesions were recorded, ranging from 1 (in 3 patients) to 33 (in 1 patient);
2. In JIA, a total of 296 lesions were recorded; the number of lesions ranged from 0 (in 14 patients) to 31 lesions (in 1 patient);

3. In OS, a total of 82 lesions were recorded; the number of lesions ranged from 0 (in 1 patient) to 22 (in 1 patient);
4. In NA, a total of 56 lesions were recorded; the number of lesions ranged from 0 (in 78 patients) to 21 (in 1 patient).

The hands and elbows were not consistently visualized (especially in older children) in 10 children (37%) with CRMO, in 10 (20%) of JIA patients, in 4 (50%) with OS, and in 21 (23.9%) of NA patients.

In isolated cases, artefacts (mainly motion) hindered WB-MRI interpretation, which occurred in 2 patients (7.4%) with CRMO, 10 (20%) with JIA, 2 (25%) with OS, and 12 with (13.6%) NA.

3.2.1. Bone Marrow Edema Lesions

BME lesions were present in all the diseases analyzed (Figures 1–3).

In CRMO, BME was the most common lesion, found in all 26 juveniles (100%); Table 3 and Figure 4 present the distribution of BME lesions in CRMO in the skeleton. BME was most commonly found bilaterally in the tibia and femur, in 12 (46.2%) and 10 (38.5%) children, respectively. With regard to long bones, BME was most frequently localized in the distal meta-physes of the femur and tibia (Table 4). Unilateral BME occurred most frequently in the calcaneus (5 children, 19.2%).

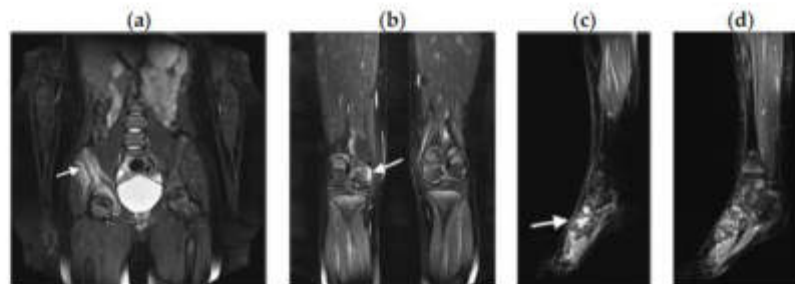


Figure 1. A 13-year-old girl with chronic recurrent multifocal osteomyelitis (CRMO), TIRM (Turbo Inversion Recovery Magnitude) images in coronal and sagittal planes. Bone marrow edema (BME, arrow) in the anterior iliac bone with soft tissue edema (enthesitis) (a), in the posterior condyle of the right femur (b), and in the tarsum bilaterally (c,d), being more intensive on the right side (c).

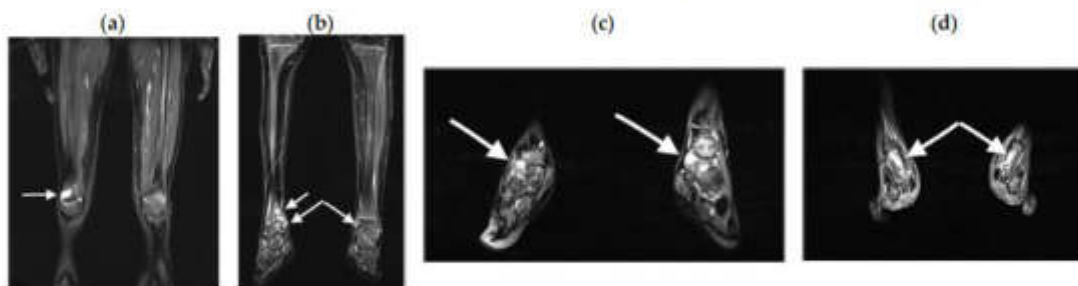


Figure 2. A 12-year-old boy with juvenile idiopathic arthritis (JIA), TIRM images in coronal planes. Knee joint effusion (arrow in (a)), BME in the distal metaphysis (short arrow) of the right tibia and distal epiphysis of tibia bilaterally (long arrows) (b), in the tarsum bilaterally (arrows in (c)), and in the 1st metatarsal bones (arrows in (d)).

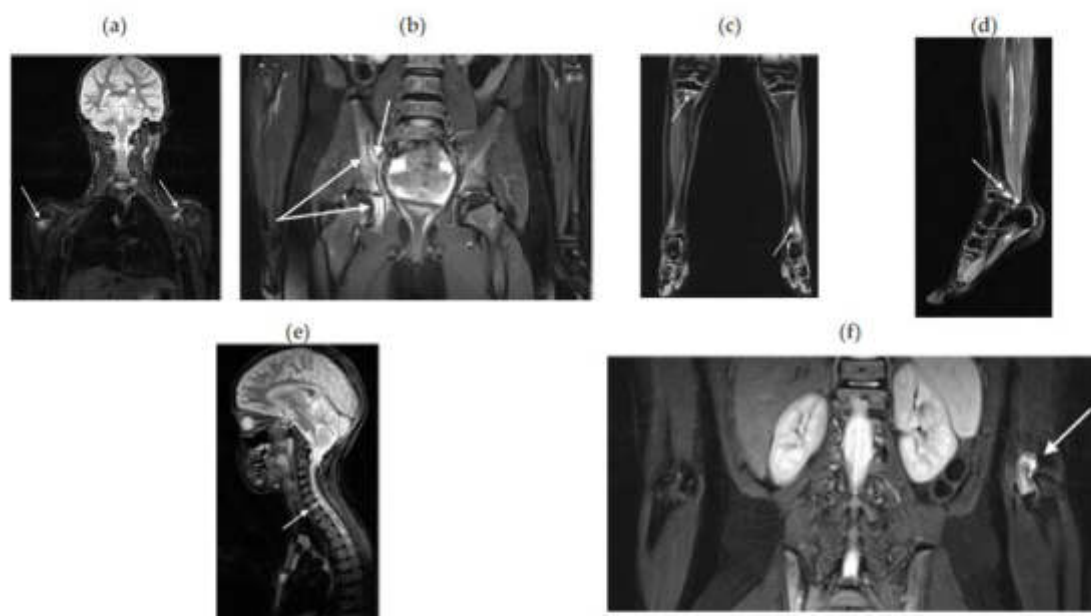


Figure 3. An 8-year-old girl with an overlapping syndrome of JIA and CRMO, TIRM images in coronal and sagittal views. (a) BME in the right humeral metaphysis and effusion in the left shoulder (arrows); (b) BME in the right triradiate cartilage and periarticularly in the right iliac bone (long arrows), and effusion in the right sacroiliac joint (short arrow); (c) BME in the proximal metaphysis of the right tibia and distal metaphysis of the left tibia (arrows); (d) BME in the distal epiphysis of the left tibia (arrow); (e) BME in the Th1 vertebra (arrow); (f) BME in the left elbow joint (arrow).

In JIA, BME was found in 28 of 51 (54.9%) patients. Most commonly, BME was found bilaterally in the femur and midfoot, in 12 (23.5%) and 7 (13.7%) children, respectively. Unilateral BME was most common in the femur (six children, 11.8%) (Table 3 and Figure 4). With regard to the long bones, BME was most commonly located in the distal epiphysis of the femur, followed by the distal metaphysis of this bone (Table 5).

In OS, BME was found in seven of eight patients (88%). BME was most commonly found bilaterally in the femur and ankle, being found in both of these locations in three children (37.5%). Unilateral BME occurred most frequently in the femur and tibia, with equal frequency in two children (25%) in both bones (Table 3 and Figure 4).

In NA, BME was found in 10 of 88 patients (11%). Most commonly, BME occurred unilaterally in the tibia (in four children; 4.4%), and bilaterally, it was most common in the talus bone (three children; 3.3%) (Table 3 and Figure 4).

BME in vertebrae was mainly seen in CRMO (four patients; 15.4%), followed by JIA (four patients; 7.87%), OS (one patient; 12.5%), and no patients with NA. Spondylitis was the only seen lesion. The thoracic spine was most frequently involved: in three patients (11.5%) with CRMO; in two (3.9%) with JIA, and in one (12.5%) with OS, followed by the lumbar spine (in two patients (7.7%) with CRMO; in three patients (5.9%) with JIA). The least frequently affected was the cervical spine, in only one patient (3.8%) with CRMO.

Table 3. BME lesions in 4 study groups.

Lesion	CRMO ¹ n = 26		JIA n = 51		OS n = 8		NA n = 88	
	Unilateral	Bilateral	Unilateral	Bilateral	Unilateral	Bilateral	Unilateral	Bilateral
Mandibula	4 (15.4%)	0	0	0	0	0	0	0
Scapula, SCJ, ACJ	1 (3.8%)	1 (3.8%)	1 (2.0%)	0	0	0	0	0
Clavicle	2 (7.7%)	1 (3.8%)	0	1 (2.0%)	0	0	0	0
Humerus	3 (11.5%)	1 (3.8%)	2 (3.9%)	0	0	1 (12.5%)	0	0
Ulna	0	1 (3.8%)	0	1 (2.0%)	0	0	0	0
Radius	2 (7.7%)	1 (3.8%)	0	2 (3.9%)	0	0	0	0
Hand and wrist	0	2 (7.7%)	0	0	0	0	0	0
Pelvis	2 (7.7%)	1 (3.8%)	4 (7.8%)	5 (9.8%)	0	1 (12.5%)	0	0
Patella	1 (3.8%)	1 (3.8%)	1 (2.0%)	0	0	0	0	0
Femur	3 (11.5%)	10 (38.5%)	6 (11.8%)	12 (23.5%)	2 (25.0%)	3 (37.5%)	1 (1.1%)	1 (1.1%)
Tibia	4 (15.4%)	12 (46.2%)	1 (2.0%)	6 (11.8%)	2 (25.0%)	2 (25.0%)	4 (4.4%)	0
Fibula	3 (11.5%)	1 (3.8%)	1 (2.0%)	1 (2.0%)	0	0	1 (1.1%)	0
Talus	4 (15.4%)	5 (19.2%)	5 (9.8%)	6 (11.8%)	0	3 (37.5%)	2 (2.2%)	3 (3.3%)
Calcaneus	5 (19.2%)	3 (11.5%)	1 (2.0%)	6 (11.8%)	1 (12.5%)	2 (25.0%)	1 (1.1%)	2 (2.2%)
Midfoot	3 (11.5%)	4 (15.4%)	3 (5.9%)	7 (13.7%)	0	2 (25.0%)	1 (1.1%)	1 (1.1%)
Metatarsal/s	4 (15.4%)	2 (7.7%)	0	1 (2.0%)	0	0	2 (2.2%)	2 (2.2%)
Toes	0	1 (3.8%)	0	0	0	0	1 (1.1%)	1 (1.1%)

¹ CRMO—chronic recurrent multifocal osteomyelitis; JIA—juvenile idiopathic arthritis; OS—JIA with CRMO overlapping syndrome; NA—non-specific arthropathy; n—number of patients; SCJ—sterno-clavicular joint; ACJ—acromio-clavicular joint.

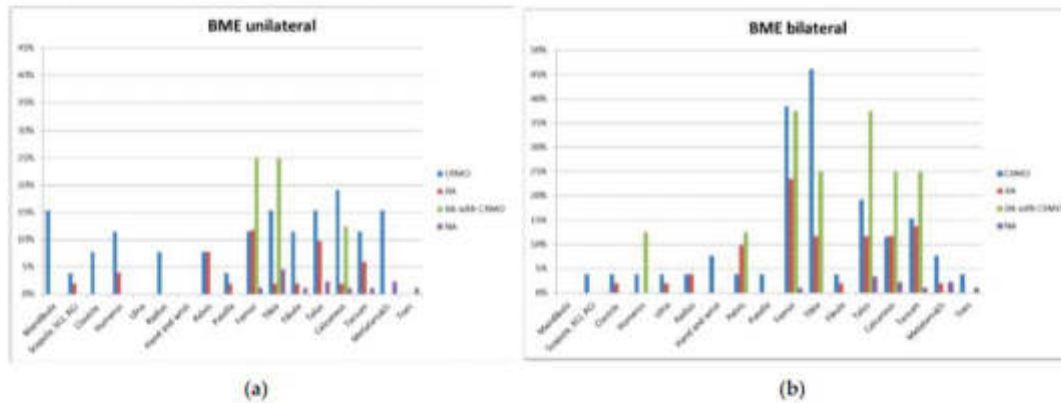


Figure 4. Distribution of bone lesions in skeleton of patients with CRMO, JIA, OS, and NA with unilateral (a) and bilateral BME lesions (b).

Table 4. Number of patients with CRMO and JIA with at least 1 lesion at proximal and distal meta-taphyses and epiphyses.

An Affected Bone	Proximal Metaphysis		Proximal Epiphysis		Distal Metaphysis		Distal Epiphysis	
	CRMO	JIA	CRMO	JIA	CRMO	JIA	CRMO	JIA
Humerus	0	0	2	1	0	0	1	1
Ulna	1	0	1	0	1	1	1	0
Radius	2	0	2	0	1	2	2	2
Femur	5	6	3	2	10	8	9	12
Tibia	6	5	4	3	10	5	10	1
Fibula	0	1	0	1	2	1	2	0

Table 5. Effusions in patients with CRMO, JIA, JIA and CRMO overlapping syndrome, and NA.

Lesion	CRMO n = 26		JIA n = 51		OS n = 8		NA n = 88	
	Unilateral	Bilateral	Unilateral	Bilateral	Unilateral	Bilateral	Unilateral	Bilateral
Shoulder	0	0	5 (9.8%)	0	1 (12.5%)	0	0	0
Elbow	0	0	1 (2.0%)	1 (2.0%)	1 (12.5%)	1 (12.5%)	1 (1.1%)	0
Wrist	0	0	1 (2.0%)	0	0	0	1 (1.1%)	0
SJ	0	0	1 (2.0%)	0	0	0	0	0
Hip	0	0	4 (7.8%)	8 (15.7%)	1 (12.5%)	3 (37.5%)	0	0
Knee	0	2 (7.7%)	9 (17.6%)	8 (15.7%)	0	1 (12.5%)	1 (1.1%)	0
Ankle	0	1 (3.8%)	3 (5.9%)	3 (5.9%)	1 (12.5%)	1 (12.5%)	1 (1.1%)	0
Foot	0	0	1 (2.0%)	0	1 (12.5%)	1 (12.5%)	0	0
Symphysis pubis	0	0	1 (2.0%)	0	1 (12.5%)	0	0	0

3.2.2. Effusions

Effusions were found predominantly in patients with JIA, in 27 out from 51 children (52.9%) (Table 5, Figure 2).

In OS, effusion was seen on WB-MRI in five of eight patients (62.5%). In the three patients in whom no effusion was visualized on WB-MRI, two were 14-year-old children whose hands and feet were outside the imaging range (effusions in the MCP and MTP joints were found on ultrasound). In a third eight-year-old child, due to strong artefacts, the small joints were not evaluable on MR, and exudates in the forefoot were confirmed on ultrasound.

Effusions in the other entities (CRMO, NA) were sporadic.

3.2.3. Myositis

Myositis was found in two patients with JIA (3.9%) and in one patient with OS (12.5%). In both JIA patients, the muscles were involved bilaterally (in one both gluteal muscles and in the second patient both infraspinatus, quadratus femoris, teres major, and multifidus). In OS, the right quadratus femoris was affected.

3.2.4. Enthesitis

Enthesitis was found in four patients with JIA (7.8%) and in one patient with CRMO (3.8%); no enthesitis was found in OS and NA. In JIA, unilateral trochanter major enthesitis was seen in one patient, bilateral trochanter major enthesitis was diagnosed in one patient, and bilateral enthesitis of the ischial tuberosity was seen in one patient. In CRMO, only one patient developed unilateral enthesitis in the iliac bone.

No other lesions were found in the study group, such as juxtaphyseal nodules, periosteal edema, fasciitis, vertebra plana, early physeal fusion, bone deformities, premature degenerative arthrosis, kyphosis deformities, thoracic outlet type syndrome, and pathologic fractures [1,8,15].

4. Discussion

The two main WB-MRI referrals for non-oncologic indications in pediatry include in approximately 80% of two rheumatologic diseases: ERA subtype of JIA and CRMO [1]. Both diseases have clinical similarities due to their respective extra-bony and extra-articular manifestations. Their concurrent involvement in one patient is possible as well as the evolution from one to another [16].

The aim of our retrospective study within a single large pediatric referral center was to determine and compare the initial distribution of lesions in the WB-MRI in those patients with CRMO, JIA, their OS, and with NA.

4.1. WB-MRI in CRMO

A systematic review conducted by Zadig et al. [40] showed that CRMO was the most frequent indication for performing a WB-MRI. In our study of 173 included patients, the most numerous group was children with JIA (51 patients), followed by CRMO (26 patients), and OS (8 patients). In the remaining 88 children referred for WB-MRI by rheumatologists, non-specific MSK complaints (NA) were finally diagnosed.

CRMO is the entity to which relatively most publications on the use of WB-MRI have been devoted. The disease is generally more common in boys; in our study, CRMO was slightly more frequently diagnosed in boys (58% vs. 42%), similarly to the results of Tasar et al. [41] (65%).

BME featured in our series of all 26 children (100%) with CRMO.

Most BME lesions demonstrated multifocal ill-defined bone marrow hyperintensity on STIR images (in 23 children; 88.5%). The results from Aden et al. [42] showed 68% of patients had multiple lesions. Based on their WB-MRI assessments, the average number of sites per patient at the diagnosis of CRMO has been reported to be five [42]. In our series, 263 lesions were detected in 26 children, with lesions ranking from 1 (in 3 patients) to 33 (in 1 patient); the median number of lesions in our CRMO group was 7.5 (IQR: 3–14). In Kieninger et al. [13] baseline WB-MRI performed in 20 children, 206 bone lesions were detected (median number of lesions per patient, 8; range, 2–40). All patients had multifocal bone lesions (88.5% in our group).

Unifocal disease at diagnosis in another study [34] was found in about 30% of patients. In our series, only three patients (11.5%) had only one BME lesion.

The characteristic skeletal lesions of CRMO are typically in the periphyseal locations, in metaphysis and epiphyseal equivalent areas in appendicular and axial skeleton without a fluid collection [8,10,13,14]. The bones of the lower extremities were the most affected body regions in our series, consistent with the literature [9,10,15,43]. The most frequent locations were bilaterally in the tibia and femur in 11 (42.3%) and 10 (38.5%) children, respectively (Table 4). Unilaterally, BME occurred most frequently in the calcaneus (five children, 19.2%). The most commonly affected lower limb regions in a study by Panwar et al. [10] occurred, in descending order, in the distal tibial metaepiphysis (66%), proximal tibial metaepiphysis (50%), distal femur metaepiphysis (50%), and distal fibular metaepiphysis (31%). The distal tibia (14.7% of total lesions) was also the most common location in the peripheral skeleton in Domasio et al. series [15]. In our study, we found similar results (Table 4): distal tibial and femoral metaphysis (38.4% each), and distal tibial and femoral epiphysis (34.6% each) were the most common locations of BME.

In the study by Papakonstantinou et al., a total of 236 lesions ranging from 1 to 31 per patient (mean: 11.8 ± 9.06 SD) was detected in a comparably sized group of 20 children [44]. The tibia was the most frequent site of lesions as at least one tibial lesion was observed in 14 (70%) of the patients (in our study, 11 patients had tibial lesions; 42.3%). The distal tibia was followed by the calcaneus (60%) and fibula (50%) [44], whereas in our study, BME lesions in the distal metaphysis of the femur and the tibia were followed by their distal epiphyses (in 18 out of 26 patients; 69.2%; Table 4). Distal tibial metaphyses or distal femoral metaphyses, most often with transphyseal extension, were the most frequently affected sites in many other cohorts [44]. Bhat et al. [45] found distal tibia as the most frequent site of disease, affecting 49.6% of their patients in a large series of 122 CRMO patients with WB-MRI, while D'Angelo et al. [46] reported femur and tibia as the most frequently affected sites (61.3% and 64.5%, respectively) followed by pelvis and spine in a series of 75 children.

Panwar et al. [10] found lesions in the bones of the feet were more common than in the hand, which is in keeping with the predilection of disease to involve the lower limb. In our case, this difference was significant: metatarsals and toes were involved in 26.9% of patients, and hands and wrists in only 7.7%. To a large extent, however, this may have been due to artefacts: in our study, the hands and feet were not well visualized in 37% of patients with CRMO.

Panwar et al. [10] found that upper extremity involvement was considerably less common, affecting the distal ulnar and radial meta-epiphysis in 20%. In our cohort of CRMO patients, the humerus, radius, ulna, hand, and wrist lesions were found in 38.4% of the patients. In the Papakonstantinou et al. group [44], upper limb BME lesions were found in 15% of patients, whereas Zhao et al. reported only in 9% of patients the involvement of the upper extremities, including humerus, radius, and hand. [9].

A classical bilateral pattern of bone lesions in our study was not evident and we obtained an almost equal distribution of uni- and bilateral involvement. The most frequent bone types showing bilateral involvement in our study were tibia and femur, followed by talus and midfoot. In Papakonstantinou et al. group [44] it was the tibia, followed by the talus, the calcaneus, and the femur.

The pelvis, spine, clavicle, mandible, skull, sternum, and ribs were also involved to a variable extent [10].

The pelvis was one of the commonest sites of involvement in several studies, ranging from 15% to 40% [10,13,41,43,44]. Typical sites of CRMO involvement include metaphyseal equivalents, pelvic synchondroses, and the sacroiliac joints, of which the latter resembles inflammatory sacroiliitis [8]. In our study, the pelvis was involved in only three children (11.5%), the ischium in one child, and the sacroiliac joints in two children.

As many as 13–30% of patients diagnosed with CRMO are reported to have spinal involvement [13,14]; in the Damasio et al. study [15], spinal segments in CRMO were the most frequent location of disease, representing 33% of total lesions. In our group, the spine in CRMO was affected in four patients (15.4%), followed by JIA (four patients; 7.87%), and one patient with OS (12.5%). The thoracic spine was affected in CRMO in 19% to 36% in the previous series [9,44]. In our patients with CRMO, it was also most often involved (11.5%). In contrast, Papakonstantinou et al. [44] found no cases of spinal involvement.

Spondylitis was the only lesion seen in our series. In our initial WB-MRI, we did not find spondylodiscitis, sclerotic/nonactive lesions, paravertebral ossifications, or osteolytic lesions with variable degrees of vertebral body collapse, commonly seen in the thoracic spine by other groups [10,41]. Such changes generally arise in up to 40% of patients with the disease duration, including structural vertebral body deformities extending from wedging to crush fractures [8]. However, Kieninger et al. reported deformities and complications early [13]; in their initial WB-MRI performed in 20 patients with CRMO up to 6 months, scoliosis, thoracic hyperkyphosis, a fractured pubic bone, deformity of the temporomandibular joint, and vertebral body fractures were detected [13]. For the growing skeleton, the loss of vertebral height may limit growth and ultimately lead to a decrease in the height of the child [14]. Detecting asymptomatic vertebral lesions at their earliest is imperative for the prevention of vertebral height loss, and this is where WB-MRI is crucial [14].

The involvement of the medial clavicle and mandible was less common in our study. When it is involved, CRMO should be strongly suspected [12]. Andronikou et al. [47] found that the clavicle was the most common lesion location in patients with CRMO, followed by the femoral and tibial metaphysis (38%). In our group, the clavicle was affected in 11.5% of patients, similarly to Damasio et al. (4%) [15], whereas Kieninger et al. and Papakonstantinou et al. found that it was involved in 15% of patients [13,44]. The mandible is involved in CRMO in about 5% of cases, with symptoms of recurring pain, trismus, and paresthesia [8]. In our cohort, BME in the mandible was found in 15.4% of cases, while none were found in the Papakonstantinou et al. group [44].

Periosteal reaction was not observed in our study despite the fact that such lesions without mass effect has been considered part of the CRMO spectrum, and other authors have found it occasionally [44,46].

Lesions were absent within our cohort in manubrium/sternum and ribs and skull, similarly to another study by Zhao et al. [9]. They also found no lesions in scapula, and ulna, which occurred, respectively, in a few patients in our group.

In addition to BME, another pathology in CRMO was effusion found in only two patients (7.7%), namely bilaterally in the knee and ankle joints (Table 5). Mild joint effusion

was seen in only five patients (25%) by Papakonstantinou et al. [44], with nearby bones being affected (three ankles, one hip, and one knee joint). In the Tasar et al. study [41], joint involvement was present in 20 patients (14%). The sacroiliac joint was the most commonly involved, followed by the knee, the sternoclavicular joint, and the ankle.

Enthesitis was found in only 1 of 26 patients (3.8%). No patients had any clinical or radiological evidence of enthesitis in the study by Tasar et al. [41].

4.2. WB-MRI in JIA

Although there are no clear-cut guidelines available for the standardized acquisition, interpretation, and quantification of JIA on WB-MRI, it has been increasingly used in the pediatric population for the evaluation of various neoplastic and nonneoplastic conditions [7]. Because of its multiplanar capabilities and excellent soft tissue contrast, MRI allows the evaluation of the peripheral joints, entheses, and the axial skeleton [7].

In JIA, the primary abnormality is synovitis. WB-MRI can be performed to assess for asymptomatic joint arthritis and can map the joints involved in the polyarticular and/or atypical forms of arthritis, especially in those locations that are not easily accessible clinically or with ultrasound, such as temporomandibular and sacroiliac joints [7,11,15]. The early detection of factors of poor prognosis in the disease is essential for suitable treatment selection. WB-MRI helps by calculating the total inflammatory burden and in guiding therapy in JIA [7].

Despite clear advantages, the ESSR survey in 2021 [3] highlighted that WB-MRI is not routinely applied for various systemic musculoskeletal inflammatory diseases, with the exceptions of myositis and CRMO. The lack of a standardized protocol, a long acquisition time, and variable reimbursement are the main factors that hinder its more widespread use [48].

Our cohort of 51 patients differs from previous studies, as JIA was the most common indication for the WB-MRI. Depending on the JIA subtype, the disease may be more common in girls or boys [49]. In our study group JIA was diagnosed almost twice as often in girls (66% vs. 34%). The number of visualized WB-MRI lesions (296) ranged from 0 (in 14 patients) to 31 lesions (in 1 patient). BME, arthritis (effusions), enthesitis, and myositis were diagnosed.

The most frequent lesion found in children with JIA was BME (55% of patients). It was most often bilateral in the femur and midfoot, in 23.5% and 13.7% of children, respectively (Table 3 and Figure 4). With regard to the long bones, BME was most frequently localized in the distal epiphysis of the femur (51%) (Table 5), which is similar to the location of BME in rheumatoid arthritis in adults. However, there have been no studies dedicated to the frequency and location of BME on WB-MRI in children with JIA.

Tarsitis (BME and effusion/synovitis in midfoot) has been reported in up to one third of children at disease onset and is a characteristic finding in juvenile spondyloarthritis [11]. This location of BME was also common in our patients (Table 3).

A cohort study involving 59 children with ERA reported the development of MRI evidence of sacroiliitis in 30% of children within 1 year of disease onset [11]. In our patients, the pelvis was involved most frequently in children with JIA (17.6%), including 7.8% cases unilaterally (one patient with sacroiliitis, two cases of BME in the pubic bone) and 9.8% bilaterally (four patients with sacroiliitis, one with BME in the pubic bone). In CRMO, the pelvis was involved slightly less frequently (three cases, 11.5%), and only one case was found in OS (12.5%) (Table 3).

In our cohort, the spine was involved in 7.8% of subjects. Although JIA typically occupies the cervical spine, BME in the thoracic and lumbar vertebral bodies was also found.

Effusions were detected in about 20% of children. The knee was most often involved joint (Table 5, Figure 2). However, it is possible that these findings are skewed due to poor visualization of the hand and foot, which affected 36% of children with JIA. Effusions were visualized in 62.5% of OS patients, whereas in CRMO and NA, it was sporadic.

Enthesitis is a predominant finding in juvenile spondyloarthritis and has been shown to affect 60–80% of JIA patients [11,50,51]. Characteristic locations include the following: the inferior pole of the patella, ischial tuberosity and various ligamentous and muscular attachments of the pelvis, and greater trochanter and calcaneus [11]. A cross-sectional study by Rachlis et al. [52] that utilized whole-body MRI identified the hip extensor insertion at the greater trochanter as the most common site of involvement. A separate study demonstrated midfoot enthesitis in 88% of patients with active inflammatory disease at short-term follow-up [51].

Enthesitis in our series was seen on the WB-MRI in three patients with JIA (5.9%). All cases involved the pelvis: trochanter major and ischial tuberosity. In CRMO, we found only one case of enthesitis, and in OS and NA, no features of enthesitis.

We did not find features of enthesitis in the spine, despite the fact that corner lesions, or Romanus lesions, can also be seen in juvenile spondyloarthritis; these lesions represent enthesitis of the annulus fibrosus, with BME or osteitis at the vertebral body endplates, with further development of sclerosis and erosions [11,53]. Sagittal images of the spine would have increased the conspicuity of any corner lesions.

Myositis was found in JIA in 4% of children, in five locations, all bilaterally. Myositis is rarely analyzed in the context of JIA, despite the fact it can occur in some patients in a systemic subtype of JIA, or may be triggered by biological treatment in JIA [19].

In 2021, Panwar et al. [10] developed a standardized WB-MRI scoring system to quantify the total inflammatory burden in children with JIA through formal consensus methods among an interdisciplinary group of experts. The working group decided to limit the scope of the scoring system to synovial and enthesal inflammation in peripheral and axial joints [10]. Nevertheless, the scoring included a number of items, including 100 peripheral joints, 76 axial joints, 23 joints of the chest, and 64 entheses. Chronic osteochondral changes and the total damage were not scored as they were highly challenging and unreliable considering the low spatial resolution and large field of view of WB-MRI [10]. Also, costovertebral, costotransverse, and temporomandibular joints were excluded from the scoring system due to the wide FOV and out-of-plane imaging of these articulations on WB-MRI [10].

4.3. WB-MRI in OS

The diagnosis of CRMO and JIA overlapping syndrome is based on the presence of multiple sites of bone marrow edema (representing CRMO) and enthesitis, and the inflammation of peripheral and axial joints, including the spine (typical for JIA, including ERA) [7].

Our work is the first report of the use of WB-MRI in this disease entity. In our study, WB-MRI lesions ranged from 0 (in one patient) to 22 (in one patient).

The most common abnormality was BME, seen in eight patients (88%), most commonly bilaterally in the femur and ankle (37.5% each). In only one child was a BME lesion detected in the thoracic spine.

Effusions were found in five of eight patients (62.5%). In the remaining three patients, no features of effusion were found on WB-MRI. However, two were 14-year-old juveniles whose hands and feet were outside the imaging range, with effusions in the MCP and MTP joints that were found on ultrasound.

There was only one case of myositis (12.5%) and no cases of enthesitis in OS. There is evidence that CRMO frequently affects first-degree or second-degree family members with psoriasis or other autoimmune disorders [14]. As many as 26% to 50% of patients with CRMO may have inflammatory monoarticular or polyarticular joint involvement either at presentation or later during the course of the disease [14]. This could explain the absence of enthesitis in our initial WB-MRI.

4.4. WB-MRI in NA

In recent years, there has been a significant increase in the frequency of various musculoskeletal complaints in children, particularly in girls. MR examination has an important role in the broad differential diagnosis [37]. In addition to diagnosis and monitoring of the effectiveness of treatment, economic considerations cannot be ignored. For example, in the case of multiple joint pain (>4–5), the cost of multiple ultrasound examinations exceeds the cost of performing a single WB-MRI [54–59].

In our WB-MRI of 88 patients with non-specific musculoskeletal symptoms, as in the previously described diseases, BME dominated in lower extremities. Effusions were sporadic, and no other lesions were found in this group.

There were several limitations in our study. These include its retrospective nature and the limited number of patients with OS. Interobserver agreement was not explored; however, the radiologists were both aware of the imaging findings. Some regions such as the hand and feet were not well represented, especially in large children, as highlighted by other researchers [9,10,15,60]. The lack of dedicated hand imaging in our protocol likely led to the underestimation of bone lesions particularly in this location, and can be addressed in future prospective studies by placing the hands on thighs for better visibility, as indicated by Panwar et al. [10]. In individual cases, artefacts (mainly motion) prevented WB-MRI interpretation, which occurred in 2 patients (7.4%) with CRMO, 10 (20%) with JIA, 2 (25%) with OS, and 12 with (13.6%) NA. Furthermore, in this study, the analysis only considered TIRM sequences, as in most published work [1,40,47], in two planes, coronal and sagittal. Future considerations might involve changing the sequences used, adding acquisition planes and changing the positioning of the hand during the examination. The ESSR survey by Giraudo et al. [3] confirmed a heterogeneous approach emerged regarding the scanning plane [7,11,40]. Finally, although BME was one of the most important diagnostic and differential features, recent work by Zadig et al. [61] showed that focal areas of high signal intensity on WB-MRI fat suppressed images that cause concern, as in our study group, are seen in more than half of healthy, asymptomatic children and adolescents. An awareness of this is important when interpreting WB-MRI in this age group as some findings may resemble clinically silent lesions in children with suspected multifocal skeletal disease [61,62].

5. Conclusions

Our study showed that this group of inflammatory childhood diseases share imaging features on WB-MRI; however, several key features can help to distinguish them.

BME was the most common abnormality in our series, being seen in 100% of patients with CRMO, 88% with OS, 55% with JIA, and 11% with NA. The bones of the lower extremities were the most affected body regions in all compared entities. Effusion was another common lesion in JIA (53% of patients) and in OS (63%), whereas in CRMO and NA, it occurred occasionally. Myositis was found only in patients with OS and JIA, and enthesitis was only seen in JIA in a small percentage of patients, presumably due to a short history of the disease. Because of artefacts, the assessment of the small joints of the hands and feet remained problematic, and their assessment often requires complementary examination, usually ultrasonography or dedicated MRI.

Author Contributions: Conceptualization, M.L. and I.S.-S.; methodology, M.L., I.S.-S., P.G. and M.M.; writing—original draft preparation, M.L., I.S.-S., P.G. and M.M.; writing—review and editing, M.L., I.S.-S., P.G. and M.M. All authors have read and agreed to the published version of the manuscript.

Funding: This research received no external funding.

Institutional Review Board Statement: The study was conducted according to the guidelines of the Declaration of Helsinki, and approved by the Institutional Ethics Committee of the National Institute of Geriatrics, Rheumatology and Rehabilitation in Warsaw (26/04/2018, No KBT-3/1/2018).

Informed Consent Statement: Informed consent was obtained from all subjects involved in the study.

Data Availability Statement: Data presented in this study are available on request from the corresponding author.

Conflicts of Interest: The authors declare no conflicts of interest.

References

- Greer, M.L.C. Whole-body magnetic resonance imaging: Techniques and nononcologic indications. *Pediatr. Radiol.* **2018**, *48*, 1348–1363. [\[CrossRef\]](#) [\[PubMed\]](#)
- Schaefer, J.F.; Berthold, L.D.; Hahn, G.; von Kalle, T.; Moritz, J.D.; Schröder, C.; Stegmann, J.; Steinborn, M.; Weidemann, J.; Wursch, R.; et al. Whole-Body MRI in Children and Adolescents—S1 Guidelines. *Fortschr. Röntgenstr.* **2019**, *191*, 618–625. [\[CrossRef\]](#) [\[PubMed\]](#)
- Giraudo, C.; Lecouvet, F.E.; Cotton, A.; Eshed, I.; Jans, L.; Jurik, A.G.; Maas, M.; Weber, M.; Sudol-Szopińska, I. Whole-body magnetic resonance imaging in inflammatory diseases: Where are we now? Results of an International Survey by the European Society of Musculoskeletal Radiology. *Eur. J. Radiol.* **2021**, *136*, 109533. [\[CrossRef\]](#) [\[PubMed\]](#)
- Spalkit, S.; Sinha, A.; Prakash, M.; Sandhu, M.S. Dermatomyositis: Patterns of MRI findings in muscles, fascia and skin of pelvis and thigh. *Eur. J. Radiol.* **2021**, *141*, 109812. [\[CrossRef\]](#) [\[PubMed\]](#)
- Sreelal, T.V.; Bhatia, A.; Suri, D.; Singh, S.; Saxena, A.K.; Tao, T.Y.; Sodhi, K.S. Whole-body MR imaging in evaluation of children with juvenile dermatomyositis. *Eur. J. Radiol.* **2022**, *155*, 110475. [\[CrossRef\]](#) [\[PubMed\]](#)
- Schaal, M.C.; Gendler, L.; Ammann, B.; Eberhardt, N.; Janda, A.; Morbach, H.; Darge, K.; Girschick, H.; Beer, M. Imaging in non-bacterial osteomyelitis in children and adolescents: Diagnosis, differential diagnosis and follow-up—An educational review based on a literature survey and own clinical experiences. *Insights Imaging* **2021**, *12*, 113. [\[CrossRef\]](#)
- Malattia, C.; Tolend, M.; Mazzoni, M.; Panwar, J.; Zlotnik, M.; Otoho, T.; Vidarsson, L.; Doria, A.S. Current status of MR imaging of juvenile idiopathic arthritis. *Best Pract. Res. Clin. Rheumatol.* **2020**, *34*, 101629. [\[CrossRef\]](#)
- Koneru, S.; Magid, M.S.; Fritz, J. Case of the Season: Asymmetric Chronic Recurrent Multifocal Osteomyelitis. *Semin. Roentgenol.* **2021**, *57*, 184–190. [\[CrossRef\]](#)
- Zhao, Y.; Sato, T.S.; Nielsen, S.M.; Beer, M.; Huang, M.; Iyer, R.S.; McGuire, M.; Ngo, A.; Otjen, J.P.; Panwar, J.; et al. Development of a Scoring Tool for Chronic Nonbacterial Osteomyelitis Magnetic Resonance Imaging and Evaluation of its Interrater Reliability. *J. Rheumatol.* **2020**, *47*, 739–747. [\[CrossRef\]](#)
- Panwar, J.; Tolend, M.; Lim, L.; Shirley, M.; Tse, S.M.; Doria, A.S.; Laxer, R.M.; Stimec, J. Whole-body MRI Quantification for Assessment of Bone Lesions in Chronic Nonbacterial Osteomyelitis Patients Treated with Pamidronate: A Prevalence, Reproducibility, and Responsiveness Study. *J. Rheumatol.* **2021**, *48*, 751–759. [\[CrossRef\]](#)
- Aquino, M.R.; Tse, S.M.L.; Gupta, S.; Rachlis, A.C.; Stimec, J. Whole-body MRI of juvenile spondyloarthritis: Protocols and pictorial review of characteristic patterns. *Pediatr. Radiol.* **2015**, *45*, 754–762. [\[CrossRef\]](#)
- Sato, T.S.; Watal, P.; Ferguson, P.J. Imaging mimics of chronic recurrent multifocal osteomyelitis: Avoiding pitfalls in a diagnosis of exclusion. *Pediatr. Radiol.* **2020**, *50*, 124–136. [\[CrossRef\]](#) [\[PubMed\]](#)
- Kieninger, A.; Schäfer, J.F.; Tsiflikas, I.; Moll, M.; Kümmerle-Deschner, J.; Kraus, M.S.; Esser, M. Early diagnosis and response assessment in chronic recurrent multifocal osteomyelitis: Changes in lesion volume and signal intensity assessed by whole-body MRI. *Br. J. Radiol.* **2021**, *95*, 20211091. [\[CrossRef\]](#) [\[PubMed\]](#)
- Shah, A.; Rosenkranz, M.; Thapa, M. Review of spinal involvement in Chronic recurrent multifocal osteomyelitis (CRMO): What radiologists need to know about CRMO and its imitators. *Clin. Imaging* **2022**, *81*, 122–135. [\[CrossRef\]](#) [\[PubMed\]](#)
- Damasio, M.B.; Magnaguagno, F.; Stagnaro, G. Whole-body MRI: Non-oncological applications in paediatrics. *Radiol. Med.* **2016**, *121*, 454–461. [\[CrossRef\]](#) [\[PubMed\]](#)
- Koné-Paut, I.; Mannes, I.; Dusser, P. Chronic Recurrent Multifocal Osteomyelitis (CRMO) and Juvenile Spondyloarthritis (JSpA): To What Extent Are They Related? *J. Clin. Med.* **2023**, *12*, 453. [\[CrossRef\]](#) [\[PubMed\]](#)
- Pracoń, G.; Simoni, O.P.; Gietka, P.; Aparisi, P.; Sudol-Szopińska, I. Conventional Radiography and Ultrasound Imaging of Rheumatic Diseases Affecting the Pediatric Population. *Semin. Musculoskelet. Radiol.* **2021**, *25*, 68–81. [\[CrossRef\]](#) [\[PubMed\]](#)
- Sudol-Szopińska, I.; Gietka, P.; Znajdek, M.; Matuszewska, G.; Boguczevska, M.; Damjanovska-Krstik, L.; Ivanoski, S. Imaging of Juvenile Spondyloarthritis. Part I: Classifications and Radiographs. *J. Ultrason.* **2017**, *17*, 167–175. [\[CrossRef\]](#)
- Sudol-Szopińska, I.; Herregods, N.; Doria, A.S.; Taljanovic, M.S.; Gietka, P.; Tzaribachev, N.; Klausner, A.S. Advances in Musculoskeletal Imaging in Juvenile Idiopathic Arthritis. *Biomedicines* **2022**, *10*, 2417. [\[CrossRef\]](#)
- Sudol-Szopińska, I.; Giraudo, C.; Oei, E.H.G.; Jans, L. Imaging update in inflammatory arthritis. *J. Clin. Orthop. Trauma* **2021**, *20*, 101491. [\[CrossRef\]](#)
- Malievskiy, V. Arthralgia in children: The epidemiological study. *Pediatr. Rheumatol.* **2011**, *9* (Suppl. S1), P144. [\[CrossRef\]](#)
- De Inocencio, J.; Carro, M.A.; Flores, M.; Carpio, C.; Mesa, S.; Marín, M. Epidemiology of musculoskeletal pain in a pediatric emergency department. *Rheumatol. Int.* **2016**, *36*, 83–89. [\[CrossRef\]](#)
- De Inocencio, J. Epidemiology of musculoskeletal pain in primary care. *Arch. Dis. Child.* **2004**, *89*, 431–434. [\[CrossRef\]](#)
- Remvig, L.; Jensen, D.V.; Ward, R.C. Epidemiology of General Joint Hypermobility and Basis for the Proposed Criteria for Benign Joint Hypermobility Syndrome: Review of the Literature. *J. Rheumatol.* **2007**, *34*, 804–809. [\[PubMed\]](#)
- Mohanta, M.P. Growing pains: Practitioners' dilemma. *Indian Pediatr.* **2014**, *51*, 379–383. [\[CrossRef\]](#)

26. Weiss, J.; Stinson, J.N. Pediatric pain syndromes and noninflammatory musculoskeletal pain. *Pediatr. Clin. N. Am.* **2018**, *65*, 801–826. [[CrossRef](#)] [[PubMed](#)]
27. Uziel, Y.; Hashkes, P.J. Growing pains in children. *Pediatrics* **2008**, *147*, 809–811. [[CrossRef](#)] [[PubMed](#)]
28. Evans, A.; Scutter, S. Prevalence of “growing pains” in young children. *J. Pediatr.* **2004**, *145*, 255–258. [[CrossRef](#)] [[PubMed](#)]
29. Roderick, M.R.; Shah, R.; Rogers, V.; Finn, A.; Ramanan, A.V. Chronic recurrent multifocal osteomyelitis (CRMO)—Advancing the diagnosis. *Pediatr. Rheumatol. Online J.* **2016**, *14*, 47. [[CrossRef](#)] [[PubMed](#)]
30. Petty, R.E.; TR Southwood, T.R.; Baum, J.; Betay, E.; Glass, D.N.; Manners, P.; Maldonado-Cocco, J.; Suarez-Almazor, M.; Orozco-Alcala, J.; Prieur, A.M.; et al. Revision of the proposed classification criteria for juvenile idiopathic arthritis: Durban, 1997. *J. Rheumatol.* **1998**, *25*, 1991–1994. [[PubMed](#)]
31. Cebecauerová, D.; Malcová, H.; Koukolská, V.; Květalová, Z.; Souček, O.; Wagenknecht, L.; Bronský, J.; Šumník, Z.; Kyněl, M.; Cebecauer, M.; et al. Two phenotypes of chronic recurrent multifocal osteomyelitis with different patterns of bone involvement. *J. Pediatr. Rheumatol.* **2022**, *20*, 108. [[CrossRef](#)] [[PubMed](#)]
32. Hofmann, S.R.; Kappush, F.; Girchick, H.J.; Morbach, H.; Pablik, J.; Ferguson, P.J.; Hedrich, C.H.M. Chronic Recurrent Multifocal Osteomyelitis (CRMO): Presentation, Pathogenesis and treatment. *Curr. Osteoporos. Rep.* **2017**, *15*, 542–554. [[CrossRef](#)] [[PubMed](#)]
33. Martini, A.; Ravelli, A.; Avcin, T.; Beresford, M.W.; Burgos-Vargas, R.; Cuttica, R.; Ilowite, N.T.; Khubchandani, R.; Laxer, R.M.; Lovell, D.J.; et al. Toward New Classification Criteria for Juvenile Idiopathic Arthritis: First Steps, Pediatric Rheumatology International Trials Organization International Consensus. *J. Rheumatol.* **2019**, *46*, 190–197. [[CrossRef](#)] [[PubMed](#)]
34. Barnes, M.G.; Grom, A.A.; Thompson, S.D.; Griffin, T.A.; Luyrink, L.K.; Colbert, R.A.; Glass, D.N. Biologic similarities based on age at onset in oligoarticular and polyarticular subtypes of juvenile idiopathic arthritis. *Arthritis Rheum.* **2010**, *62*, 3249. [[CrossRef](#)] [[PubMed](#)]
35. Weiss, P.F.; Colbert, R.A. Juvenile Spondyloarthritis: A Distinct Form of Juvenile Arthritis. *Pediatr. Clin. N. Am.* **2018**, *65*, 675–690. [[CrossRef](#)]
36. Yıldız, M.; Haşlak, F.; Adroviç, A.; Şahin, S.; Barut, K.; Kasapoçur, Ö. Juvenile spondyloarthropathies. *Eur. J. Rheumatol.* **2022**, *9*, 42–49. [[CrossRef](#)]
37. Gunz, A.C.; Canizares, M.; MacKay, C.; Badley, A.M. Magnitude of impact and healthcare use for musculoskeletal disorders in the paediatric: A population-based study. *BMC Musculoskelet. Disord.* **2012**, *13*, 98. [[CrossRef](#)]
38. King, S.; Chambers, C.T.; Huguet, A.; MacNevin, R.C.; McGrath, P.J.; Parker, L.; MacDonald, A.J. The epidemiology of chronic pain in children and adolescents revisited: A systematic review. *Pain* **2011**, *152*, 2729–2738. [[CrossRef](#)]
39. Turecki, M.B.; Taljanovic, M.S.; Stubbs, A.Y.; Graham, A.R.; Holden, D.A.; Hunter, T.B.; Rogers, L.F. Imaging of musculoskeletal soft tissue infections. *Skelet. Radiol.* **2010**, *39*, 957–971. [[CrossRef](#)]
40. Zadig, P.; von Brandis, E.; Küfner, L.; Rosendahl, K.; Avenarius, D.; Ording Müller, L. Whole-body magnetic resonance imaging in children—How and why? A systematic review. *Pediatr. Radiol.* **2021**, *51*, 14–24. [[CrossRef](#)]
41. Taşar, S.; Sözeri, B. Whole-body MRI in Pediatric Patients with Chronic Recurrent Multifocal Osteomyelitis. *Med. J. Bakirkoy* **2023**, *19*, 78–85. [[CrossRef](#)]
42. Aderi, S.; Won, S.; Yang, C.; Bui, T.; Higa, T.; Scheck, J.; Iyer, R.S.; Egbert, M.; Lindberg, A.; Zhao, Y. Increasing Cases of Chronic Nonbacterial Osteomyelitis in Children: A Series of 215 Cases from a Single Tertiary Referral Center. *J. Rheumatol.* **2022**, *49*, 929–934. [[CrossRef](#)]
43. Menashe, S.J.; Iyer, R.S.; Ngo, A.; Rosenwasser, N.L.; Zhao, Y.; Maloney, E. Whole-body MRI at initial presentation of pediatric chronic recurrent multifocal osteomyelitis and correlation with clinical assessment. *Pediatr. Radiol.* **2022**, *52*, 2377–2387. [[CrossRef](#)] [[PubMed](#)]
44. Papakonstantinou, P.; Proutzou, S.; Karavasilis, E.; Atsali, E.; Bizimi, V.; Alexopoulou, E.; Fotis, L. Whole-body magnetic resonance imaging findings and patterns of chronic nonbacterial osteomyelitis in a series of Greek pediatric Patients. *Acta Radiol. Open* **2022**, *11*, 1–10. [[CrossRef](#)]
45. Bhat, C.S.; Anderson, C.; Harbinson, A.; McCann, L.J.; Roderick, M.; Finn, A.; Davidson, J.E.; Ramanan, A.V. Chronic nonbacterial osteitis— a multicenter study. *Pediatr. Rheumatol.* **2018**, *16*, 4. [[CrossRef](#)] [[PubMed](#)]
46. D’ Angelo, P.; Tanturri de Horatio, L.; Toma, P.; Ording Miller, L.; Avenarius, D.; von Brandis, E.; Zadig, P.; Casazza, I.; Pardeo, M.; Pires-Marafon, D.; et al. Chronic nonbacterial osteomyelitis—Clinical and magnetic resonance imaging features. *Pediatr. Radiol.* **2021**, *51*, 282–288. [[CrossRef](#)] [[PubMed](#)]
47. Andronikou, S.; Kraft, J.K.; Offiah, A.C.; Jones, J.; Douis, H.; Thyagarajan, M.; Barrera, C.A.; Zouvani, A.; Ramanan, A.V. Whole-body MRI in the diagnosis of paediatric CNO/CRMO. *Rheumatology* **2020**, *59*, 2671–2680. [[CrossRef](#)] [[PubMed](#)]
48. Chang, E.Y.; Chen, K.C.; Huang, B.K.; Kavanaugh, A. Adult inflammatory arthritides: What the radiologist should know. *Radiographics* **2016**, *36*, 1849–1870. [[CrossRef](#)]
49. Moradi, A.; Amin, R.M.; Thorne, J.E. The Role of Gender in Juvenile Idiopathic Arthritis-Associated Uveitis. *J. Ophthalmol.* **2014**, *2014*, 61078. [[CrossRef](#)]
50. Li, J.; Zhu, Y.; Guo, G. Enthesitis-related arthritis: The clinical characteristics and factors related to MRI remission of sacroiliitis. *BMC Musculoskelet. Disord.* **2022**, *23*, 1054. [[CrossRef](#)]
51. Burgos-Vargas, R.; Pacheco-Tena, C.; Vazquez-Mellado, J. A short-term follow-up of enthesitis and arthritis in the active phase of juvenile onset spondyloarthropathies. *Clin. Exp. Rheumatol.* **2002**, *20*, 727–731.

52. Rachlis, A.C.; Babyn, P.S.; Lobo-Mueller, E.W.; Benseler, S.M.; Stimec, J. Whole body magnetic resonance imaging in juvenile spondyloarthritis: Will it provide vital information compared to clinical exam alone? *Arthritis Rheum.* **2011**, *63*, 29.
53. Sudol-Szopińska, I.; Matuszewska, G.; Pracoń, G. Juvenile spondyloarthritis. In *Radiographic Atlas of Inflammatory Rheumatic Diseases*, 1st ed.; Sudol-Szopińska, I., Matuszewska, G., Pracoń, G., Eds.; Medisfera: Otwock, Poland, 2022; pp. 215–219.
54. Coles, M.L.; Weissmann, R.; Uziel, Y. Juvenile primary fibromyalgia syndrome: Epidemiology, etiology, pathogenesis, clinical manifestations and diagnosis. *Pediatr. Rheumatol.* **2021**, *19*, 22. [[CrossRef](#)]
55. Weissmann, R.; Uziel, Y. Pediatric complex regional pain syndrome: A review. *Pediatr. Rheumatol. Online J.* **2016**, *14*, 29. [[CrossRef](#)]
56. Pavone, V.; Vescio, A.; Valenti, F.; Sapienza, M.; Sessa, G.; Testa, G. Growing pains: What do we know about etiology? A systematic review. *World J. Orthop.* **2019**, *10*, 192–205. [[CrossRef](#)] [[PubMed](#)]
57. Sperotto, F.; Brachi, S.; Zulian, F.; Vittadello, F. Musculoskeletal pain in schoolchildren across puberty: A 3-year follow-up study. *Pediatr. Rheumatol.* **2015**, *13*, A723–A724. [[CrossRef](#)] [[PubMed](#)]
58. Le Blanc, C.; Houghton, K. Noninflammatory musculoskeletal pain conditions. In *Textbook of Pediatric Rheumatology*; Cassidy, J.T., Petty, R.E., Eds.; Elsevier Saunders: Amsterdam, The Netherlands, 2011; pp. 697–717.
59. De Somer, L.; Wouters, C.; Pans, S. Total body MRI, a guide to diagnosis in patients with osteo-articular pain and inflammation. *Pediatr. Rheumatol. Online J.* **2014**, *12* (Suppl. S1), P164. [[CrossRef](#)]
60. Pasoglou, V.; Van Nieuwenhove, S.; Peeters, F.; Duchêne, G.; Kirchgessner, T.; Lecouvet, F.E. 3D Whole-Body MRI of the Musculoskeletal System. *Semin. Musculoskelet. Radiol.* **2021**, *25*, 441–454. [[CrossRef](#)] [[PubMed](#)]
61. Zadig, P.K.; von Brandis, E.; Flatø, B.; Müller, L.S.O.; Nordal, E.B.; de Horatio, L.T.; Rosendahl, K.; Avenarius, D.F. Whole body magnetic resonance imaging in healthy children and adolescents Bone marrow appearances of the appendicular skeleton. *Eur. J. Radiol.* **2022**, *153*, 110365. [[CrossRef](#)] [[PubMed](#)]
62. von Brandis, E.; Zadig, P.K.; Avenarius, D.F.M.; Flatø, B.; Knudsen, P.K.; Lilleby, V.; Nguyen, B.; Rosendahl, K.; Müller, L.S.O. Whole body magnetic resonance imaging in healthy children and adolescents. Bone marrow appearances of the axial skeleton. *Eur. J. Radiol.* **2022**, *154*, 110425. [[CrossRef](#)]

Disclaimer/Publisher's Note: The statements, opinions and data contained in all publications are solely those of the individual author(s) and contributor(s) and not of MDPI and/or the editor(s). MDPI and/or the editor(s) disclaim responsibility for any injury to people or property resulting from any ideas, methods, instructions or products referred to in the content.

Publikacja 2.

Whole - Body Magnetic Resonance Imaging in Rheumatology.

Chianca Vito, Michał Lanckoroński, Marco Curti, Majid Chalian, Iwona Sudoł-Szopińska, Chiara Giraud, Filippo Del Grande. Whole-Body Magnetic Resonance Imaging in Rheumatology.

Radiologic Clinics of North America, 2024;62:865-876.

S0033838924000216. <https://doi.org/10.1016/j.rcl.2024.02.008>

Whole-Body Magnetic Resonance Imaging in Rheumatology



Vito Chianca, MD^{a,*}, Michał Lanckoroński, MD^b, Marco Curti, MD^a,
Majid Chalian, MD^c, Iwona Sudol-Szopińska, MD^b,
Chiara Giraud, MD, PhD^d, Filippo Del Grande, MD^{a,e}

KEYWORDS

• Whole-body MRI • Bone • Muscles • Joint • Rheumatology

KEY POINTS

- Whole-body magnetic resonance imaging is an imaging tool that enables an optimal evaluation of soft tissue and bones.
- The main use of WB MRI in rheumatology is the evaluation of seronegative spondyloarthritis and inflammatory myopathies.
- Both 1.5 or 3.0 T scanners are eligible for imaging acquisition.
- Seronegative spondyloarthropathies are a group of diseases characterized by inflammatory arthritis with axial involvement.

INTRODUCTION

Whole-body magnetic resonance imaging (WB-MRI) is an imaging method that provides high spatial and contrast resolution images without ionizing radiation.^{1,2} Its first clinical applications were in assessing skeletal involvement in pathologic conditions such as lymphoma, myeloma, and solid tumor metastases.³ WB-MRI expanded its clinical applications after showing promising results compared with bone scintigraphy and PET allowing the evaluation of the multi-district involvement of inflammatory pathologies. As such, it is widely used in rheumatology for staging, follow-up, and clinical outcome evaluation. In particular, WB-MRI is able to provide information on inflammatory processes that are asymptomatic at the time of the investigation.

IMAGING TECHNIQUE

Recent technological advances have revolutionized the WB-MRI acquisition technique. In the past, the patients had to be repositioned during the acquisition because older-generation scanners could not acquire the whole body in a single scan and required coil exchange with increasing scan time. New scanner generations use multiple phased-array coils covering a field of view (FOV) of 15 to 40 cm along the longitudinal axis, allowing the acquisition of the whole body in a single session in a reasonable scan time. Head, neck, thoracic, abdominal, spine, and lower extremities coils are used simultaneously; only the upper limbs are not included in the acquisition and need a separate investigation if necessary.⁴ Both 1.5 T (T) or 3.0 T scanners are eligible for proper

^a Istituto di Imaging Della Svizzera Italiana (IIMSI), Ente Ospedaliero Cantonale (EOC), Via Tesserete 46, Lugano 6900 Switzerland; ^b Department of Radiology, National Institute of Geriatrics, Rheumatology and Rehabilitation, Spartanska 1 Street, Warsaw 02-637, Poland; ^c Division of Musculoskeletal Imaging and Intervention, Department of Radiology, University of Washington, Seattle, WA, USA; ^d Department of Cardiac, Thoracic, Vascular Sciences and Public Health – DCTV, University of Padova, Padova, Italy; ^e Facoltà di Scienze Biomediche, Università Della Svizzera Italiana, Via Buffi 13, Lugano 6900, Switzerland

* Corresponding author. Clinica di Radiologia, EOC Istituto di Imaging della, Svizzera Italiana (IIMSI), Via Tesserete 46, Lugano 6900, Switzerland.

E-mail address: vitochianca@gmail.com

acquisition. 1.5 T is preferable in children because it is reported to produce better images.⁵

Several protocols for WB-MRI acquisition are reported in the literature, and almost all can be completed within 45 minutes; most of them, including the recommended protocol by the Arthritis Subcommittee of the European Society of Musculoskeletal Radiology (ESSR), suggest the application of Short Tau Inversion Recovery (STIR) and T1w sequences only.⁶

T1w sequences are able to give anatomic information, and breath-hold acquisition is preferred for its quick acquisition time.⁷ STIR sequence provides the appropriate identification of bone or soft tissue acute inflammatory sites.⁸ However, the Dixon technique is increasingly used because of its homogeneous fat signal suppression over a large FOV.^{9,10} DWI sequences give qualitative and quantitative information (through the calculation of the ADC values) regarding the cellularity of the pathologic process¹¹ and are able to better evaluate the inflammatory areas. Moreover, a protocol that includes the DWI allows for exhaustive information without the injection of a contrast agent, which causes an increase in scanning times and could potentially lead to the pathologic accumulation of gadolinium in patients undergoing follow-up.^{12,13} Three b values can be recommended for an appropriate ADC quantification; in our institution, a b value of 50 s/mm², 400 s/mm², and 800 s/mm² were selected based on the optimal signal-to-noise ratio.

WHOLE-BODY MAGNETIC RESONANCE IMAGING: INDICATIONS IN RHEUMATOLOGY Spondyloarthropathies

Spondyloarthropathies (aca spondyloarthritis, spondyloarthritis, former name seronegative spondyloarthropathies) are a group of diseases characterized by inflammatory peripheral arthritis and enthesitis with axial involvement. They are commonly associated with extra-articular inflammatory findings of the skin, eyes, and gastrointestinal involvement.¹⁴ Ankylosing spondylitis (AS), psoriatic arthritis (PA), reactive arthritis (RA), and enteropathic arthropathies are included in this group.

Ankylosing spondylitis

AS is a chronic inflammatory autoimmune disease mainly affecting young adults linked with human leukocyte antigen (HLA)-27 and interleukin-23/17.¹⁵ The pathogenesis of AS has not been fully understood. AS typically affects the sacroiliac joints (SIJ) and the discovertebral junctions with the involvement of adjacent soft tissues, such as

tendons and ligaments. Other alterations can be located at peripheral joints and entheses.¹⁶ The main AS structural findings include bone sclerosis, erosions, SIJs, and spine ankylosis.¹⁷ These are findings assessable by radiographic examination in an advanced stage. MRI is able to evaluate early bone and soft tissue involvement, such as bone marrow edema (BME), in the preradiological stage of the disease. As such, it is possible to start new effective therapy (TNF-alpha inhibitors) in the early phase, limiting the evolution of the disease.¹⁸ The WB MRI allows visualization in a single examination of the inflammatory lesion of the SIJ, the entire spine, the shoulder girdles, the chest wall, hip joints, and the symphysis pubis.¹⁹ Subchondral BME at SIJ is the major diagnostic criterion for AS; the diagnosis requires the presence of BME on 2 consecutive MRI sections or 2 distinct BME areas in the same section. During the chronic stage of the disease, fatty infiltration replaces BME, followed by sclerosis, erosions, and ankylosis. It is important to note that adipose infiltration areas may also be present after an effective treatment, but in this case, erosions and sclerosis will not be present.²⁰ AS can involve the manubriosternal, sternoclavicular, and chondrosternal joints with BME and edema of the neighboring soft tissue.²¹

Extra-axial findings include synovitis, enthesitis, and dactylitis (mainly in patients with PsA, but not ideally seen on the WB-MRI), which are reported to affect about 77% of the patients.¹⁸

Juvenile Spondyloarthritis

According to the ESSG (European Spondyloarthropathy Study Group), JSpAs are a group of several pathologic conditions such as enthesitis-related arthritis (ERA), seronegative enthesopathy and arthropathy syndrome (SEA), juvenile psoriatic arthritis (JPAs), arthritis associated with inflammatory bowel diseases (IBD), and undifferentiated arthritis categories^{22,23} (Box 1). Musculoskeletal symptoms include nonsymmetric peripheral arthritis, mainly of the lower limbs, enthesitis, and axial skeleton involvement, which begins before 16 years old. Systemic inflammation can affect the eyes, bowels, skin, and, rarely, heart and lungs.²⁴ The mean age at diagnosis of these conditions is 9 to 11 years, with a male preponderance.²⁵ The radiographic evaluation of these alterations is complex due to the late onset of the radiographic findings and the not-always-reported symptoms by children. WB-MRI can demonstrate BME, synovitis, tenosynovitis, enthesitis, and bursitis (Fig. 1). Tarsal involvement is typical; hips, knees, and ankles are also frequently

Box 1

Juvenile spondyloarthropathies divided into differentiated and undifferentiated forms according to ESSG

Undifferentiated forms

Seronegative enthesopathy and arthritis syndrome (SEA)

Differentiated forms

Juvenile ankylosing spondylitis (JAS)

Reactive arthritis (formerly including Reiter's syndrome)

Arthritis associated with inflammatory bowel diseases (IBD) 4. Juvenile psoriatic arthritis (JPsA)

affected. Regarding enthesitis, the most commonly involved sites are the patella (inferior pole), calcaneal insertion of the plantar fascia, and Achilles tendon.²⁶ Axial involvement is less common at presentation compared with adult spondyloarthritis. It can be present after several years of disease and typically starts with the SIJ.²⁷ The higher the number of skeletal segments involved, the greater the possibility of developing sacroiliitis. MRI is an effective tool for monitoring both peripheral joint and progressive axial skeletal involvement.

Psoriatic Arthritis and Rheumatoid Arthritis

Psoriatic arthritis (PsA) and rheumatoid arthritis (RA) are chronic autoimmune inflammatory diseases affecting peripheral joints and the axial

skeleton. RA is the most common chronic autoimmune inflammatory disease affecting peripheral joints and the axial skeleton. RA is typically symmetrically distributed and characterized by the involvement of the small joints of the hands and feet. PsA is usually asymmetric and tends to involve axial and peripheral joints.²⁸ MR imaging is particularly useful in detecting synovitis and enthesitis in PsA and the cervical spine involvement in both entities. WB-MRI imaging is also helpful in monitoring inflammation changes during follow-up, playing a crucial role in the evaluation of treatment response. However, RA-related lesions in hands, wrists, feet, and ankles are sometimes indistinguishable without serology from PsA, which is the 1st subtype (symmetric polyarthritis).²⁹

Systemic Sclerosis

Systemic sclerosis (SSc; scleroderma) is one of the most severe systemic rheumatological diseases with the highest mortality rate.³⁰ SSc is an autoimmune disease characterized by intense inflammation and fibrosis of the skin, the subcutaneous tissue, the tendons, and the muscles with the potential involvement of internal organs such as the lungs, heart, esophagus, and kidney.³¹ The course of the disease is very variable and ranges from slow progression to aggressive and rapid evolution. WB-MRI shows the multifocal and often symmetric involvement of musculoskeletal structures; the most frequent findings are fascial and subcutaneous thickening/edema caused by inflammation, fascia or perifascial post-contrast enhancement, and articular synovitis with

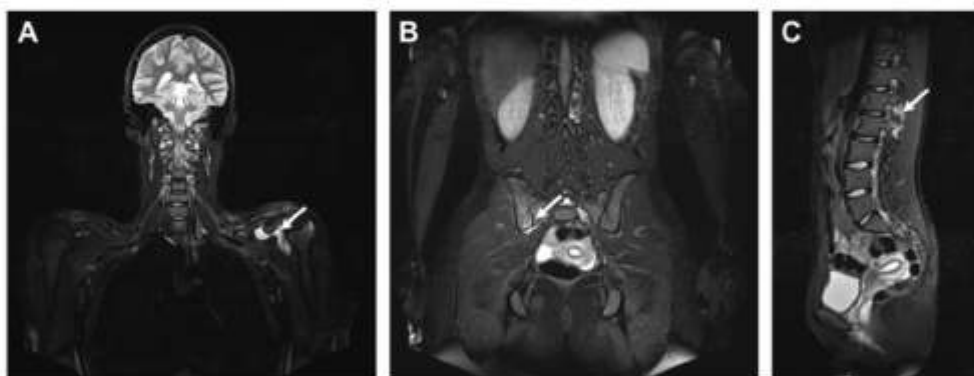


Fig. 1. Whole body MRI in a 17-year-old girl with juvenile idiopathic arthritis (JIA) enthesitis-related arthritis (ERA) subtype, HLA-B27 positive. T2 TIRM images in coronal (A and B) and sagittal (C) planes show synovitis in the left shoulder with some bone marrow edema in the proximal metaphysis of the humerus (A), right-sided sacroiliitis (B) and L1/2 left intervertebral joint synovitis with some bone marrow and soft tissue swelling of surrounding tissues.

BME. Intense muscle edema reflecting myositis is also present and mainly involves the proximal region of both the lower extremities.³² Symmetric high signal abnormality on fluid sensitive sequences is present in almost 50% of the patients and is directly correlated with the risk of organ involvement. In chronic stage fibrosis of the affected tissues is seen. Additionally, WB-MRI is helpful for the follow-up after immunosuppressive treatments.³³

Polymyalgia Rheumatica

Polymyalgia rheumatica (PR) is a chronic, inflammatory disease affecting patients generally more than the age of 50 years.³⁴ Patients with PR suffer from bilateral shoulder, hip, and thigh stiffness that are typically worse in the morning and improves during the day.³⁵ These nonspecific musculoskeletal symptoms may be associated with an elevation of serum inflammatory markers.³⁵ Prolonged glucocorticoid therapy is effective to reduce the multi-district inflammatory state. The main imaging findings of PR are subacromial-subdeltoid (SASD) bursitis, glenohumeral and hip joint effusion, peritendinitis, and capsular edema.³⁶ Furthermore, extracapsular inflammatory edema located near the acetabular space and the pubic symphysis are other common findings in patients with PR.³⁷ WB-MRI shows multiple joint inflammation and play a role in the evaluation of treatment response after glucocorticoid treatment.¹⁶

Idiopathic Inflammatory Myopathies

Idiopathic inflammatory myopathies (IIM) are rare heterogeneous autoimmune disorders characterized by proximal symmetric muscle weakness and nonsuppurative muscle inflammation, except for inclusion body myositis (IBM), which is usually characterized by distal and asymmetric muscle weakness. Extramuscular involvement such as interstitial lung pathology (ILP), cutaneous alterations in dermatomyositis (DM), and systemic or joint involvement with increased risk of malignancy in DM³⁸ are also present (Fig. 2).

Antisynthetase Syndrome

Antisynthetase syndrome (ASS) is an autoimmune disease characterized by autoantibodies against one of the many aminoacyl tRNA synthetases.³⁹ Its clinical findings are the following: interstitial lung disease, nonerosive arthritis, myositis, synovitis, tenosynovitis, and Raynaud's phenomenon.⁴⁰ Muscle involvement can present a hypotrophic or pseudohypertrophic pattern.⁴¹ While muscle biopsy is crucial for the diagnosis of other IIMs, there are no clinical indications about

the use of muscle biopsy for AAS diagnosis.⁴² WB MRI is useful for the evaluation of muscular and extramuscular involvement and for the evaluation of the extension of the disease. It is also helpful in the differential diagnosis of rheumatoid arthritis, especially in the initial stages of the disease.⁴³

Infective Myositis

Infective myositis (IM) is a group of myopathies caused by a wide range of infective agents (viral, bacterial, fungal, and parasitic),⁴⁴ secondary to a hematogenous spreading (mainly present in immunocompromised patients) or from a direct spreading after surgical procedures. Pyomyositis refers specifically to a bacterial infection of skeletal muscle. IM is characterized by an acute, subacute, or chronic manifestations causing pain, tenderness, swelling, and weakness.⁴⁴ WB-MRI may show muscle edema (Fig. 3) and fluid collections (incl. abscesses) with peripheral contrast enhancement. There may also be diffuse muscle enlargement.

MULTIFOCAL ASEPTIC MUSCULOSKELETAL DISORDERS

Synovitis, Acne, Pustulosis, Hyperostosis, and Osteitis Syndrome

Synovitis, acne, pustulosis, hyperostosis, and osteitis (SAPHO) syndrome (also known as Chronic Non-Bacterial Osteitis" (CNO) is characterized by a combination of musculoskeletal and cutaneous manifestations.⁴⁵ The preferred involved sites are the sternoclavicular, costosternal, and manubriosternal joints, followed by the lumbar and cervical spine.⁴⁶ There is no gender or age predominance.⁴⁷ Acute findings are edema with end-plate erosion at the medium/anterior part of the discovertebral junction, paravertebral soft tissue edema, and a height reduction of the intervertebral disk that may show enhancement after the intravenous administration of a gadolinium-based contrast agent.⁴⁸ Chronic findings are fatty infiltration, sclerosis, hypertrophy of the medial ends of the clavicles, sternum and upper ribs, and ultimately ankylosis. WB-MRI allows early diagnosis by the recognition of multifocal osteitis, also located in extra-axial bony segments, avoiding several complications such as kyphosis and flat vertebrae deformation (Fig. 4). Furthermore, WB MRI can be compared with bone scintigraphy, showing higher sensitivity in the recognition of juxta-physeal lesions.⁴⁹

Chronic Recurrent Multifocal Osteomyelitis

Chronic recurrent multifocal osteomyelitis (CRMO) or-postulated new name- chronic non-bacterial

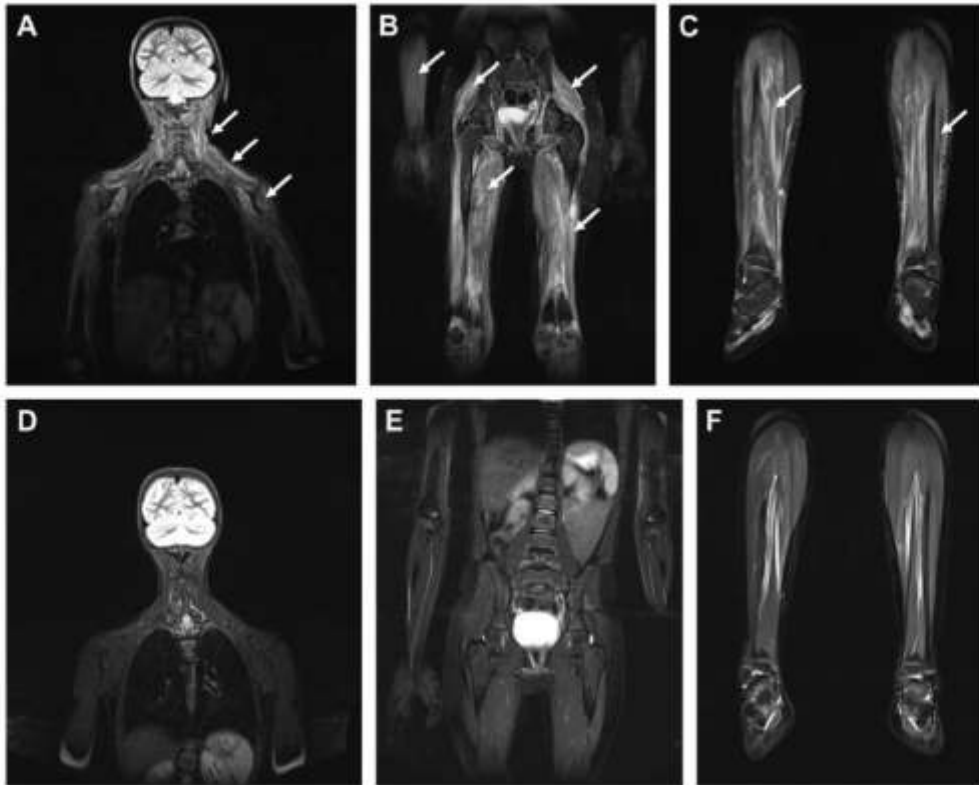


Fig. 2. Whole body MRI in an A 6-year-old girl with juvenile dermatomyositis. Coronal T2 TIRM images. Initial examination (A-C) shows multiple areas of increased signal in muscles of the neck, upper and lower girdle, forearms and crura; follow-up 8 months later (D-F) shows complete resolution of all lesions.

osteomyelitis (CNO), is an autoimmune inflammatory bone disorder mainly affecting adolescents and children.⁵⁰ Clinical findings include multifocal, frequently recurrent bone inflammation/osteomyelitis, which heals to lytic, sclerotic, or mixed lytic and sclerotic lesions. The metaphysis of long bones, the spine, and the shoulder girdle are the most involved sites.⁵¹

Inflammation of the surrounding peripheral nerves and vessels, bowel inflammation, and synovitis are additional symptoms.⁵¹ WB MRI has replaced bone scintigraphy due to its high sensitivity to assess multifocal bone and soft tissue involvement. MRI findings include BME, enhancement after the intravenous administration of gadolinium-based contrast, periosteal reaction, and extensive soft tissue edema (Fig. 5).

The most common sites of disease are the metaphyses or metaphyseal equivalents of the long bones, most frequently in the tibia, often in a symmetric distribution.⁵² Three patterns have been described with the use of whole-body MRI⁵³⁻⁵⁵.

- Multifocal pattern with tibial lesions, without clavicular involvement.
- Clavicular lesions with only a few spinal lesions without tibial involvement.
- Tibia-clavicular pattern in which there are both tibial and clavicular lesions.

Avascular Multifocal Osteonecrosis

Avascular multifocal osteonecrosis (AMO) is a rare pathologic condition, frequently occurs in patients from 20 to 50 years old, characterized by local bone necrosis that affects at least 3 or more separate anatomic sites concurrently or consecutively.⁵⁶ AMO may lead to severe secondary arthropathy if early diagnosis and treatment are missed, which is possible due to the asymptomatic course of the pathology in the early stages.⁵⁷ AMO can be secondary to several causes, including renal failure, hematological, oncological, or rheumatic diseases, such as lupus erythematosus. However, the main risk factor for AMO is high-

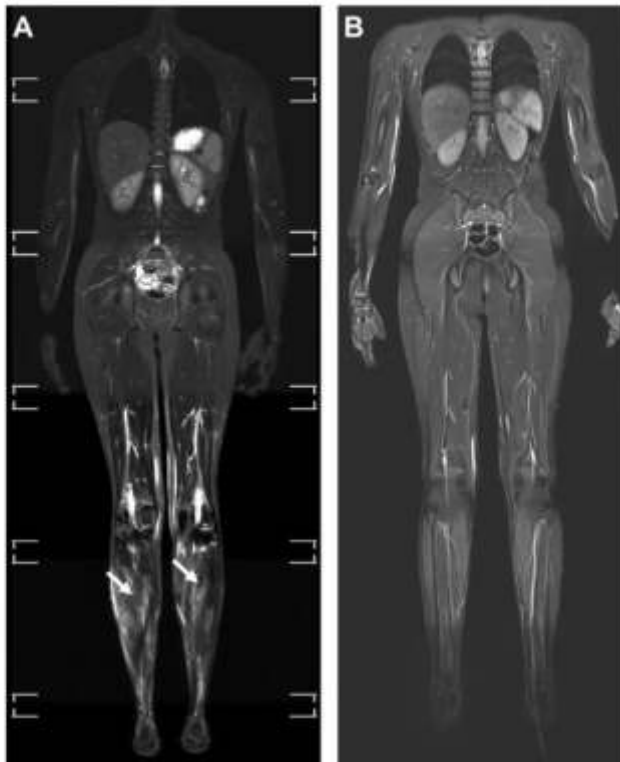


Fig. 3. WB MRI of a 15-year-old girl with benign acute childhood myositis due to Influenza B showing diffuse muscle edema in the calves on the coronal STIR (Arrows) in A. WB-MRI performed as follow-up 1 month later demonstrating a complete resolution of the muscle edema (coronal STIR in B).

dose corticosteroid treatments.⁵⁸ MRI is the gold standard for the diagnosis and follow-up of osteonecrosis, which appears as an ischemic lesion characterized by low intensity on T1-weighted images with a peripheral geographic rim of hyperintensity on T2-weighted images⁵⁹ between normal marrow and ischemic marrow. WB-MRI allows evaluating all potential sites of AMO to be evaluated in a single acquisition.⁶⁰

Sarcoidosis

Sarcoidosis is a multi-system inflammatory disease of unknown etiology characterized by multiple non-caseating granulomas. About 70% of cases involved patients between 25 and 40 years old, with a second peak of incidence in female patients more than 50 years old.⁶¹ Up to 90% of the patients show an intrathoracic involvement with a symmetric bilateral hilar adenopathy. 25% to 50% of the patients show extrathoracic findings such as skin granuloma, liver or splenic involvement, abdominal lymphadenopathy, and peripheral arthritis.⁶² A multisite involvement of the axial skeleton can be present, and it might be challenging to differentiate it from bone metastases. WB MRI provides

information regarding the extension and activity of the disease and allows the distinction between active lesions and inactive fatty lesions.

Langerhans Cell Histiocytosis

Langerhans cell histiocytosis (LCH) is a rare proliferative disorder characterized by the accumulation of Langerhans cells in several organs.⁶³ Although almost every organ could potentially be affected, in up to 80% of the patients, bone involvement is seen.⁶⁴ Splenomegaly with potential solid or cystic lesions, lung with centrilobular nodules or cysts,⁶⁴ lymph nodes, particularly at the neck,⁶⁵ and the central nervous system can be involved as well.

The MRI appearance of LCH lesions is nonspecific. Frequent findings are bone marrow replacement with BME, soft tissue edema, periosteal reaction, and endosteal scalloping in aggressive lesions.⁶⁶ These nonspecific findings mimic malignancy or infections, and a biopsy is mandatory.

Polyostotic Fibrous Dysplasia

Fibrous dysplasia (FD) is a genetic, noninheritable skeletal disorder in which pathologic bone

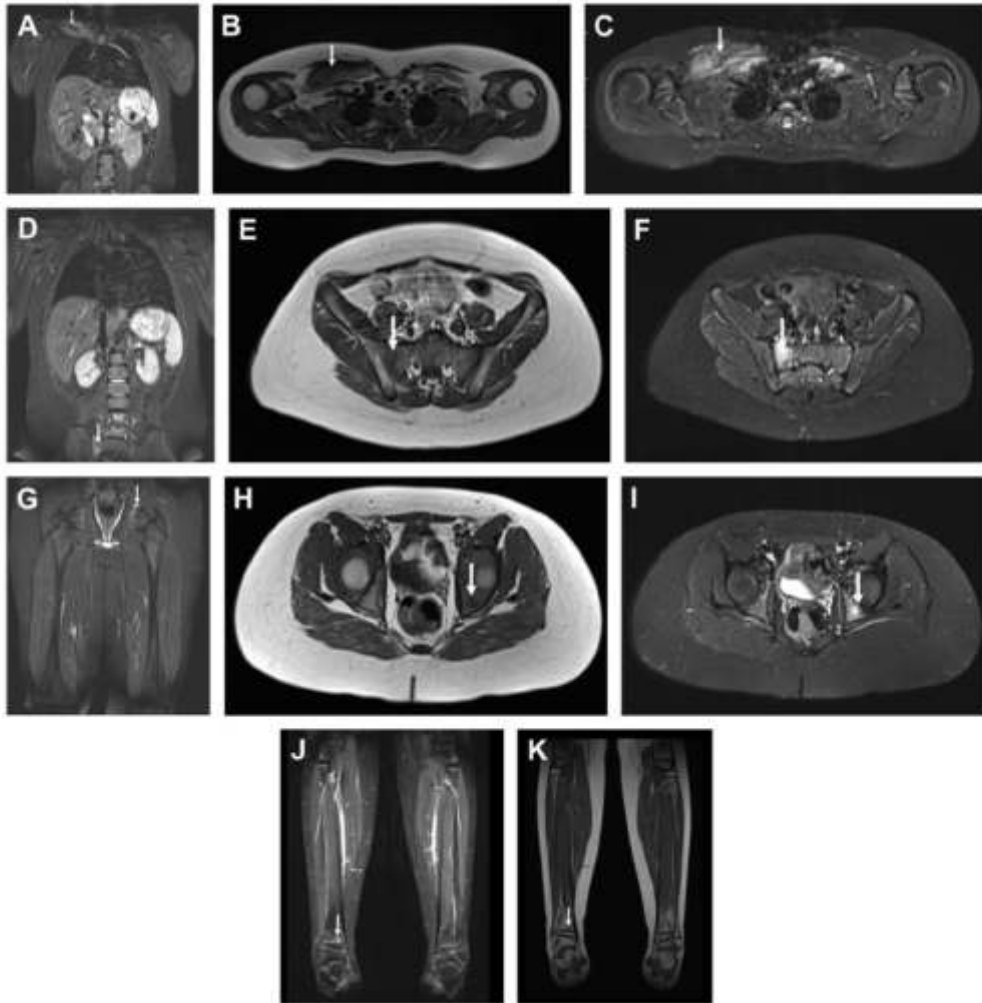


Fig. 4. WB MRI of an 11-year-old boy with SAPHO syndrome demonstrating the edema and periosteal reaction of the right clavicle (coronal short tau inversion recovery-STIR in A, axial T1weighted turbo spin echo-TSE in B and axial STIR in C), bone marrow edema in the right sacrum (coronal STIR in D, axial T1w TSE in E, and axial STIR in F), in the left acetabulum (coronal STIR in G, axial T1w TSE in H, and axial STIR in I), and in the distal metaphyseal area of the right tibia (coronal STIR in J and coronal T1w TSE in K).

architecture replaces normal bone.⁶⁷ Skeletal lesions often develop during the first decade of life⁶⁷; FD can involve only one bone (monostotic form, present in 70%–80% of patients) or multiple skeletal sites (polyostotic form present in 20%–30% of the patients) may be affected. The lesions are usually asymptomatic, but they can lead to pathologic fractures, deformities, compression, pain, and functional impairment. In patients with craniofacial FD presentation, facial bone asymmetry can lead to compression of the optic nerve, causing functional alteration. FD can be associated with several

syndromes, such as McCune-Albright syndrome (MAS) and Mazabraud's syndrome. MAS is characterized by the presence of FD, café-au-lait skin alterations, and precocious puberty.⁶⁸ Mazabraud syndrome is a rare disorder characterized by the presence of polyostotic FD with associated intramuscular myxomas.⁶⁹ The diagnosis of FD is generally based on radiography, but the WB MRI is helpful for the evaluation of the extension of the disease and for monitoring potential pathologic progression. WB MRI is also useful for the assessment of myxomas in the case of Mazabraud syndrome.

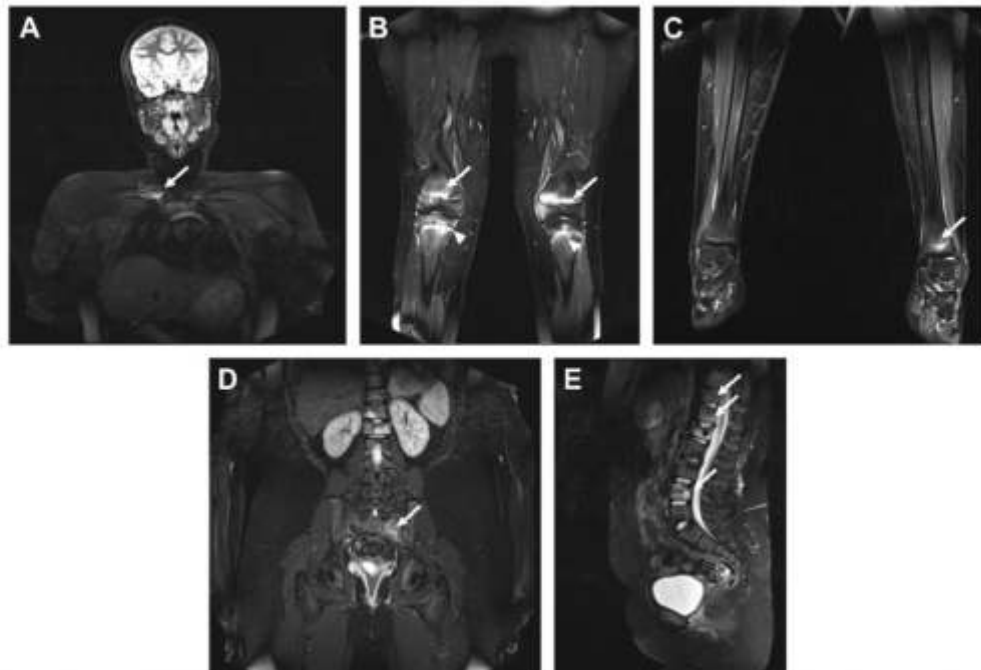


Fig. 5. Whole body MRI in a 12-year-old girl with chronic recurrent multifocal osteomyelitis (CRMO). T2 TIRM images show bone marrow oedema of the sternal end of the right clavicle with oedema of the surrounding tissues (A), bone marrow oedema of the distal femoral epiphysis, proximal tibial epiphysis, and to a minor extent in a knee joint epiphyses bilaterally (B), bone marrow edema in the left distal tibial epiphysis (C), left-sided sacroiliitis (D), and bone marrow oedema of several vertebral bodies of the thoracic and lumbar regions, with a fracture of the L1 vertebral body (E).

Muscle Evaluation

The pathologic involvement of the muscle characterizes many of the pathologies described above in our article. Muscles can undergo tropism and composition changes, which may include increased water (acute inflammatory phases) or fat molecules (chronic phases) content. Qualitative and quantitative methods are available for the WB assessment of the muscle.

- Dixon sequence based on the chemical-shift principle of different water and fat protons precession frequencies at a specific magnetic field strength.⁷⁰ Multi-echo Dixon techniques are able to quantify fat content through fat-fraction maps whereby the gray value of different pixels is directly linked with the fat infiltration.
- T2 mapping is an MRI sequence based on measuring T2 relaxation times in body tissues included in the selected region of interest (ROI). T₂ mapping in myopathies and dystrophies is not always easy to evaluate due to

the potential simultaneous presence of edema and fatty infiltration, both conditions that increase the T₂ values.⁷¹ Another limit is the absence of defined cut-offs in the literature, making the identification of diagnostic criteria based on its measurements difficult.

- Diffusion tensor imaging (DTI) is based on the concept of nonisotropic mobility of water molecules in human tissues due to the presence of cell membranes and sheaths of muscle fibers that restrict molecule diffusion.^{72,73} The integrity of the muscle fibers is measured by fractional anisotropy, which measures between 0 and 1. A value close to 0 will indicate a greater diffusion of the molecules due to the lesion of the muscle fibers. In contrast, a value tending to 1 will indicate the integrity of the fibers. In the case of fatty infiltration (more than 45% of the muscle belly), there is a paradoxical increase in the FA values of the selected ROI.⁷⁴⁻⁷⁶ Tractography is an application of DTI that allows the graphic evaluation of some muscle architecture findings such as pennation angle, curvature of fibers, and fiber length.⁷⁷ In

cases of fatty infiltration, tractography shows fibers that are decreased in number, length, and organization. DTI's disadvantages are the sequence's complexity and the need for high performance gradients. Another disadvantage is the long time of acquisition, reported in the literature of about 80 minutes, which is unsuitable for the study of patients with claustrophobic⁷⁸ or many patients with rheumatoid, including juveniles, suffering pain.

SUMMARY

Due to recent improvements in MRI techniques, WB-MRI is increasingly used for the detection and the follow up of rheumatic diseases and for target biopsy when needed. It is a unique imaging method that, through its large FOV, allows the detection of muscular, skeletal, abdominal, and thoracic findings. In the clinical practice WB MRI in rheumatology is mainly used for the evaluation of spondyloarthritis and for inflammatory myopathies. Furthermore, WB MRI is also used in the suspect of CRMO and SAPHO syndrome and for an accurate assessment of the extent of multifocal findings in the case of eosinophilic granuloma and sarcoidosis.

CLINICS CARE POINTS

- In the rheumatologic field, a protocol with the application of Short Tau Inversion Recovery (STIR) and T1w sequences only is recommended.
- In recent years, interest in the quantitative evaluation of pathologic findings has increased. T2 mapping, diffusion tensor imaging, and dixon sequences can be effective optional sequences.
- A whole-body MRI examination includes information regarding the head, neck, thoracic, abdominal, spine, and lower extremities; only the upper limbs usually need a separate investigation.

FUNDING

The authors declare that no funds, grants, or other support were received during the preparation of this article.

AUTHOR CONTRIBUTIONS

All authors contributed to the study conception. Material preparation and data collection were

performed by Vito Chianca, Michal Lanckoronsk, Iwona Sudol-Szopińska, and Chiara Giraudo. The first draft of the article was written by Vito Chianca. Marco Curti and Filippo Del Grande revised the article.

DISCLOSURE

The authors have no relevant financial or nonfinancial interests to disclose.

REFERENCES

1. Giraudo C, Lecouvet FE, Cotten A, et al. Whole-body magnetic resonance imaging in inflammatory diseases: Where are we now? Results of an International Survey by the European Society of Musculoskeletal Radiology. *Eur J Radiol* 2021;136. <https://doi.org/10.1016/j.ejrad.2021.109533>.
2. Summers P, Saia G, Colombo A, et al. Whole-body magnetic resonance imaging: Technique, guidelines and key applications. *Ecancermedicalscience* 2021; 15. <https://doi.org/10.3332/ECANCER.2021.1164>.
3. Pasoglou V, Michoux N, Larbi A, et al. Whole body MRI and oncology: Recent major advances. *Br J Radiol* 2018;91(1090). <https://doi.org/10.1259/bjr.20170664>.
4. Sudol-Szopińska I, Praćoń G. Diagnostyka obrazowa łuszczykowego zapalenia stawów. Część II: rezonans magnetyczny i ultrasonografia. *J Ultrason* 2016;16(65):163-74.
5. Mohan S, Moineddin R, Chavhan GB. Pediatric whole-body magnetic resonance imaging: Intra-individual comparison of technical quality, artifacts, and fixed structure visibility at 1.5 and 3 T. *Indian J Radiol Imaging* 2015;25(4):353-8.
6. Sudol-Szopińska I, Jurk AG, Eshed I, et al. Recommendations of the ESSR Arthritis Subcommittee for the Use of Magnetic Resonance Imaging in Musculoskeletal Rheumatic Diseases. *Semin Musculoskelet Radiol* 2015;19(4):396-411.
7. Morone M, Bail MA, Tunariu N, et al. Whole-body MRI: Current applications in oncology. *Am J Roentgenol* 2017;209(6):W336-49.
8. Panwar J, Patel H, Tolend M, et al. Toward Developing a Semiquantitative Whole Body-MRI Scoring for Juvenile Idiopathic Arthritis: Critical Appraisal of the State of the Art, Challenges, and Opportunities. *Acad Radiol* 2021;28(2):271-86.
9. Costelloe CM, Madewell JE, Kundra V, et al. Conspicuity of bone metastases on fast Dixon-based multi-sequence whole-body MRI: Clinical utility per sequence. *Magn Reson Imaging* 2013;31(5): 669-75.
10. Grande F Del, Santini F, Herzka DA, et al. Fat-suppression techniques for 3-T MR imaging of the musculoskeletal system. *Radiographics* 2014; 34(1):217-33.

11. Robba T, Chianca V, Albano D, et al. Diffusion-weighted imaging for the cellularity assessment and matrix characterization of soft tissue tumour. *Radiol Medica* 2017;122(11). <https://doi.org/10.1007/s11547-017-0787-x>.
12. Doniselli FM, Albano D, Chianca V, et al. Gadolinium accumulation after contrast-enhanced magnetic resonance imaging: what rheumatologists should know. *Clin Rheumatol* 2017;36(5):977–80.
13. Savarino E, Chianca V, Bodini G, et al. Gadolinium accumulation after contrast-enhanced magnetic resonance imaging: Which implications in patients with Crohn's disease? *Dig Liver Dis* 2017;49(7). <https://doi.org/10.1016/j.dld.2017.04.010>.
14. Duba AS, Mathew SD. The Seronegative Spondyloarthropathies. *Prim Care Clin Off Pract* 2018; 45(2):271–87.
15. Zhu W, He X, Cheng K, et al. Ankylosing spondylitis: etiology, pathogenesis, and treatments. *Bone Res* 2019;7(1). <https://doi.org/10.1038/s41413-019-0057-8>.
16. Barakat E, Kirchgessner T, Triqueneaux P, et al. Whole-Body Magnetic Resonance Imaging in Rheumatic and Systemic Diseases: From Emerging to Validated Indications. *Magn Reson Imaging Clin N Am* 2018;26(4):581–97.
17. Lecouvet FE, Michoux N, Toukap AN, et al. The Increasing Spectrum of Indications of Whole-Body MRI beyond Oncology: Imaging Answers to Clinical Needs. *Semin Musculoskelet Radiol* 2015;19(4): 348–62.
18. Althoff CE, Seper J, Song IH, et al. Active inflammation and structural change in early active axial spondyloarthritis as detected by whole-body MRI. *Ann Rheum Dis* 2013;72(6):967–73.
19. Weber U, Pfirmann CWA, Kissling RO, et al. Whole body MR imaging in ankylosing spondylitis: A descriptive pilot study in patients with suspected early and active confirmed ankylosing spondylitis. *BMC Musculoskelet Disord* 2007;8:20.
20. Van Onna M, Van Tubergen A, Van Der Heijde DM, et al. Bone marrow edema on Magnetic Resonance Imaging (MRI) of the sacroiliac joints is associated with development of fatty lesions on MRI over a 1-year interval in patients with early inflammatory low back pain: A 2-year followup study. *J Rheumatol* 2014;41(6):1088–94.
21. Weber U, Lambert RGW, Rufibach K, et al. Anterior chest wall inflammation by whole-body magnetic resonance imaging in patients with spondyloarthritis: Lack of association between clinical and imaging findings in a cross-sectional study. *Arthritis Res Ther* 2012;14(1):R3.
22. Suddi-Szopińska I, Znajdek M, Gietka P, et al. Imaging of juvenile spondyloarthritis. Part II: Ultrasonography and magnetic resonance imaging. *J Ultrason* 2017;17(70):176–81.
23. Srinivasalu H, Sikora KA, Colbert RA. Recent Updates in Juvenile Spondyloarthritis. *Rheum Dis Clin North Am* 2021;47(4):565–83.
24. Burgos-Vargas R, Pacheco-Tena C, Vázquez-Mellado J. The juvenile-onset spondyloarthritis: Rationale for clinical evaluation. *Best Pract Res Clin Rheumatol* 2002;16(4):551–72.
25. Rumsey DG, Lougee A, Matsouka R, et al. Juvenile Spondyloarthritis in the Childhood Arthritis and Rheumatology Research Alliance Registry: High Biologic Use, Low Prevalence of HLA-B27, and Equal Sex Representation in Sacroiliitis. *Arthritis Care Res* 2021;73(7):940–6.
26. Aquino MR, Tse SML, Gupta S, et al. Whole-body MRI of juvenile spondyloarthritis: protocols and pictorial review of characteristic patterns. *Pediatr Radiol* 2015;45(5):754–62.
27. Pagnini I, Savelli S, Matucci-Cerinic M, et al. Early predictors of juvenile sacroiliitis in enthesitis-related arthritis. *J Rheumatol* 2010;37(11):2395–401.
28. Poulsen AEF, Axelsen MB, Poggendorf RP, et al. Whole-body magnetic resonance imaging in psoriatic arthritis, rheumatoid arthritis, and healthy controls: Interscan, intrareader, and interreader agreement and distribution of lesions. *J Rheumatol* 2021;48(2):198–216.
29. Żelnio E, Taljanovic M, Mańczak M, et al. Hand and Wrist Involvement in Seropositive Rheumatoid Arthritis, Seronegative Rheumatoid Arthritis, and Psoriatic Arthritis—The Value of Classic Radiography. *J Clin Med* 2023;12(7):2622.
30. Elhal M, Meune C, Boubaya M, et al. Mapping and predicting mortality from systemic sclerosis. *Ann Rheum Dis* 2017;76(11):1897–905.
31. Volkmann ER, Andréasson K, Smith V. Systemic sclerosis. *Lancet* 2023;401(10373):304–18.
32. Schanz S, Henes J, Ulmer A, et al. Magnetic resonance imaging findings in patients with systemic scleroderma and musculoskeletal symptoms. *Eur Radiol* 2013;23(1):212–21.
33. Schanz S, Henes J, Ulmer A, et al. Response evaluation of musculoskeletal involvement in patients with deep morphea treated with methotrexate and prednisolone: A combined MRI and clinical approach. *Am J Roentgenol* 2013;200(4). <https://doi.org/10.2214/AJR.12.9335>.
34. Kernani TA, Warrington KJ. Polymyalgia rheumatica. *Lancet* 2013;381:63–72.
35. Mahmood S Bin, Nelson E, Padniewski J, et al. Polymyalgia rheumatica: An updated review. *Cleve Clin J Med* 2020;87(9):549–56.
36. Leão RV, Calich ALG, Calich I, et al. Magnetic resonance imaging findings in patients with polymyalgia rheumatica. *Radiol Bras* 2022;55(6):346–52.
37. Mackie SL, Pease CT, Fukuba E, et al. Whole-body MRI of patients with polymyalgia rheumatica identifies a distinct subset with complete patient-

- reported response to glucocorticoids. *Ann Rheum Dis* 2015;74(12):2188–92.
38. Dimachkie MM, Barohn RJ, Amato AA. Idiopathic inflammatory myopathies. *Neurol Clin* 2014;32(3):595–628.
 39. Witt LJ, Curran JJ, Streck ME. The diagnosis and treatment of antisynthetase syndrome. *Clin Pulm Med* 2016;23(5):218–26.
 40. Connors GR, Christopher-Stine L, Oddis CV, et al. Interstitial lung disease associated with the idiopathic inflammatory myopathies: What progress has been made in the past 35 years? *Chest* 2010;138(6):1464–74.
 41. Deplano L, Piga M, Porcu M, et al. Whole-Body MRI in Rheumatology: Major Advances and Future Perspectives. *Diagnostics* 2021;11(10):1770.
 42. Dalakas MC. Muscle biopsy findings in inflammatory myopathies. *Rheum Dis Clin North Am* 2002;28(4):779–98.
 43. Cantwell C, Ryan M, O'Connell M, et al. A comparison of inflammatory myopathies at whole-body turbo STIR MRI. *Clin Radiol* 2005;60(2):261–7.
 44. Narayanappa G, Nandeesh BN. Infective myositis. *Brain Pathol* 2021;31(3). <https://doi.org/10.1111/bpa.12950>.
 45. Laredo JD, Vuillemin-Bodaghi V, Boutry N, et al. SAPHO syndrome: MR appearance of vertebral involvement. *Radiology* 2007;242(3):825–31.
 46. Takigawa T, Tanaka M, Nakahara S, et al. SAPHO syndrome with rapidly progressing destructive spondylitis: Two cases treated surgically. *Eur Spine J* 2008;17(SUPPL.2). <https://doi.org/10.1007/s00586-008-0663-4>.
 47. Chianca V, Chalian M, Harder D, et al. Imaging of Spine Infections. *Semin Musculoskelet Radiol* 2022;26(4):387–95.
 48. Nachigal A, Cardinal E, Bureau NJ, et al. Vertebral involvement in SAPHO syndrome: MRI findings. *Skeletal Radiol* 1999;28(3):163–8.
 49. Falip C, Alison M, Boutry N, et al. Chronic recurrent multifocal osteomyelitis (CRMO): A longitudinal case series review. *Pediatr Radiol* 2013;43(3):355–75.
 50. Hofmann SR, Kapplusch F, Girschick HJ, et al. Chronic Recurrent Multifocal Osteomyelitis (CRMO): Presentation, Pathogenesis, and Treatment. *Curr Osteoporos Rep* 2017;15(6):542–54.
 51. Schnabel A, Range U, Hahn G, et al. Unexpectedly high incidences of chronic non-bacterial as compared to bacterial osteomyelitis in children. *Rheumatol Int* 2016;36(12):1737–45.
 52. Iyer RS, Thapa MM, Chew FS. Chronic recurrent multifocal osteomyelitis: Review. *Am J Roentgenol* 2011;196(6 SUPPL). <https://doi.org/10.2214/AJR.09.7212>.
 53. Sergi CM, Miller E, Demellawy D El, et al. Chronic recurrent multifocal osteomyelitis. A narrative and pictorial review. *Front Immunol* 2022;13. <https://doi.org/10.3389/fimmu.2022.959675>.
 54. Himuro H, Kurata S, Nagata S, et al. Imaging features in patients with SAPHO/CRMO: a pictorial review. *Jpn J Radiol* 2020;38(7):622–9.
 55. Andronkou S, Mendes da Costa T, Hussien M, et al. Radiological diagnosis of chronic recurrent multifocal osteomyelitis using whole-body MRI-based lesion distribution patterns. *Clin Radiol* 2019;74(9):737.e3.
 56. Sun W, Shi Z, Gao F, et al. The pathogenesis of multifocal osteonecrosis. *Sci Rep* 2016;6. <https://doi.org/10.1038/srep29576>.
 57. Kaste SC, Pei D, Cheng C, et al. Utility of early screening magnetic resonance imaging for extensive hip osteonecrosis in pediatric patients treated with glucocorticoids. *J Clin Oncol* 2015;33(6):610–5.
 58. Flouzat-Lachaniette CH, Roussignol X, Poinard A, et al. Multifocal Joint Osteonecrosis in Sickle Cell Disease. *Open Orthop J* 2009;3(1):32–5.
 59. Fordyce MJF, Solomon L. Early detection of avascular necrosis of the femoral head by MRI. *J Bone Jt Surg - Ser B*. 1993;75(3):365–7.
 60. Yokota S, Sakamoto K, Shimizu Y, et al. Evaluation of whole-body modalities for diagnosis of multifocal osteonecrosis—a pilot study. *Arthritis Res Ther* 2021;23(1):1–7.
 61. Hunninghake GW, Costabel U, Ando M, et al. Statement on sarcoidosis. *Am J Respir Crit Care Med* 1999;160(2):736–55.
 62. Sève P, Pacheco Y, Durupt F, et al. Sarcoidosis: A clinical overview from symptoms to diagnosis. *Cells* 2021;10(4). <https://doi.org/10.3390/cells10040766>.
 63. Kobayashi M, Tojo A. Langerhans cell histiocytosis in adults: Advances in pathophysiology and treatment. *Cancer Sci* 2018;109(12):3707–13.
 64. Zaveri J, La O, Yarnish G, et al. More than just langerhans cell histiocytosis: A radiologic review of histiocytic disorders. *Radiographics* 2014;34(7):2008–24.
 65. Badalian-Very G, Vergillo JA, Fleming M, et al. Pathogenesis of langerhans cell histiocytosis. *Annu Rev Pathol Mech Dis* 2013;8:1–20.
 66. Samet J, Weinstein J, Fayad LM. MRI and clinical features of Langerhans cell histiocytosis (LCH) in the pelvis and extremities: can LCH really look like anything? *Skeletal Radiol* 2016;45(5):607–13.
 67. Utraiainen P, Valta H, Björnsdóttir S, et al. Polyostotic fibrous dysplasia with and without McCune-Albright syndrome-clinical features in a Nordic Pediatric cohort. *Front Endocrinol* 2018;9(MAR):336764.
 68. Dumitrescu CE, Collins MT. McCune-Albright syndrome. *Orphanet J Rare Dis* 2008;3(1):1–12.
 69. Major BCJ, Van De Sande MAJ, Appelman-Dijkstra NM, et al. Prevalence and clinical features of mazabraud syndrome: A multicenter european study. *J Bone Jt Surg - Am* 2019;101(2):160–8.
 70. Huber FA, Del Grande F, Rizzo S, et al. MRI in the assessment of adipose tissues and muscle

- composition: how to use it. *Quant Imaging Med Surg* 2020;10(8):1636649.
71. De Mello R, Ma Y, Ji Y, et al. Quantitative MRI musculoskeletal techniques: An update. *Am J Roentgenol* 2019;213(3):524–33.
 72. Chianca V, Albano D, Rizzo S, et al. Inter-vendor and inter-observer reliability of diffusion tensor imaging in the musculoskeletal system: a multiscanner MR study. *Insights into Imaging* 2023;14(1):1–9.
 73. Chianca V, Albano D, Messina C, et al. Diffusion tensor imaging in the musculoskeletal and peripheral nerve systems: from experimental to clinical applications. *Eur Radiol Exp* 2017;1(1):12.
 74. Chianca V, Vincenzo B, Cuocolo R, et al. MRI Quantitative Evaluation of Muscle Fatty Infiltration. *Magnetochemistry* 2023;9(4):111.
 75. Giraudo C, Motyka S, Weber M, et al. Weighted Mean of Signal Intensity for Unbiased Fiber Tracking of Skeletal Muscles: Development of a New Method and Comparison with Other Correction Techniques. *Invest Radiol* 2017;52(8):488–97.
 76. Giraudo C, Motyka S, Weber M, et al. Diffusion Tensor Imaging of Healthy Skeletal Muscles: A Comparison between 7 T and 3 T. *Invest Radiol* 2019;54(1):48–54.
 77. Barp A, Carraro E, Albamonte E, et al. Muscle MRI in two SMA patients on nusinersen treatment: A two years follow-up. *J Neurol Sci* 2020;417:117067.
 78. Kenkel D, Von Spiczak J, Wurnig MC, et al. Whole-body diffusion tensor imaging: A feasibility study. *J Comput Assist Tomogr* 2016;40(1):183–8.

Publikacja nr 3.

Update on MRI in rheumatic diseases.

Sudoł-Szopińska Iwona, Michał Lanckoroński, Torsten Diekhoff, Damjana Ključevšek, Filippo Del Grande, Andrea Doria.

Radiologic Clinics of North America, 2024;62:821-836.

S003383892400040X. <https://doi.org/10.1016/j.rcl.2024.03.003>

Update on MRI in Rheumatic Diseases



Iwona Sudol-Szopińska, MD, PhD^{a,*}, Michał Lanckoroński, MD^a, Torsten Diekhoff, MD^b, Damjana Ključevšek, MD, PhD^c, Filippo Del Grande, MD, MBA, MHEM^d, Andrea Doria, MD, PhD, MSc, MBA^{e,f}

KEYWORDS

• MRI • Whole body-MRI • Advances • Arthritis • Spondyloarthritis • Juvenile idiopathic arthritis • Contrast

KEY POINTS

- MRI is the modality of choice to evaluate the axial and peripheral skeleton concerning disease activity and treatment response.
- MRI is critical in early diagnosis of axial spondyloarthritis as it surpasses radiography in sensitivity to detect active inflammation and structural lesions.
- MRI, despite its low specificity, has high sensitivity in detecting peripheral inflammation, such as synovitis, tenosynovitis, bursitis, enthesitis, and osteitis.
- MRI, including whole body-MRI, proves to be the gold standard for detecting bone marrow edema, offering an accurate semi-quantitative assessment of the total inflammatory joint burden.
- MRI is an important biomarker and outcome measure of arthritis burden, treatment response or failure, and subsequent joint damage progression.

INTRODUCTION

Imaging is crucial in the evaluation of rheumatic diseases, aiding in complementing clinical examinations, corroborating or refuting diagnoses, revealing alternate symptom etiologies, determining disease activity, assessing chronic structural changes, gauging disease burden, assessing treatment efficacy, and identifying potential complications from the disease or treatment. To this end, MRI has become a key instrument for assessment of both the axial and peripheral skeletons, with its scope and utility being consistently broadening over recent years.

MRI harnesses potent magnetic fields and electromagnetic waves to acquire signals from the

patient's body, typically generated within protons found abundantly in soft tissues, fat, and water. These characteristics provide a uniquely accurate appraisal of muscles, synovium, and bone marrow while offering limited signal from cortical and trabecular bone. Hence, MRI outperforms radiography and computed tomography (CT) in detecting active inflammatory changes. While signal intensities depend on the patient's body, field strengths, and pulse sequences, making MRI inherently a non-quantitative imaging modality, contemporary techniques can assess quantitative parameters such as diffusion-weighted imaging (DWI), dynamic contrast enhancement, or mapping techniques.

^a Department of Radiology, National Institute of Geriatrics, Rheumatology and Rehabilitation, Warsaw, Poland; ^b Department of Radiology, Charité - Universitätsmedizin Berlin, Campus Mitte, Humboldt-Universität zu Berlin, Freie Universität Berlin, Berlin, Germany; ^c Department of Radiology, University Children's Hospital Ljubljana, Slovenia; ^d Clinica di Radiologia EOC, Istituto di Imaging della Svizzera Italiana (IIMS), Ente Ospedaliero Cantonale (EOC), Ospedale Civico via Tesserete 47, Lugano-Ti 6900, Switzerland; ^e Department of Diagnostic Imaging, Research Institute, The Hospital for Sick Children; ^f Department of Medical Imaging, University of Toronto, Toronto, Canada

* Corresponding author.

E-mail address: sudolszopinska@gmail.com

Radiol Clin N Am 62 (2024) 821–836
<https://doi.org/10.1016/j.rcl.2024.03.003>
0033-8389/24/© 2024 Elsevier Inc. All rights reserved.



Fig. 1. MR image of a 40-year-old male patient with suspected rheumatoid arthritis. The MR image and computed tomography (CT) scan show a pseudoerosion in the lunate. In susceptibility-weighted imaging, the lesion is more clearly outlined, and with inversion, the image has a similar contrast as compared to CT.

Although ultrasound is examiner-dependent and time-consuming, its easy integration into the rheumatologist's workflow and excellent spatial resolution and sensitivity to active inflammatory lesions offer it a competitive advantage. Conversely, MRI is time-consuming, positions the patient uncomfortably, and depends on contrast media administration for reliable soft-tissue inflammation detection. Addressing the latter issue, some research groups propose that unenhanced high-resolution sequences could suffice for patient follow-up with established diagnoses.²⁷ Dixon sequences may also reduce scan time.²⁸ Others use double-inversion recovery sequences to saturate fat and effusion, leaving synovitis as the only bright structure and differentiating effusion from synovitis in unenhanced images, rendering gadolinium application unnecessary.²⁹

Conversely, contrast enhancement provides additional synovial microenvironment information when assessed over time.^{30,31} DCE MRI detects soft-tissue or bone inflammation and characterizes inflammation according to enhancement-patterns and relative enhancement measurements. Further processing with fractal analysis might yield insights into neoangiogenesis and other pathophysiological processes in rheumatoid arthritis (RA) (Fig. 3).³²

While less critical for primary diagnosis compared to axSpA, structural lesions of the peripheral skeleton carry significant prognostic weight and

support an inflammatory disease diagnosis when present. Similar to the axial skeleton, special magnetic resonance (MR) sequences display the cortical bone and enable a more accurate joint erosion assessment.³³ Moreover, degeneration and loss of joint cartilage have been investigated. Researchers found that delayed gadolinium-enhanced MRI of cartilage can reveal patterns of cartilage microenvironment changes.³⁴ Similar results were obtained using quantitative T2-mapping methods and glycosaminoglycan chemical exchange saturation transfer imaging and sodium-sensitive MRI.³⁵ However, the latter require specialized equipment, such as ultra-high-field machines and specific coils.

In addition to peripheral joints, RA also affects the axial skeleton, particularly the cervical spine. Chronic ligament damage can cause C1/C2 level instability, posing a risk to the myelon. Those instabilities are a dynamic phenomenon that cannot be assessed by conventional MRI. Nonetheless, DWI has shown promise to identify early changes of myelon at this level in cases of atlanto-axial subluxation in RA.³⁶

Other Peripheral Joint Disease

The differentiation between various inflammatory conditions using MRI can be a challenge, particularly when it comes to distinguishing RA from other ailments such as psoriatic arthritis.³⁷ Advanced AI

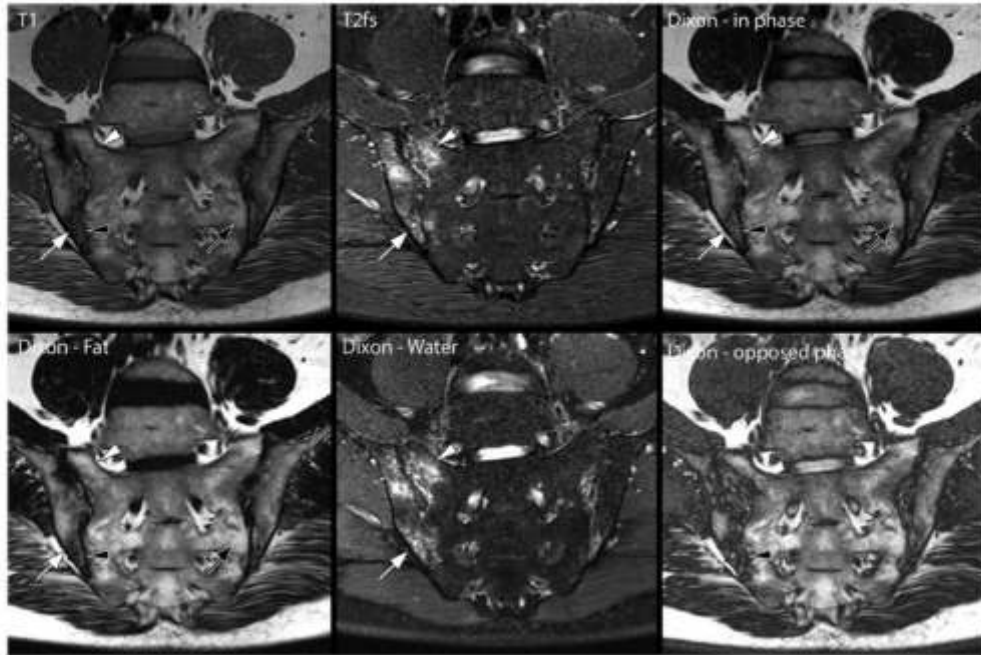


Fig. 2. MR image of the sacroiliac joints of a 45-year-old patient with advanced axial spondyloarthritis. One single T2-Dixon sequence with 4 contrasts (in-phase, opposed-phase, and fat and water image) is compared to standard T1 and T2 fat saturation (fs). Bone marrow edema (white arrow, high signal intensity in T2 fs, in-phase and water image, low signal in T1 and fat image) can clearly be differentiated from fat lesions (black arrow, high signal in T1, in-phase, and fat image). Edema within a fat lesion is also visible (white arrowhead). Dixon opposed phase can help detecting erosions (black arrowhead).

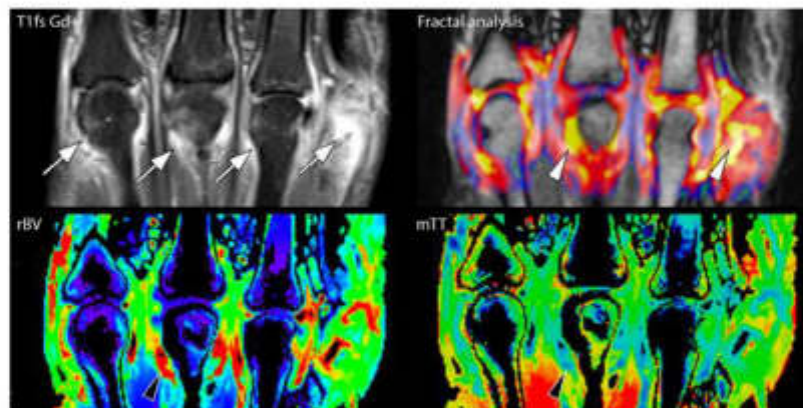


Fig. 3. Dynamic contrast-enhanced MR imaging of the hand. A 56-year-old male patient presenting with hand and finger arthritis due to late-onset rheumatoid arthritis. The synovium of all metacarpophalangeal joints is enhanced after contrast administration (arrows). Fractal analysis shows neoangiogenesis in heavily inflamed tissues (white arrowheads). In the perfusion analysis, the relative blood volume is increased while the mean transit time is decreased in synovitis.

approaches achieve only moderate accuracy when differentiating rheumatoid arthritis and psoriatic arthritis (area under the curve [AUC] of 75%).³⁸ Although MRI has a low specificity in this regard, its sensitivity in detecting peripheral inflammation such as synovitis, tenosynovitis, bursitis, and enthesitis is substantial, as shown in Fig. 4. For conditions such as psoriatic arthritis, the detection of enthesitis (inflammation at the sites where tendons or ligaments insert into the bone) is paramount. Here, MRI proves to be the gold standard for detecting bone marrow edema, offering sensitive and semi-quantitative assessment.^{39,40} Of note, crystal arthropathies (eg, gouty arthritis, calcium pyrophosphate, or hydroxyapatite deposition disease) may not be easily discernible through MRI and may mimic other inflammatory conditions.⁴¹ However, recent advancements in imaging techniques, such as special sequences or ultra-high-field MRI, show promise in the detection of small calcifications.⁴²

Other Clinical Applications

In cases of polymyalgia rheumatica, MRI is particularly helpful in visualizing inflammation around the shoulder, such as in the subacromial bursa.⁴³ It also helps in revealing distinctive patterns of extracapsular inflammation in areas like the pelvic and hand regions.^{44,45} Compared to ultrasound, MRI is advantageous for assessing complex anatomic sites, especially within the axial skeleton.⁴⁶ Advancements in black-blood sequences offer a unique approach to image large vessel vasculitis, allowing selective assessment of the vessel wall without the distraction of contrast media.^{47,48} This has been used in various regions, including thoracic, abdominal, and intracranial vessels. Moreover, ultra-short echo-time MRI provides high-resolution images of the lung for assessing lung structure and function, offering a radiation-free option for lung disease depiction.⁴⁹⁻⁵¹ Innovations are also being made in lung

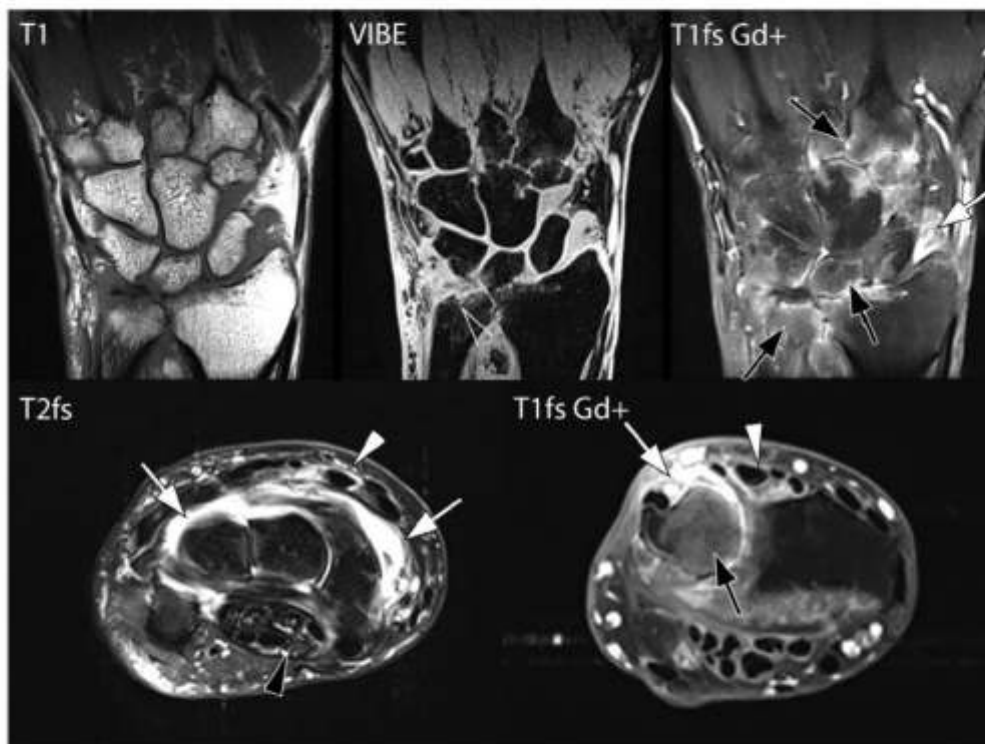


Fig. 4. Wrist MR image of a 49-year-old man with dermatomyositis complicated by septic inflammation on immunosuppressive therapy. The images show active inflammatory changes: wrist joints with synovitis (white arrow), osteitis (black arrow), minor tenosynovitis in several compartments of extensor and flexor tendons (white arrowheads), and tendinopathy of deep flexor muscle of the fingers in the carpal tunnel (black arrowhead). Osteolytic lesions with cartilage loss of numerous bones are best appreciated on a volumetric interpolated breath-hold examination sequence.

perfusion and special contrast agents to visualize specific biomarkers for particular diseases.^{52,53}

Whole Body-MRI in Adults

Whole body-MRI (WB-MRI) presents a powerful tool for systemic diseases, allowing for an all-encompassing view of potential inflammation even in areas that may not be clinically symptomatic. WB-MRI has proven effective in detecting unnoticed inflammation⁵⁴ and assessing treatment response.⁵⁵ It has shown potential for a global assessment of structural and active inflammatory lesions, and reliability in patients with conditions like psoriatic arthritis⁵⁶ and rheumatoid arthritis.⁵⁷ The utility of WB-MRI has also been demonstrated in assessing treatment responses and relapses in patients with synovitis, acne, pustulosis, hyperostosis, and osteitis syndrome.⁵⁸

Beyond joint inflammation, WB-MRI serves to identify early muscle inflammation and guide muscle biopsy locations, as shown in Fig. 5.⁵⁹ It can comprehensively evaluate treatment responses,⁶⁰ although standardizing WB-MRI and performing it within a reasonable timeframe remains challenging, especially for patients with joint diseases and pain. However, the Outcome Measures in Rheumatology Clinical Trials (OMERACT) has introduced protocol recommendations and pathology definitions for joint diseases to further foster the technique.^{61,62} This underscores the importance of balancing image quality, number of different sequences, and scan time, recognizing that information about individual joints will always be more limited compared to focused MRI.

UPDATE IN MRI OF JUVENILE RHEUMATIC DISEASES

MRI is a valuable technique for the assessment of pediatric musculoskeletal pathologies and is the most validated technique.⁶³ It is the most suitable technique for detecting synovial hypertrophy and other features of rheumatic diseases, such as tenosynovitis, enthesitis, bursitis, myositis, inflammatory cysts, and erosions, and it is the only technique that can visualize BME (osteitis).⁶⁴⁻⁶⁶ MRI has the advantages of allowing the three-dimensional (3D) evaluation of the peripheral and axial joints and is especially valuable in the evaluation of the complex or deep-seated joints.⁶⁷

Considerable improvements to the MRI diagnosis of both peripheral and axial arthritis in pediatric rheumatology have been achieved over the recent years. This update will address these latest advancements in the peripheral and axial skeleton along with implementation of the WB-MRI technique for screening of inflammation. The authors



Fig. 5. Whole body (WB) MR image of a 56-year-old woman with scleromyositis, T2 turbo inversion recovery magnitude (TIRM) images with majority of the muscle high signal representing myositis. Superficial soft tissue swelling of the lower extremities, likely representing skin and subdermis inflammation (arrows).

also discuss post-contrast MR assessment of joints in children.

Juvenile Idiopathic Arthritis

Juvenile idiopathic arthritis (JIA) is the most common chronic arthropathy in the pediatric population.⁶⁷ Although MRI has become an important tool for diagnostic joint assessment, its utilization is challenging in the pediatric population given the need for discrimination between pathologic and physiologic changes in the growing skeleton.⁶⁷ Recently published papers on non-specific high-signal bone marrow changes on T2-weighted fat-suppressed images in the axial and appendicular skeleton commonly found in healthy, asymptomatic children on WB-MRI make their interpretation more challenging, particularly in the assessment

of clinically silent lesions in children with suspected multifocal skeletal disease.^{68,69} Several multicentric multidisciplinary organizations have made major efforts over the past decades to standardize, quantify, and validate scoring systems to measure joint changes both cross-sectionally and longitudinally according to rigorous methodological standards.⁶⁷ Recently updated recommendations by the ESSR and the European Society of Pediatric Radiology musculoskeletal imaging taskforce include the current indications to perform MRI for diagnosis, monitoring, and prediction, along with MRI protocols for the most commonly involved joints in JIA.⁶³ For monitoring disease course and treatment efficacy, semiquantitative grading systems have been devised to quantify the degree of inflammation and osteochondral changes in the large and small joints of JIA patients.⁶⁷

Peripheral Joints

The knee is the most commonly affected joint in JIA, followed by the hand and wrist.⁶⁶ Over the past decade, a dedicated MRI scoring system for assessment of the knee (Juvenile Arthritis MRI Scoring; JAMRIS) has been developed and validated by the OMERACT MRI in JIA group.^{70,71} Recommendations for the MRI protocol of the wrist in JIA patients were published by the Health-e-Child project and OMERACT MRI in JIA group.⁷²

Hip is affected in approximately 20% to 50% of patients with JIA and is considered a predictor of severe disease and disability, **Fig. 6**.⁷³ Although the validation process of an MRI scoring system for the hips in JIA is in its early stage, Porter-Young et al. in 2018 indicated the most reliable MRI parameters on which a scoring system might be based.⁷⁴ Then, Ostrowska et al. in 2021 proposed a comprehensive scoring system for hip arthritis, including 24 active, chronic, and developmental hip lesions, and proposed the MRI summarized score, a sum of the scores of these lesions in an individual patient that showed 25% sensitivity and 100% specificity in discriminating hip arthritis from hip pain in juveniles without JIA.⁷⁵ Tanturri and colleagues in 2023 published another scoring, including mostly the same lesions and showed good interobserver agreement for them.⁷³ Additional items included in this scoring, such as joint space width, caput-collum-diaphyseal angle, femoral neck-head length, femoral width, and trochanteric distance were imprecise.

The temporomandibular joint (TMJ) is affected in 39% to 78% of JIA patients.⁷⁶ If left untreated, or in treatment-resistant cases, arthritis of the TMJ can lead to growth disturbance of the TMJ condyle and damage to the articular disk, leading to severe

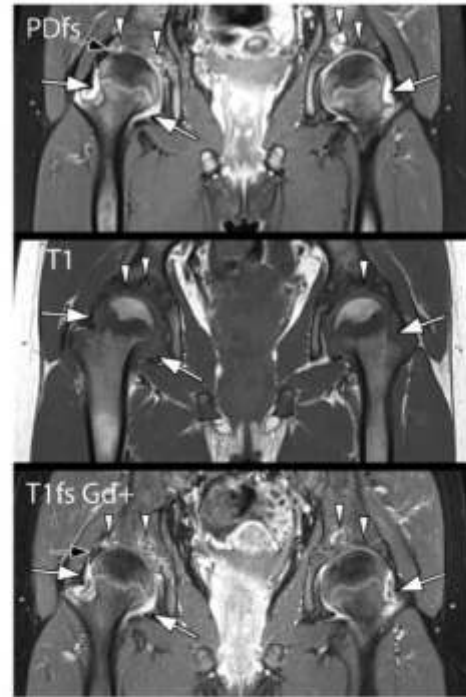


Fig. 6. MR image of both the hips of a 14-year-old girl with systemic juvenile idiopathic arthritis (JIA) treated by biologics. Bilateral hip joint effusions with moderate synovial thickening (arrows, PD fs) and synovial enhancement (arrows, T1 FS gd+), hip joint space narrowing (more pronounced on the right) with thinned joint cartilage (black arrows). Bone architecture changes of acetabular roof (arrowheads) with geodes (non-enhanced changes) and synovial cysts rim enhancement, the largest on the left (medial arrowhead).

orofacial outcomes such as facial asymmetry, reduced or asymmetric mouth opening, retrognathia as well as functional abnormalities with mastication, orofacial pain, and reduced quality of life.^{67,76} Because of the complex nature of this joint, MRI has become the modality of choice for the assessment of early inflammatory changes as well as chronic abnormalities.⁶³ Both closed-mouth and open-mouth views should be performed for the optimal assessment of the joint and the disc position, see **Fig. 7**. Although MRI scoring systems for TMJ involvement by JIA are available, any proven precise nor was validated.⁷⁶⁻⁷⁸ Angenette and colleagues in 2022 indicated a precise MRI-based scoring system consisting of 7 variables in the osteochondral domain and 4 variables in the inflammatory domain.⁷⁶ For most of the lesions, inter-observer and intra-observer agreements were good. Several of the commonly used markers

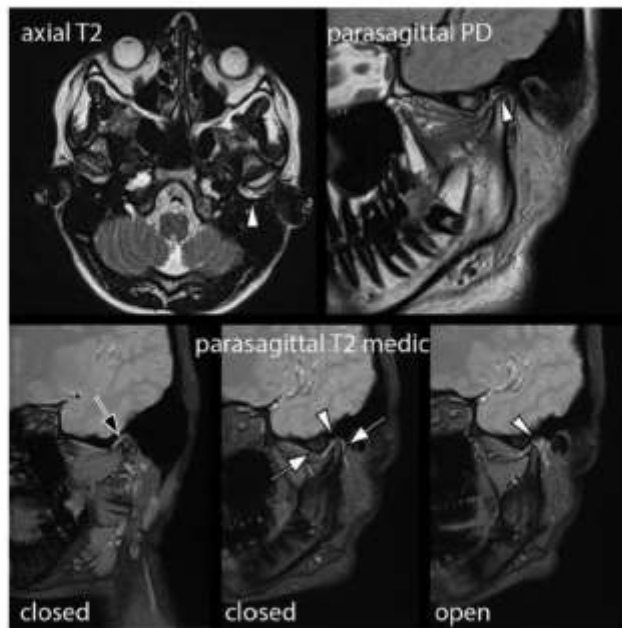


Fig. 7. A 16-year-old female patient with JIA and bilateral inflammatory lesions in the temporomandibular joints. The images show increased fluid with thickening of the synovial membrane (white arrowhead on axial T2), bone marrow edema of the mandibular head, and articular eminence (white arrows) with erosions (black arrow on parasagittal T2 multi-echo data image combination [MEDIC]). Features of limited joint mobility and of the perforation of the articular disc in the central part—in close-up its position is normal (white arrowheads on “close” parasagittal PD and T2 MEDIC), in opening the posterior band immobile (white arrowhead on “open” parasagittal T2 MEDIC).

performed poorly in particular assessment of synovial thickness and joint enhancement, as well as measurements of joint fluid.⁷⁶ Therefore, although with contrast injection, the interpretation of the signal localization in the TMJ remains challenging.⁶⁷ The presence of a small amount of synovial enhancement and joint effusion are commonly seen even in nonrheumatological patients; hence, these must be interpreted with caution in the absence of correlative osteochondral and clinical changes.⁶⁷ Also, similarly to other bones, the physiologic growth-related hematopoietic-to-fatty marrow conversion in children makes the identification of pathologic bone marrow changes within the mandibular condyle subjective and challenging.⁶⁷ When assessing the degree of osteochondral damage in JIA using MRI, the surface irregularities, erosions, and flattening of the condyle need to be interpreted in reference to the expected age-matched size and morphologic configuration of the condylar head that changes over time in children with and without JIA.⁶⁷ What is more, the same spectrum of lesions, including morphologic changes of condyle such as flattening, synovitis, erosions, and disc degeneration with malalignment may be seen in congenital, maldevelopmental conditions or even after minor trauma of TMJ. TMJs problems, including disc pathology, are further linked to the widespread use of smartphones.⁷⁹ While cone beam CT remains the better standard for higher detailed assessment of

cortical irregularities and other osteophytic changes, optimized 3D gradient echo MRI sequences have shown similar measurement agreement and reliability to CT.⁶⁷ Clemente and colleagues in 2018 showed that inter-reader reliability and qualitative measures of image quality for assessment of TMJ improved with the coil offering higher resolution, and not increased magnet strength 1,5 versus 3,0 Tesla.⁸⁰

Contrast-Enhanced Versus Non-Contrast MRI in Juvenile Idiopathic Arthritis in Peripheral Joints

The question concerning the validity of intravenous contrast administration remains open. On the 1 hand, many studies point toward the increased sensitivity of contrast-enhanced MRI in the detection of synovitis and tenosynovitis in JIA.⁸¹ In 2013, Hemke and colleagues reported that the reliability of the JAMRIS score for the assessment of synovial thickening decreases when omitting contrast agents in MRI examinations of the knee at 1 T⁸². Boesen and colleagues showed that DCE MRI was found to be able to differentiate between active and inactive JIA in the knee and wrist based on the differences in signal intensity curve shapes.⁸² The maximum enhancement values of the synovium in the wrist of JIA patients in remission seem to be able to predict clinical flares.⁸³ Mazzoini and colleagues in

2023 based on a postcontrast MRI studies of 90 JIA patients showed MRI-detected subclinical synovitis in a large proportion (65.5%) of the patients in wrists, hips, ankles, and knees in clinical remission.⁸⁴ The presence of subclinical synovitis was the best predictor of the disease flare on multivariable regression analysis.

On the other side, the recently described possible accumulation of gadolinium in deep brain nuclei such as the dentate nucleus and globus pallidus with uncertain long-term consequences leads to stricter indications for the use of contrast agents in MRI.^{81,85} Therefore, application and especially repetitive application of MR contrast agents in children and adolescents must be well justified and should, if possible, be omitted.^{81,85}

Ostrowska and colleagues showed that the non-contrast MRI of hip joints in JIA enables discrimination between JIA and not JIA in hip arthralgia.⁷⁵ In the latest publication from 2023, Chjieu et al. compared unenhanced versus enhanced knee joint MRI to assess disease activity of JIA using a 3T scanner.⁸⁵ Their results suggested that contrast agent application could be omitted in JIA patients and the proper diagnosis regarding synovial activity can be done based on proton density (PD) sequences and assuring the standardization of image acquisition timing after contrast administration. Based on their data, no significant difference in

diagnostic accuracy when using enhanced or unenhanced images could be found when using the clinical Juvenile Arthritis Disease Activity Score (JADAS10) as a reference. A challenge in contrast agent application for the detection of disease activity of JIA is the standardization of image acquisition delay after administration. Otherwise, significant differences in synovial thickness measurements and enhancement may be seen, as it has been proven already.⁸⁵⁻⁸⁷

Advances in MRI hardware and software development and the resulting improved image quality as well as image interpretation using AI programs will likely help to better assess unenhanced images.⁸⁵ DWI has been evaluated as a non-invasive parameter to detect disease activity in patients with JIA^{85,88} and its high accuracy for the detection of arthritis in agreement with contrast-enhanced MRI has been found already in 2010 by Roemer and colleagues⁸⁹ Other imaging sequences are studied in order to decrease the use of contrast agent. Verkuil and colleagues used double inversion recovery (DIR) MRI as a potential sequence which accentuates the knee synovium in children with JIA without using contrast agents.⁹⁰ Their results demonstrate that DIR MRI should be considered as a child-friendly alternative to contrast-enhanced MRI for evaluation of synovitis in children.

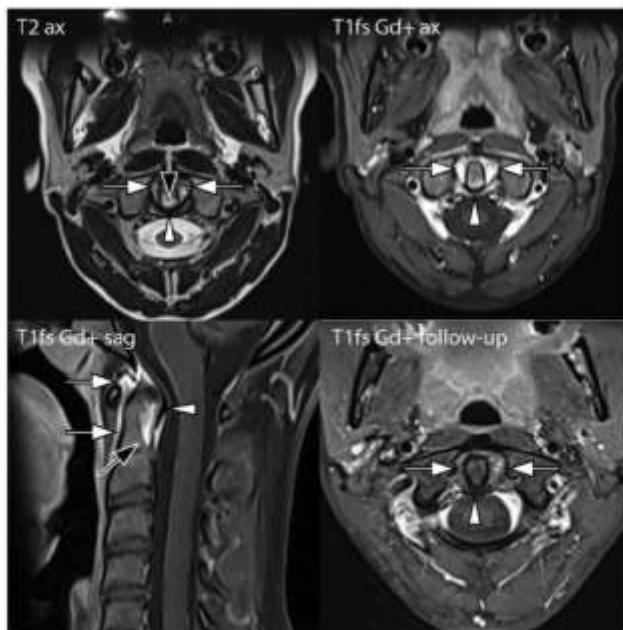


Fig. 8. A series of MR images of the cervical spine of 14-year-old and 16-year-old girls with extended oligoarticular JIA, antinuclear antibodies-positive baseline images in T2 axial, T1 fs contrast-enhanced axial and sagittal, and follow-up T1 fs postcontrast image in axial plane (last bottom image). Baseline T2 turbo spin-echo axial shows asymmetrically thickened atlanto-axial synovium (arrows), area of hyperintense bone marrow signal in the posterior part of the dens (black arrow), and thickened transversal ligament (arrowhead). Contrast-enhanced MR image in axial and sagittal planes shows homogenous intensive synovial enhancement, enhancement of the posterior part of the dens and thickened transverse ligament, and no signs of anterior atlantoaxial subluxation. The contrast-enhanced MR image on follow-up obtained 2 years later, during which time the girl was treated with biologics, shows slightly asymmetric thickened synovium with minimal non-homogenous enhancement

(arrows on T1fs Gd+ follow-up) and thickened transversal ligament (arrowhead). The girl was symptom-free and had normal laboratory data.

Advanced quantitative MRI techniques, such as T2-mapping and T1-rho mapping, might play an important role in the future for the evaluation of inflammatory changes in the knee, but these sequences are not yet part of routine imaging.^{85,88} Recently, radiomics have been developed as an image analysis technique that quantifies image characteristics on the basis of the distribution of pixels and their surface intensity or patterns.⁹¹ Hu and colleagues captured the radiomics signature by quantifying and developing the radiomics-related model for predicting the existence of the juvenile dermatomyositis (JDM).⁹¹ The combination of radiomics features extracted from MRIs of the thighs and non-invasive clinical characteristics obtained a pronounced discriminative performance to assist in diagnosing JDM.⁹¹

Axial Spine

For a complete assessment of the cervical spine involvement in JIA, contrast-enhanced MRI

appears indispensable. The latest publication by Kotecki and colleagues showed that the cervical spine lesions in JIA, despite optimized diagnosis and treatment in the last years, may affect up to 35% of JIA patients, and 25% of them develop serious complications, such as atlanto-axial subluxations and ankylosis, see Fig. 8.⁹² Despite clear advantages of MRI in terms of imaging of early inflammatory lesions in soft tissues and bone, radiography shows superiority in the diagnosis of atlanto-axial subluxation (AAS) and subaxial subluxations (SAS).⁹² The predominance of chronic features, such as SAS, AAS, and ankylosis, over early inflammatory abnormalities, including BME and synovitis, along with the several years of history of JIA suggests that clinical manifestation of cervical spine involvement is discrete or even absent in the first years of the disease, which lets the cervical arthritis progress unrecognized until a more advanced stage.⁹² Kljucsek D et al. have demonstrated that early treatment with

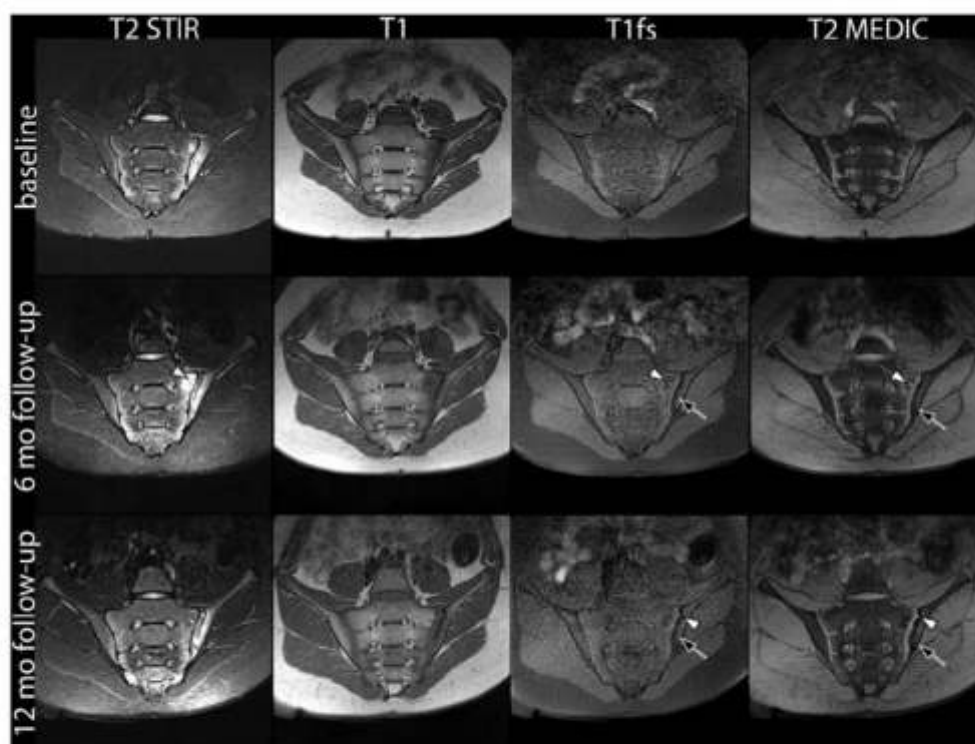


Fig. 9. An 11-year-old boy with JIA enthesitis-related arthritis subtype. The initial examination was obtained at the age of 11 years; first follow-up MR imaging was obtained 6 months later, and second follow-up, 12 months after baseline. Left-sided sacroiliitis: semicoronal T2 short-tau inversion recovery images show bone marrow edema in the left ilium, joint space inflammation, capsulitis, and active erosion in the left sacral bone (evident in the first follow-up examination; arrow). T1, T1 fat-suppressed, and T2 MEDIC consecutive examinations show increasing number of erosions (white arrows) and bone marrow fatty metaplasia (black arrows).

anti-TNF α drugs resulted in significantly reduced inflammation and prevented the development of cervical spine joints malalignments including atlantoaxial instability with a potential risk of cord or brainstem compression, cervical bone deformities, and ankylosis.⁹³

Recent years have been groundbreaking in terms of the imaging of juvenile sacroiliitis. In 2019, the OMERACT Juvenile Idiopathic Arthritis MRI Working Group published the first recommendations for the definitions of sacroiliac joint (SIJ) findings in JIA.⁹⁴ An example is shown in Fig. 9. The same international group subsequently in 2021 developed and updated a semiquantitative MRI-based scoring system for the evaluation of SIJ inflammation and structural changes in children with JIA, the Juvenile Idiopathic Arthritis MRI Scoring System (JAMRIS-SIJ) score.⁹⁵ In the wake of this, the group issued an atlas of MRI findings of juvenile sacroiliitis to illustrate the updated preliminary OMERACT pediatric JAMRIS scoring system for active and structural lesions.⁹⁶ In 2023, they ran the project which used a formal conjoint analysis-based survey to elicit expert preferences on the relative weights of measurement items and grades to determine the relative weightings for SIJ pathologies in the OMERACT JAMRIS-SIJ score.⁹⁷ The 2 most important inflammation domain measurement items were BE and osteitis, and their weights were equivalent and for the JAMRIS-SIJ damage domain, ankylosis was the most important measurement item.⁹⁷

Finally, there has been a tendency for an additional MRI sequence, volume-interpolated breath-hold examination (VIBE), to be entered into imaging protocols, both for the SIJs and peripheral joints, improving the performance of interpretation of osseous abnormalities, such as erosions, sclerosis, and ankylosis due to high contrast between the cortex and a subchondral bone marrow. VIBE is a 3D gradient echo MRI sequence that has the advantage of higher spatial resolution, lower partial volume effects, and multi-planar reconstruction.^{8,9,64}

Whole Body-MRI

WB-MRI has increasingly been used for the evaluation of rheumatologic diseases, enabling the assessment of the extent and activity of the disease involving the peripheral and axial joints, entheses, muscles, and bone marrow of the entire body in a single scanning session.⁶² Because of its high tissue contrast resolution, it detects subtle early inflammatory changes and provides an objective tool to assess disease burden and activity.⁶⁷ An ESSR survey conducted by Giraud and colleagues in 2018 among radiologists identified the most common clinical indications used for WB-MRI that included inflammatory idiopathic myositis and chronic recurrent multifocal osteomyelitis (CRMO)/chronic nonbacterial osteomyelitis, followed by overlapping syndromes (an example is CRMO and JIA), JIA alone, and other

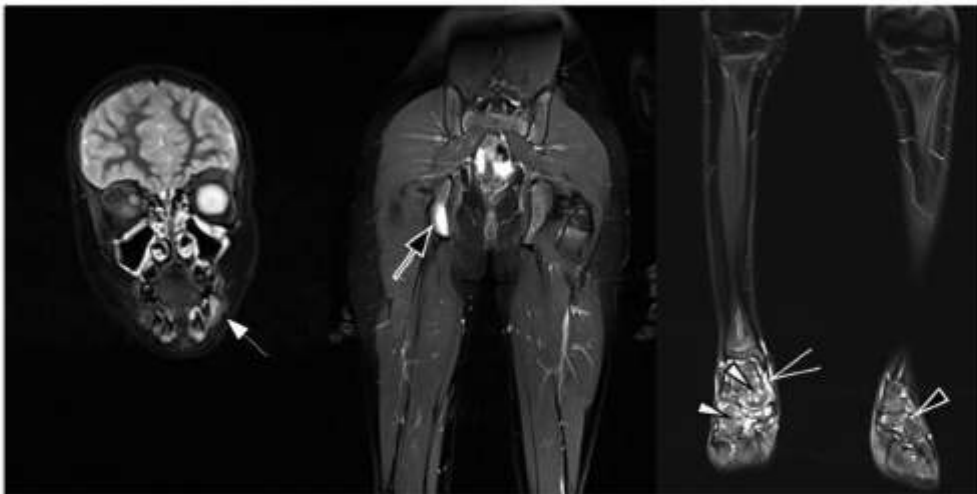


Fig. 10. An 8-year-old girl with chronic recurrent multifocal osteomyelitis (CRMO). Coronal T2 TIRM images show areas of increased marrow signal in the inferior ramus and angle of the mandibula on the left side (*white arrow*), and in the right ischium (*black arrow*). The numerous areas of abnormal signal in the right ankle and tarsal bones (*white arrowheads*) with minor effusion (*open arrowhead*), less severe in the left ankle (*black arrowhead*) may represent stress-related mechanical abnormalities which are in differential for CRMO-related lesions.

rheumatic diseases.⁵⁹ The identification of specific patterns of skeletal involvement in patients with overlapping features (not rarely clinically occult CRMO overlapping cases) may have an impact on identifying those with genetic predisposition and also affects treatment strategies and long-term follow-up, see Fig. 10.⁶⁷ If not optimally treated, both CRMO and spondyloarthropathies can lead to bone deformities and morbidity, which result in a significant effect on the quality of life. WB-MRI demonstrates typical sites of involvement and can show the progression or improvement of the disease following treatment. However, as mentioned earlier, caution is needed when interpreting bone marrow changes, as they are often seen in healthy children.^{68,69}

In 2021, Panwar and colleagues developed a standardized WB-MRI scoring system to quantify the total inflammatory burden in children with JIA and provided recommendations on anatomic MRI planes and sequences as the minimally necessary imaging protocol for the scoring system.⁶² The developed scoring system includes 100 peripheral, 23 chests, and 76 axial joints, and 64 entheses, with 2 to 4 diagnostic parameters graded in each of the regions, using binary (presence or absence) and 2 to 3-level ordinal scores. The tables and figures in the article, which illustrate the elements required for analysis of the numerous locations potentially subject to inflammation in JIA, provide additional educational material.

SUMMARY

In conclusion, continuous developments of MRI have improved the management of rheumatic patients, and allowed more objective and standardized evaluation. Advances in the hardware and software of MRI scanners, along with new definitions of pathologic findings, and new semiquantitative and quantitative assessments introduced and validated in the recent years perfect the MRI ability to diagnose and monitor peripheral and axial arthritis. Future research in this field is needed to further optimize the MRI protocols to improve specificity of MRI diagnosis, provide early diagnosis, identify patients at risk of rapid progression to prevent joint damage, and maximize quality of life and ability to function. Further studies are needed on how to validate, interpret, and manage subclinical synovitis seen on MRI, as predictor for treatment response or damage,⁹⁸ and on the importance of BME as a biomarker of flair and joint damage progression. Imaging with MR is one of JIA biomarkers along with clinical, serum, cellular, and genetic biomarkers, and the results of MRI

have to be interpreted in conjunction with all these data.

CLINICS CARE POINTS

- MRI has become a key instrument in rheumatology for assessment of both the axial and peripheral skeleton; however, correlation with clinical data is mandatory.
- In axial spondyloarthritis, MRI enables detection of active inflammation, and also surpasses radiography in sensitivity to structural lesions.
- Although WB-MRI is time-consuming and patient positioning may be uncomfortable, it represents a powerful tool for systemic diseases, as it can detect inflammation even in areas that may not be clinically symptomatic, and it is useful in assessing treatment response.
- In the pediatric population, MRI has become an important tool for joint assessment, although its utilization is challenging, given the need for discrimination between pathologic and physiologic changes in the growing skeleton.

DISCLOSURE

The authors have nothing to disclose.

REFERENCES

1. Protopopov M, Proft F, Wichuk S, et al. Comparing MRI and conventional radiography for the detection of structural changes indicative of axial spondyloarthritis in the ASAS cohort. *Rheumatology (Oxford, England)* 2023;62(4):1631-5.
2. Greese J, Diekhoff T, Sieper J, et al. Detection of Sacroiliitis by Short-tau Inversion Recovery and T2-weighted Turbo Spin Echo Sequences: Results from the SIMACT Study. *J Rheumatol* 2019;46(4):376-83.
3. Zhang H, Huang H, Zhang Y, et al. Diffusion-Weighted MRI to Assess Sacroiliitis: Improved Image Quality and Diagnostic Performance of Readout-Segmented Echo-Planar Imaging (EPI) Over Conventional Single-Shot EPI. *AJR Am J Roentgenol* 2021;217(2):450-9.
4. Wang D, Yin H, Liu W, et al. Comparative analysis of the diagnostic values of T2 mapping and diffusion-weighted imaging for sacroiliitis in ankylosing spondylitis. *Skeletal Radiol* 2020;49(10):1597-606.
5. Beltran LS, Samim M, Gyftopoulos S, et al. Does the Addition of DWI to Fluid-Sensitive Conventional MRI

- of the Sacroiliac Joints Improve the Diagnosis of Sacroiliitis? *AJR Am J Roentgenol* 2018;210(6):1309–16.
6. Albano D, Bignone R, Chianca V, et al. T2 mapping of the sacroiliac joints in patients with axial spondyloarthritis. *Eur J Radiol* 2020;131:109246.
 7. Martín-Noguerol T, Casado-Verdugo OL, Beltrán LS, et al. Role of advanced MRI techniques for sacroiliitis assessment and quantification. *Eur J Radiol* 2023;163:110793.
 8. Gaalen F, van der Heijde D, Huizinga T, et al. Magnetic resonance imaging of the sacroiliac joints in the early detection of spondyloarthritis: no added value of gadolinium compared with short tau inversion recovery sequence. *Rheumatology (Oxford)* 2013;52:1220–4.
 9. Giraudou C, Weber M, Puchner A, et al. Which MR sequences should we use for the reliable detection and localization of bone marrow edema in spondyloarthritis? *Radiol Med* 2017;122:752–60.
 10. Diekhoff T, Greese J, Sieper J, et al. Improved detection of erosions in the sacroiliac joints on MRI with volumetric interpolated breath-hold examination (VIBE): results from the SIMACT study. *Ann Rheum Dis* 2018;77(11):1585–9.
 11. Baraliakos X, Hoffmann F, Deng X, et al. Detection of Erosions in Sacroiliac Joints of Patients with Axial Spondyloarthritis Using the Magnetic Resonance Imaging Volumetric Interpolated Breath-hold Examination. *J Rheumatol* 2019;46(11):1445–9.
 12. Algin O, Gokalp G, Ocakoglu G. Evaluation of bone cortex and cartilage of spondyloarthropathic sacroiliac joint: efficiency of different fat-saturated MRI sequences (T1-weighted, 3D-FLASH, and 3D-DESS). *Acad Radiol* 2010;17(10):1292–8.
 13. Jans LBO, Chen M, Elewaut D, et al. MRI-based Synthetic CT in the Detection of Structural Lesions in Patients with Suspected Sacroiliitis: Comparison with MRI. *Radiology* 2021;298(2):343–9.
 14. Deppe D, Hermann KG, Proft F, et al. CT-like images of the sacroiliac joint generated from MRI using susceptibility-weighted imaging (SWI) in patients with axial spondyloarthritis. *RMD Open* 2021;7(2).
 15. Hahn S, Song JS, Choi EJ, et al. Can Bone Erosion in Axial Spondyloarthropathy be Detected by Ultra-short Echo Time Imaging? A Comparison With Computed Tomography in the Sacroiliac Joint. *J Magn Reson Imag* 2022;56(5):1580–90.
 16. Lin C, Liu D, Wen H, et al. Zero echo time MRI improved detection of erosions and sclerosis in the sacroiliac joint in comparison with LAVA-flex. *Front Endocrinol* 2023;14:1167334.
 17. Wolham L, Guggenberger R, Higashigaito K, et al. Detailed bone assessment of the sacroiliac joint in a prospective imaging study: comparison between computed tomography, zero echo time, and black bone magnetic resonance imaging. *Skeletal Radiol* 2022;51(12):2307–15.
 18. Adelsmayer G, Haidmayer A, Spreizer C, et al. The value of MRI compared to conventional radiography in analysing morphologic changes in the spine in axial spondyloarthritis. *Insights into imaging* 2021;12(1):183.
 19. de Koning A, de Bruin F, van den Berg R, et al. Low-dose CT detects more progression of bone formation in comparison to conventional radiography in patients with ankylosing spondylitis: results from the SIAS cohort. *Ann Rheum Dis* 2018;77(2):293–9.
 20. Alhashash M, Shousha M, Heyde CE, et al. Cervical spine fractures in ankylosing spondylitis patients: an analysis of the presentation and clinical results of 110 surgically managed patients in two spine centers. *Eur Spine J* 2023;32(6):2131–9.
 21. Baraliakos X, Pournara E, Coates LC, et al. Magnetic resonance imaging characteristics in patients with psoriatic arthritis and axial manifestations from the MAXIMISE cohort. *Rheumatology (Oxford, England)* 2023. <https://doi.org/10.1093/rheumatology/kead162>.
 22. Regierer AC, Weiß A, Proft F, et al. Comparison of patients with axial PsA and patients with axSpA and concomitant psoriasis: an analysis of the German register RABBIT-SpA. *RMD open* Mar 2023;9(1).
 23. Poddubnyy D, Baraliakos X, Van den Bosch F, et al. Axial Involvement in Psoriatic Arthritis cohort (AXIS): the protocol of a joint project of the Assessment of SpondyloArthritis International Society (ASAS) and the Group for Research and Assessment of Psoriasis and Psoriatic Arthritis (GRAPPA). *Therapeutic advances in musculoskeletal disease* 2021;13:1759720x211057975.
 24. Huang H, Zhang Y, Zhang H, et al. Qualitative and quantitative assessment of sacroiliitis in axial spondyloarthropathy: can a single T2-weighted dixon sequence replace the standard protocol? *Clin Radiol* 2020;75(4):321.e13–20.
 25. Maksymowych WP, Lambert RG, Østergaard M, et al. MRI lesions in the sacroiliac joints of patients with spondyloarthritis: an update of definitions and validation by the ASAS MRI working group. *Ann Rheum Dis* 2019;78(11):1550–8.
 26. Bressemer KK, Adams LC, Proft F, et al. Deep Learning Detects Changes Indicative of Axial Spondyloarthritis at MRI of Sacroiliac Joints. *Radiology* 2023;307(3):e239007.
 27. Franken M, Rüksam G, Mewes A, et al. To Contrast or Not to Contrast? On the Role of Contrast Enhancement in Hand MRI Studies of Patients with Rheumatoid Arthritis. *Diagnostics* 2022;12(2):12.
 28. Boeren AMP, Niemantsverdriet E, Verstappen M, et al. Towards a simplified fluid-sensitive MRI protocol in small joints of the hand in early arthritis patients: reliability between modified Dixon and regular Gadolinium enhanced TSE fat saturated MRI-sequences. *Skeletal Radiol* 2023;52(6):1193–202.

29. Ma W, Cai J, Zhang W, et al. Diagnostic performance of double inversion recovery MRI sequence for synovitis of the wrist joints in rheumatoid arthritis. *Radiol Med* 2023;128(8):978–88.
30. Tripathi D, Awasthi R, Agarwal V, et al. Diffusion Tensor and Dynamic Contrast-Enhanced Magnetic Resonance Imaging Correlate with Molecular Markers of Inflammation in the Synovium. *Diagnos-tics* 2022;12(12).
31. Ulas ST, Hermann KG, Makowski MR, et al. Perfu-sion in hand arthritis on dynamic contrast-enhanced computed tomography: a randomized prospective study using MRI as a standard of refer-ence. *Skeletal Radiol* 2021;50(1):59–68.
32. Michałek F, Ulas ST, Poddubnyy D, et al. Fractal analysis of perfusion imaging in synovitis: a novel imaging biomarker for grading inflammatory activity based on assessing angiogenesis. *RMD Open* 2022;8(1).
33. Ulas ST, Diekhoff T, Hermann KGA, et al. Suscepti-bility-weighted MR imaging to improve the speci-ficity of erosion detection: a prospective feasibility study in hand arthritis. *Skeletal Radiol* 2019;48(5): 721–8.
34. Abrar DB, Schleich C, Frenken M, et al. DGEMRIC in the Assessment of Pre-Morphological Cartilage Degeneration in Rheumatic Disease: Rheumatoid Arthritis vs. Psoriatic Arthritis. *Diagnostics* 2021; 11(2).
35. Renner N, Kleyer A, Krönke G, et al. T2 Mapping as a New Method for Quantitative Assessment of Carti-lage Damage in Rheumatoid Arthritis. *J Rheumatol* 2020;47(6):820–5.
36. Mańczak M, Pracoń G, Sudół-Szopińska I, et al. Apparent diffusion coefficient as an indicator of spi-nal cord compression due to anterior atlanto-axial subluxation in rheumatoid arthritis patients. *Eur Spine J* 2019;28(10):2352–8.
37. Diekhoff T, Ulas ST, Poddubnyy D, et al. Ultra-low-dose CT detects synovitis in patients with suspected rheumatoid arthritis. *Ann Rheum Dis* 2019;78(1): 31–5.
38. Folle L, Bayat S, Kleyer A, et al. Advanced neural networks for classification of MRI in psoriatic arthritis, seronegative, and seropositive rheumatoid arthritis. *Rheumatology (Oxford, England)* 2022; 61(12):4945–51.
39. Mathew AJ, Krabbe S, Kirubakaran R, et al. Utility of Magnetic Resonance Imaging in Diagnosis and Monitoring Enthesitis in Patients with Spondyloarthri-tis: An OMERACT Systematic Literature Review. *J Rheumatol* 2019;46(9):1207–14.
40. Mathew AJ, Østergaard M, Eder L. Imaging in pso-riatic arthritis: Status and recent advances. *Best Pract Res Clin Rheumatol* 2021;35(2):101690.
41. Tedeschi SK, Becce F, Pascart T, et al. Imaging Fea-tures of Calcium Pyrophosphate Deposition Disease: Consensus Definitions From an International Multidis-ciplinary Working Group. *Arthritis Care Res* 2023; 75(4):825–34.
42. Germann C, Galley J, Falkowski AL, et al. Ultra-high resolution 3D MRI for chondrocalcinosis detection in the knee—a prospective diagnostic accuracy study comparing 7-tesla and 3-tesla MRI with CT. *Eur Ra-di-ol* 2021;31(12):9436–45.
43. Salvarani C, Cantini F, Olivieri I, et al. Proximal bursitis in active polymyalgia rheumatica. *Ann Intern Med* 1997;127(1):27–31.
44. Fruth M, Seggewiss A, Kozik J, et al. Diagnostic capability of contrast-enhanced pelvic girdle mag-netic resonance imaging in polymyalgia rheumatica. *Rheumatology (Oxford, England)* 2020;59(10): 2864–71.
45. Marzo-Ortega H, Rhodes LA, Tan AL, et al. Evidence for a different anatomic basis for joint disease local-ization in polymyalgia rheumatica in comparison with rheumatoid arthritis. *Arthritis Rheum* 2007; 56(10):3496–501.
46. Huwart A, Garrigues F, Jousse-Joulin S, et al. Ultra-sonography and magnetic resonance imaging changes in patients with polymyalgia rheumatica treated by tocilizumab. *Arthritis Res Ther* 2018; 20(1):11.
47. Maurus S, Sommer NN, Kooijman H, et al. 3D black-blood 3T-MRI for the diagnosis of abdominal large vessel vasculitis. *Eur Radiol* 2020;30(2):1041–4.
48. Treitl KM, Maurus S, Sommer NN, et al. 3D-black-blood 3T-MRI for the diagnosis of thoracic large vessel vasculitis: A feasibility study. *Eur Radiol* 2017;27(5):2119–28.
49. Dourmes G, Menuf F, Macey J, et al. Lung morphology assessment of cystic fibrosis using MRI with ultra-short echo time at submillimeter spatial resolution. *Eur Radiol* 2016;26(11):3811–20.
50. Delacoste J, Chaptinel J, Beigelman-Aubry C, et al. A double echo ultra short echo time (UTE) acquisi-tion for respiratory motion-suppressed high resolu-tion imaging of the lung. *Magn Reson Med* 2018; 79(4):2297–305.
51. Heidenreich JF, Kuhl PJ, Grunz JP, et al. Lung Func-tion in Patients with Cystic Fibrosis before and dur-ing CFTR-Modulator Therapy Using 3D Ultrashort Echo Time MRI. *Radiology* 2023;308(1):e230084.
52. Ibhagui OY, Li D, Han H, et al. Early Detection and Staging of Lung Fibrosis Enabled by Collagen-Targeted MRI Protein Contrast Agent. *Chem Biomed Eng* 2023;1(3):268–85.
53. Frenk NE, Montesi SB, Chen T, et al. Free-breathing dynamic contrast-enhanced magnetic resonance of interstitial lung fibrosis. *Magn Reson Imag* 2020;69: 16–21.
54. Althoff CE, Sieper J, Song IH, et al. Comparison of Clinical Examination versus Whole-body Magnetic Resonance Imaging of Enthesitis in Patients with

- Early Axial Spondyloarthritis during 3 Years of Continuous Etanercept Treatment. *J Rheumatol* 2016;43(3):618–24.
55. Althoff CE, Sieper J, Song IH, et al. Active inflammation and structural change in early active axial spondyloarthritis as detected by whole-body MRI. *Ann Rheum Dis* 2013;72(6):967–73.
 56. Axelsen MB, Eshed I, Duer-Jensen A, et al. Whole-body MRI assessment of disease activity and structural damage in rheumatoid arthritis: first step towards an MRI joint count. *Rheumatology (Oxford, England)* 2014;53(5):845–53.
 57. Poulsen AEF, Axelsen MB, Foggenborg RP, et al. Whole-body Magnetic Resonance Imaging in Psoriatic Arthritis, Rheumatoid Arthritis, and Healthy Controls: Interscan, Intrareader, and Interreader Agreement and Distribution of Lesions. *J Rheumatol* 2021;48(2):198–206.
 58. Assmann G, Kueck O, Kirchhoff T, et al. Efficacy of antibiotic therapy for SAPHO syndrome is lost after its discontinuation: an interventional study. *Arthritis Res Ther* 2009;11(5):R140.
 59. Giraudo C, Lecouvet FE, Cotten A, et al. Whole-body magnetic resonance imaging in inflammatory diseases: Where are we now? Results of an International Survey by the European Society of Musculoskeletal Radiology. *Eur J Radiol* 2021;136:109533.
 60. Bellutti Enders F, Bader-Meurier B, Baldam E, et al. Consensus-based recommendations for the management of juvenile dermatomyositis. *Ann Rheum Dis* 2017;76(2):329–40.
 61. Østergaard M, Eshed I, Althoff CE, et al. Whole-body Magnetic Resonance Imaging in Inflammatory Arthritis: Systematic Literature Review and First Steps Toward Standardization and an OMERACT Scoring System. *J Rheumatol* 2017;44(11):1699–705.
 62. Panwar J, Tolend M, Redd B, et al. Consensus-driven conceptual development of a standardized whole body-MRI scoring system for assessment of disease activity in juvenile idiopathic arthritis: MRI in JIA OMERACT working group. *Semin Arthritis Rheum* 2021;51(6):1350–9.
 63. Hemke R, Herregods N, Jaremko JL, et al. Imaging assessment of children presenting with suspected or known juvenile idiopathic arthritis: ESSR-ESPR points to consider. *Eur Radiol* 2020;30:5237–49.
 64. Suddi-Szopifiska I, Giraudo C, Oel EHG, et al. Imaging update in inflammatory arthritis. *J Clin Orthop Trauma* 2021;20:101491.
 65. Paramalingam IMS, Conaghan PG, Keen HI. An update on imaging in rheumatoid arthritis. *Curr Treat Options Rheum* 2020;8:370–81.
 66. Suddi-Szopifiska I, Teh J, Cotton A. Rheumatoid Hand and Other Hand-deforming Rheumatic Conditions. *Semin Musculoskelet Radiol* 2021;25:232–45.
 67. Malattia C, Tolend M, Mazzoni M, et al. Current status of MR imaging of juvenile idiopathic arthritis. *Best Pract Res Clin Rheumatol* 2020;34:101629.
 68. Zadig PK, von Brandis E, Fiata B, et al. Whole body magnetic resonance imaging in healthy children and adolescents: Bone marrow appearances of the appendicular skeleton. *Eur J Radiol* 2022;153:110365.
 69. von Brandis E, Zadig PK, Avenarius DFM, et al. Whole body magnetic resonance imaging in healthy children and adolescents. Bone marrow appearances of the axial skeleton. *Eur J Radiol* 2022;154:110425.
 70. Hemke R, Van Rossum MAJ, van Veenendaal M, et al. Reliability and responsiveness of the Juvenile Arthritis MRI Scoring (JAMRIS) system for the knee. *Eur Radiol* 2013;23:1075–83.
 71. Hemke R, Tzaribachev N, Nusman CM, et al. Magnetic Resonance Imaging (MRI) of the knee as an outcome measure in juvenile idiopathic arthritis: An OMERACT reliability study on MRI scales. *J Rheumatol* 2017;44:1224–30.
 72. Avenarius DFM, Nusman C, Malattia C, et al. Current status of wrist imaging in juvenile idiopathic arthritis. *Pediatr Radiol* 2018;48:801–10.
 73. Tanturi de Horatio L, Shelmerdine SC, d'Angelo P, et al. A novel magnetic resonance imaging scoring system for active and chronic changes in children and adolescents with juvenile idiopathic arthritis of the hip. *Pediatr Radiol* 2023;53:426–37.
 74. Porter-Young FM, Offiah AC, Broadley P, et al. Inter- and intra-observer reliability of contrast-enhanced magnetic resonance imaging parameters in children with suspected juvenile idiopathic arthritis of the hip. *Pediatr Radiol* 2018;48:1891–900.
 75. Ostrowska M, Gietka P, Mańczak M, et al. MRI Findings in Hip in Juvenile Idiopathic Arthritis. *J Clin Med* 2021;10:5252.
 76. Angenete OW, Augdal TA, Rygg M, et al. MRI in the Assessment of TMJArthritis in Children with JIA: Repeatability of a Newly Devised Scoring System. *Acad Radiol* 2022;29:1362–77.
 77. Tolend MA, Twilt M, Cron RQ, et al. Toward establishing a standardized magnetic resonance imaging scoring system for temporomandibular joints in juvenile idiopathic arthritis. *Arthritis Care Res* 2018;70(5):758–67.
 78. Tolend M, Doria AS, Meyers AB, et al. Assessing the Reliability of the OMERACT Juvenile Idiopathic Arthritis Magnetic Resonance Scoring System for Temporomandibular Joints (JAMRIS-TMJ). *J Clin Med* 2021;10:4047.
 79. Pei YP, Li HC, Zhong JW, et al. The association between problematic smartphone use and the severity of temporomandibular disorders: A cross-sectional study. *Front Public Health* 2022;23:1042147.
 80. Clemente EJI, Tolend M, Junhasavasdikul T, et al. Qualitative and semi-quantitative assessment of

- temporomandibular joint MRI protocols for juvenile idiopathic arthritis at 1.5 and 3.0T. *Eur J Radiol* 2018;98:90–9.
81. Sudoł-Szopińska I, Herregods N, Doria AS, et al. Advances in Musculoskeletal Imaging in Juvenile Idiopathic Arthritis. *Biomedicines* 2022;10:2417.
 82. Boesen M, Kubassova O, Sudoł-Szopińska I, et al. MR Imaging of Joint Infection and Inflammation with Emphasis on Dynamic Contrast-Enhanced MR Imaging. *Pet Clin* 2018;13:523–50.
 83. Nusman CM, Henke R, Lavini C, et al. Dynamic contrast-enhanced magnetic resonance imaging can play a role in predicting flare in juvenile idiopathic arthritis. *Eur J Radiol* 2017;88:77–81.
 84. Mazzoni A, Pistorio A, Magnaguagno F, et al. Predictive Value of Magnetic Resonance Imaging in Patients With Juvenile Idiopathic Arthritis in Clinical Remission. *Arthritis Care Res* 2023;75(1):198–206.
 85. Chieu VDV, Chieu VV, Dressler F, et al. Juvenile idiopathic arthritis of the knee: is contrast needed to score disease activity when using an augmented MRI protocol comprising PD-weighted sequences? *Eur Radiol* 2023;33:3775–84.
 86. Michalski E, Ostrowska M, Gietka P, et al. Magnetic resonance imaging of the knee joint in juvenile idiopathic arthritis. *Reumatologia* 2020;58(6):416–23.
 87. Barendregt AM, van Gulik EC, Groot PFC, et al. Prolonged time between intravenous contrast administration and image acquisition results in increased synovial thickness at magnetic resonance imaging in patients with juvenile idiopathic arthritis. *Pediatr Radiol* 2019;49(5):638–45.
 88. Barendregt AM, Mazzoli V, van Gulik EC, et al. Juvenile idiopathic arthritis: diffusion-weighted MRI in the assessment of arthritis in the knee. *Radiology* 2020;295(2):373–80.
 89. Roemer FW, Kassim Javaid M, Guermazi A, et al. Anatomical distribution of synovitis in knee osteoarthritis and its association with joint effusion assessed on non-enhanced and contrast-enhanced MRI. *Osteoarthritis Cartilage* 2010;18(10):1269–74.
 90. Verkuil F, Henke R, van Gulik EC, et al. Double inversion recovery MRI versus contrast-enhanced MRI for evaluation of knee synovitis in juvenile idiopathic arthritis. *Insights Imaging* 2022;13:167.
 91. Hu M, Zheng F, Ma X, et al. Assessment of Thigh MRI Radiomics and Clinical Characteristics for Assisting in Discrimination of Juvenile Dermatomyositis. *J Clin Med* 2022;11:6712.
 92. Kotecki M, Gietka P, Posadzy M, et al. Radiographs and MRI of the Cervical Spine in Juvenile Idiopathic Arthritis: A Cross-Sectional Retrospective Study. *J Clin Med* 2021;10:5798.
 93. Kijučevšek D, Emeršič N, Toplak N, et al. Clinical and MRI outcome of cervical spine lesions in children with juvenile idiopathic arthritis treated with anti-TNF α drugs early in disease course. *Pediatr Rheumatol Online J* 2017;15:38.
 94. Olobo TM, Conaghan PG, Maksymowych WP, et al. Preliminary Definitions for Sacroiliac Joint Pathologies in the OMERACT Juvenile Idiopathic Arthritis MRI Score (OMERACT JAMRIS-SIJ). *J Rheumatol* 2019;46:1192–7.
 95. Olobo TM, Herregods N, Jaremko JL, et al. Reliability of the Preliminary OMERACT Juvenile Idiopathic Arthritis MRI Score (OMERACT JAMRIS-SIJ). *J Clin Med J Clin Med* 2021;10:4564.
 96. Herregods N, Maksymowych WP, Jans L, et al. Atlas of MRI findings of sacroiliitis in pediatric sacroiliac joints to accompany the updated preliminary OMERACT pediatric JAMRIS (Juvenile Idiopathic Arthritis MRI Score) scoring system: Part I: Active lesions and part II: Structural damage lesions. *Arthritis Rheum* 2021;51:1099–107.
 97. Olobo TM, Tolend M, Meyers AB, et al. Determination of Relative Weightings for Sacroiliac Joint Pathologies in the OMERACT Juvenile Arthritis Magnetic Resonance Imaging Sacroiliac Joint Score. *J Clin Med* 2023;12:2729.
 98. Choida V, Madenidou A, Sen D, et al. The role of whole-body MRI in musculoskeletal inflammation detection and treatment response evaluation in inflammatory arthritis across age: A systematic review. *Semin Arthritis Rheum* 2022;52:151953.

9. Spis tabel i rycin

Publikacja nr 1. Whole-Body MRI at Initial Presentation of Chronic Recurrent Multifocal Osteomyelitis, Juvenile Idiopathic Arthritis, Their Overlapping Syndrome, and Non-Specific Arthropathy. Michał Lanckoroński, Piotr Gietka Małgorzata Mańczak, Iwona Sudol-Szopińska. Journal of Clinical Medicine 2024; 13, 998.

Table 1. Whole-body MRI sequence protocol.

Table 2. Demographic data of the following included patients: CRMO: chronic recurrent multifocal osteomyelitis; JIA: juvenile idiopathic arthritis; OS: JIA and CRMO overlapping syndrome; NA: Non-specific Arthropathy.

Table 3. BME lesions in 4 study groups.

Table 4. Number of patients with CRMO and JIA with at least 1 lesion at proximal and distal metaphyses and epiphyses.

Table 5. Effusions in patients with CRMO, JIA, JIA and CRMO overlapping syndrome, and NA.

Figure 1. A 13-year-old girl with chronic recurrent multifocal osteomyelitis (CRMO), TIRM (Turbo Inversion Recovery Magnitude) images in coronal and sagittal planes. Bone marrow edema (BME, arrow) in the anterior iliac bone with soft tissue edema (enthesitis) (a), in the posterior condyle of the right femur (b), and in the tarsum bilaterally (c,d), being more intensive on the right side (c).

Figure 2. A 12-year-old boy with juvenile idiopathic arthritis (JIA), TIRM images in coronal planes. Knee joint effusion (arrow in (a)), BME in the distal metaphysis (short arrow) of the right tibia and distal epiphysis of tibia bilaterally (long arrows) (b), in the tarsum bilaterally (arrows in (c)), and in the 1st metatarsal bones (arrows in (d)).

Figure 3. An 8-year-old girl with an overlapping syndrome of JIA and CRMO, TIRM images in coronal and sagittal views. (a) BME in the right humeral metaphysis and effusion in the left shoulder (arrows); (b) BME in the right triradiate cartilage and periarticularly in the right iliac bone (long arrows), and effusion in the right sacroiliac joint (short arrow); (c) BME in the proximal metaphysis of the right tibia and distal metaphysis of the left tibia (arrows); (d) BME in the distal epiphysis of the left tibia (arrow); (e) BME in the Th1 vertebra (arrow); (f) BME in the left elbow joint (arrow). unilateral (a) and bilateral BME lesions (b).

Figure 4. Distribution of bone lesions in skeleton of patients with CRMO, JIA, OS, and NA with unilateral (a) and bilateral BME lesions (b).

Publikacja nr 2. Whole - Body Magnetic Resonance Imaging in Rheumatology.
Vito Chianca, Michał Lanckoroński, Marco Curti, Majid Chalian, Iwona Sudol-Szopińska, Chiara Giraud, Filippo Del Grande. Seminars in Musculoskeletal Radiology 2024; <https://doi.org/10.1016/j.rcl.2024.02.008>.

Figure 1. Whole body MRI in a 17-year old girl with juvenile idiopathic arthritis (JIA) enthesitis-related arthritis (ERA) subtype, HLA-B27 positive. T2 TIRM images in coronal (a,b) and sagittal (c) planes show synovitis in the left shoulder with some bone marrow edema in the proximal metaphysis of the humerus (a), right-sided sacroiliitis (b) and L1/2 left intervertebral joint synovitis with some bone marrow and soft tissue swelling of surrounding tissues.

Figure 2. Whole body MRI in a 6-year old girl with juvenile dermatomyositis. Coronal T2 TIRM images. Initial exam (a-c) shows multiple areas of increased signal in muscles of the neck, upper and lower girdle, forearms and crura; follow-up 8 months later (d-f) shows complete resolution of all lesions.

Figure 3. WB MRI of a 15-year-old girl with benign acute childhood myositis due to Influenza B showing diffuse muscle edema in the calves on the coronal STIR (Arrows) in a. WB MRI performed as follow-up one month later demonstrating a complete resolution of the muscle edema (coronal STIR in b).

Figure 4. WB MRI of an 11-years-old boy with SAPHO syndrome demonstrating edema and periosteal reaction of the right clavicle (coronal short tau inversion recovery-STIR- in a, axial T1weighted turbo spin echo – TSE- in b and axial STIR in c), bone marrow edema in the right sacrum (coronal STIR in d, axial T1w TSE in e, and axial STIR in f), in the left acetabulum (coronal STIR in g, axial T1w TSE in h, and axial STIR in i), and in the distal metaphyseal area of the right tibia (coronal STIR in l and coronal T1w TSE in m).

Figure 5. Whole body MRI in a 12-year old girl with chronic recurrent multifocal osteomyelitis (CRMO). T2 TIRM images show bone marrow oedema of the sternal end of the right clavicle with oedema of the surrounding tissues (a), bone marrow oedema of the distal femoral epiphysis, proximal tibial epiphysis, and to a minor extent in a knee joint epiphyses bilaterally (b), bone marrow edema in the left distal tibial epiphysis (c), left-sided sacroiliitis (d), and bone marrow oedema of several vertebral bodies of the thoracic and lumbar regions, with a fracture of the L1 vertebral body (e).

Publikacja nr. 3. Update on MRI in rheumatic diseases. Iwona Sudol-Szopińska, Michał Lanckoroński, Torsten Diekhoff, Damjana Ključevšek, Filippo Del Grande, Andrea Doria. Radiologic Clinics of North America 2024; <https://doi.org/10.1016/j.rcl.2024.03.003> 0033-8389/24.

Figure 1. MRI of a 40-year-old male patient with suspected rheumatoid arthritis. The MRI and CT show a pseudoerosion in the lunate. In susceptibility-weighted imaging (SWI) the lesion is more clearly outlined, and with inversion, the image has a similar contrast as compared to CT.

Figure 2. MRI of the sacroiliac joints in a 45-year-old patient with advanced axial spondyloarthritis (axSpA). One single T2-Dixon sequence with four contrasts (in-phase, opposed-phase, fat and water image) is compared to standard T1 and T2fs. Bone marrow edema (white arrow, high signal intensity in T2 fat saturation (fs), in-phase and water image, low signal in T1 and fat image) can clearly be differentiated from fat lesions (black arrow, high signal in T1, in-phase and fat image). Edema within a fat lesion is also visible (white arrowhead). Dixon opposed phase can help detecting erosions (black arrowhead).

Figure 3. Dynamic contrast-enhanced MRI of the hand. A 56-year-old male patient presenting with hand and finger arthritis due to late-onset rheumatoid arthritis. The synovium of all metacarpophalangeal (MCP)-joints is enhanced after contrast administration (arrows). Fractal analysis shows neoangiogenesis in heavily inflamed tissues (white arrowheads). In the perfusion analysis, the relative blood volume (rBV) is increased while the mean transit time (mTT) is decreased in synovitis.

Figure 4. Wrist MR in a 49-year-old man with dermatomyositis (DM) complicated by septic inflammation, on immunosuppressive therapy. The images show active inflammatory changes: wrist joints with synovitis (white arrow), osteitis (black arrow), minor tenosynovitis in several compartments of extensor and flexor tendons (white arrowheads), tendinopathy of deep flexor muscle of the fingers in the carpal tunnel (black arrowhead). Osteolytic lesions with cartilage loss of numerous bones are best appreciated on a Volumetric Interpolated Breath-hold Examination (VIBE) sequence.

Figure 5. Whole body (WB)MRI in a 56-year-old woman with scleromyositis, T2 Turbo Inversion Recovery Magnitude (TIRM) images with majority of the muscle high signal representing myositis. Superficial soft tissue swelling of the lower extremities, likely representing skin and subdermis inflammation (arrows).

Figure 6. MRI of both hips in a 14-year-old girl with systemic juvenile idiopathic arthritis (JIA) treated by biologics. Bilateral hip joint effusions with moderate synovial thickening (arrows, PD fs) and synovial enhancement (arrows, T1 FS gd+), hip joint space narrowing (more pronounced on the right) with thinned joint cartilage (black arrows). Bone architecture changes of acetabular roof (arrowheads) with geodes (non-enhanced changes) and synovial cysts (rim enhancement, the largest on the left (medial arrowhead)).

Figure 7. A 16-year-old female patient with juvenile idiopathic arthritis (JIA) and bilateral inflammatory lesions in the temporomandibular joints. The images show increased fluid with thickening of the synovial membrane (white arrowhead on axial T2), bone marrow edema of the mandibular head and articular eminence (white arrows) with erosions (black arrow on parasagittal T2Medic); Features of limited joint mobility and of the perforation of the articular disc in the central part - in close-up its position is normal (white arrowheads on “close”

parasagittal PD and T2Medic), in opening the posterior band immobile (white arrowhead on “open” parasagittal T2Medic).

Figure 8. A series of MRI of cervical spine in 14 and 16-y-old girls with extended oligoarticular juvenile idiopathic arthritis (JIA), antinuclear antibodies (ANA) positive baseline images in T2 axial, T1 fat saturated (fs) contrast enhanced axial and sagittal, and follow up T1 fs postcontrast image in axial plane (last bottom image). Baseline T2 Turbo Spin-Echo (TSE) axial shows asymmetrically thickened atlanto-axial synovium (arrows), area of hyperintense bone marrow signal in the posterior part of the dens (black arrow), and thickened transversal ligament (arrowhead). Contrast-enhanced MRI in axial and sagittal planes shows homogenous intensive synovial enhancement, enhancement of the posterior part of the dens and thickened transverse ligament, and no signs of anterior atlantoaxial subluxation. The contrast-enhanced MRI follow-up obtained 2 years later, during which time the girl was treated with biologics, shows slightly asymmetric thickened synovium with minimal non-homogenous enhancement (arrows on T1 fs Gd +follow up) and thickened transversal ligament (arrowhead). The girl was symptom-free and had normal laboratory data.

Figure 9. An 11-year old boy with juvenile idiopathic arthritis (JIA) enthesitis-related arthritis (ERA) subtype. The initial exam was obtained at the age of 11 years; 1st follow MRI was obtained 6 months later, and 2nd follow, 12 months after baseline. Left-sided sacroiliitis: semicoronal T2 Short-Tau Inversion Recovery (STIR) images show bone marrow edema in the left ilium, joint space inflammation, capsulitis, and active erosion in the left sacral bone (evident in the first follow-up exam; arrow). T1, T1 fat-suppressed (fs) and T2 Multi-Echo Data Image Combination (MEDIC) consecutive exams show increasing number of erosions (white arrows) and bone marrow fatty metaplasia (black arrows).

Figure 10. 8-year old girl with chronic recurrent multifocal osteomyelitis (CRMO). Coronal T2 Turbo Inversion Recovery Magnitude (TIRM) images show areas of increased marrow signal in the inferior ramus and angle of the mandibula on the left side (white arrow), and in the right ischium (black arrow). The numerous areas of abnormal signal in the right ankle and tarsal bones (white arrowheads) with minor effusion (open arrowhead), less severe in the left ankle (black arrowhead) may represent stress-related mechanical abnormalities which are in differential for CRMO-related lesions.

10. Decyzja Komisji Bioetycznej



Warszawa, 26.04.2018 r.

Decyzja Komisji Bioetycznej przy Narodowym Instytucie Geriatrii, Reumatologii i Rehabilitacji w Warszawie nr KBT-3/1/2018

Komisja Bioetyczna przy Narodowym Instytucie Geriatrii, Reumatologii i Rehabilitacji w Warszawie, ul. Spartańska 1, działająca zgodnie z zasadami GCP, zapoznana się w dniu 26.04.2018 r. z następującymi dokumentami dotyczącymi projektu badawczego pn. „Ocena retrospektywna badań MR całego ciała (WB MRI) wykonanych w Zakładzie Radiologii NIGRiR w celu przygotowania rozprawy doktorskiej dot. określenia wartości diagnostycznej WB MRI u dzieci z podejrzeniem zmian zapalnych w układzie ruchu”:

1. Podanie głównego badacza do Komisji Bioetycznej z prośbą o zaopiniowanie projektu;
2. Opis programu badania.

Retrospektywne badanie naukowe będzie prowadzone w oparciu o dokumentację medyczną zgromadzoną w Zakładzie Radiologii oraz w Klinice i Poliklinice Reumatologii Wieku Rozwojowego Narodowego Instytutu Geriatrii, Reumatologii i Rehabilitacji. Wyniki badań będą podstawą publikacji oraz zostaną wykorzystane w pracy doktorskiej lek. Marty Wyszmołek – rezydentki w Klinice i Poliklinice Reumatologii NIGRiR. Kierownikiem projektu oraz proponowanym promotorem rozprawy doktorskiej jest prof. dr hab. n. med. Iwona Sudol-Szopińska – Kierownik Zakładu Radiologii Instytutu.

Komisja Bioetyczna przy NIGRiR w głosowaniu tajnym nad akceptacją zgłoszonego projektu wyraziła zgodę na rozpoczęcie badań zgodnie z przedstawionym protokołem.

PRZEWODNICZĄCY
KOMISJI BIOETYCZNEJ
przy Narodowym Instytucie Geriatrii,
Reumatologii i Rehabilitacji w Warszawie
prof. dr hab. n. med. Piotr Guzik

Komisja Bioetyczna
tel.: (22) 670 92 28
e-mail: monika.dabrowska@spartanska.pl

www.spartanska.pl
ul. Spartańska 1
02-637 Warszawa

11.

Warszawa, 26.04.2018 r.

**Lista obecności członków Komisji Bioetycznej przy Narodowym Instytucie Geriatrii,
Reumatologii i Rehabilitacji**

Prof. dr hab. med. Piotr Głuszko – lekarz
NIGRiR

Prof. dr hab. med. Anna Filipowicz-Sosnowska – lekarz
NIGRiR

Dr n. hum. Ewa Kujawa – etyk

P. Barbara Kurek – pielęgniarka

Prof. nadzw. dr hab. med. Robert Gasik – lekarz
NIGRiR

Prof. nadzw. dr hab. med. Brygida Kwiatkowska – lekarz
NIGRiR

Ks. dr Włodzimierz Nast – ksiądz
Chrześcijańska Akademia Teologiczna

Mec. Maria Grzeszczyk – prawnik
Państwowy Zakład Wydawnictw Lekarskich

Prof. nadzw. dr hab. med. Marzena Olesińska – lekarz
NIGRiR

Prof. dr hab. med. Lidia Rutkowska-Sak – lekarz
NIGRiR

Prof. dr hab. med. Tadeusz Styczyński – lekarz

Dr hab. n. farm. Tomasz Pawiński – farmaceuta
Warszawski Uniwersytet Medyczny

Dr n. med. Aleksandra Słabik-Ledóchowska – lekarz
Okręgowa Izba Lekarska w Warszawie

























11. Oświadczenia współautorów publikacji

Warszawa, 20.03.2024

Prof. dr hab. med. Iwona Sudol-Szopińska
Zakład Radiologii
Narodowy Instytut Geriatrii, Reumatologii i Rehabilitacji
Ul. Spartańska 1, 02-637 Warszawa

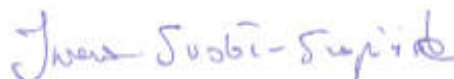
OŚWIADCZENIE

Oświadczam, że w publikacji pt.: "Whole-Body MRI at Initial Presentation of Chronic Recurrent Multifocal Osteomyelitis, Juvenile Idiopathic Arthritis, Their Overlapping Syndrome, and Non-Specific Arthropathy", Autorzy: Michał Lanckoroński, Piotr Gietka Małgorzata Mańczak, Iwona Sudol-Szopińska, opublikowanej w Journal of Clinical Medicine 2024; 13, 998. doi.org/10.3390/jcm13040998, mój wkład merytoryczny w przygotowanie publikacji polegał na:

- Zaprojektowaniu badania
- Interpretacji wyników badania
- Przygotowaniu manuskryptu
- Analizie literatury

Oceniam swój wkład procentowy w publikację na poziomie 30%. Wyrażam zgodę na przedłożenie powyższej publikacji przez doktora Michała Lanckorońskiego jako część Jego rozprawy doktorskiej w formie spójnego cyklu artykułów naukowych opublikowanych w recenzowanych czasopismach naukowych. Jednocześnie oświadczam, że samodzielna i możliwa do wyodrębnienia część powyższej publikacji wykazuje indywidualny wkład lek. Michała Lanckorońskiego przy opracowywaniu założeń, wykonania części eksperymentalnej oraz interpretacji wyników tej pracy.

Z poważaniem,



Dr n. med. Małgorzata Mańczak
Zakład Gerontologii, Zdrowia Publicznego i Dydaktyki
Narodowy Instytut Geriatrii, Reumatologii i Rehabilitacji
Ul. Spartańska 1, 02-637 Warszawa

Warszawa, 20.03.2024

OŚWIADCZENIE

Oświadczam, że w publikacji pt.: "Whole-Body MRI at Initial Presentation of Chronic Recurrent Multifocal Osteomyelitis, Juvenile Idiopathic Arthritis, Their Overlapping Syndrome, and Non-Specific Arthropathy", Autorzy: Michał Lanckoroński, Piotr Gietka, Małgorzata Mańczak, Iwona Sudół-Szopińska, opublikowanej w Journal of Clinical Medicine 2024; 13, 998. doi.org/10.3390/jcm13040998, mój wkład merytoryczny w przygotowanie publikacji polegał na:

- Przygotowaniu manuskryptu
- Analizie literatury

Oceniam swój wkład procentowy w publikację na poziomie 5%. Wyrażam zgodę na przedłożenie powyższej publikacji przez doktora Michała Lanckorońskiego jako część Jego rozprawy doktorskiej w formie spójnego cyklu artykułów naukowych opublikowanych w recenzowanych czasopismach naukowych. Jednocześnie oświadczam, że samodzielna i możliwa do wyodrębnienia część powyższej publikacji wykazuje indywidualny wkład lek. Michała Lanckorońskiego przy opracowywaniu założeń, wykonania części eksperymentalnej oraz interpretacji wyników tej pracy.

Z poważaniem,

Małgorzata Mańczak

Warszawa, 20.03.2024

Dr n.med. Piotr Gietka
Klinika i Poliklinika Reumatologii Wieku Rozwojowego
Narodowy Instytut Geriatrii, Reumatologii i Rehabilitacji
Ul. Spartańska 1, 02-637 Warszawa

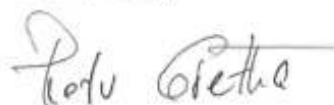
OŚWIADCZENIE

Oświadczam, że w publikacji pt.: Whole-Body MRI at Initial Presentation of Chronic Recurrent Multifocal Osteomyelitis, Juvenile Idiopathic Arthritis, Their Overlapping Syndrome, and Non-Specific Arthropathy”, Autorzy: Michał Lanckoroński, Piotr Gietka Małgorzata Mańczak, Iwona Sudol-Szopińska, opublikowanej w Journal of Clinical Medicine 2024; 13, 998. doi.org/10.3390/jcm13040998, mój wkład merytoryczny w przygotowanie publikacji polegał na:

- Przygotowaniu manuskryptu
- Analizie literatury

Oceniam swój wkład procentowy w publikację na poziomie 5%. Wyrażam zgodę na przedłożenie powyższej publikacji przez doktora Michała Lanckorońskiego jako część Jego rozprawy doktorskiej w formie spójnego cyklu artykułów naukowych opublikowanych w recenzowanych czasopismach naukowych. Jednocześnie oświadczam, że samodzielna i możliwa do wyodrębnienia część powyższej publikacji wykazuje indywidualny wkład lek. Michała Lanckorońskiego przy opracowywaniu założeń, wykonania części eksperymentalnej oraz interpretacji wyników tej pracy.

Z poważaniem,



Lugano, 02.07.2024

Dr. Vito Chianca
Clinica di Radiologia EOC
Istituto di Imaging della Svizzera Italiana (IIMSI)
Via Tesserete 46, 6900 Lugano, Switzerland

DECLARATION

I hereby declare that in the publication entitled: Whole - Body Magnetic Resonance Imaging in Rheumatology, Authors: Vito Chianca, Michał Lanckoroński, Marco Curti, Majid Chalian, Iwona Sudol-Szopińska, Chiara Giraud, Filippo Del Grande, published in *Seminars in Musculoskeletal Radiology* 2024; <https://doi.org/10.1016/j.rcl.2024.02.008>; my substantive contribution to the publication consisted of:

Designing the paper

Preparation of the manuscript

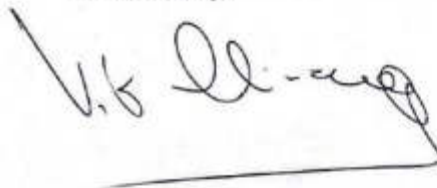
Analysis of the literature

As first and corresponding author of the above international publication, I estimate my percentage contribution to the publication at 40%, Dr Michał Lanckoroński at 35%, the other co-authors at 5%.

I agree to submit the above publication by Dr Michał Lanckoroński as part of his doctoral dissertation in the form of a coherent series of scientific articles published in peer-reviewed scientific journals.

At the same time, I declare that the independent and separable part of the above publication shows an individual contribution of dr. Michał Lanckoroński in the design of the work, preparation of the manuscript, and analysis of the literature for this work.

Yours sincerely,

A handwritten signature in black ink, appearing to read 'V. Chianca', with a long horizontal line extending to the right.

Warszawa, 20.05.2024

Prof. dr hab. med. Iwona Sudol-Szopińska
Zakład Radiologii
Narodowy Instytut Geriatrii, Reumatologii i Rehabilitacji
Ul. Spartańska 1, 02-637 Warszawa

OŚWIADCZENIE

Oświadczam, że w publikacji pt.: Update on MRI in rheumatic diseases, Autorzy: Iwona Sudol-Szopińska, Michał Lanckoroński, Torsten Diekhoff, Damjana Ključevšek, Filippo Del Grande, Andrea Doria, opublikowanej w Radiologic Clinics of North America 2024; <https://doi.org/10.1016/j.rcl.2024.03.003>, mój wkład merytoryczny w przygotowanie publikacji polegał na:

Zaprojektowaniu pracy
Przygotowaniu manuskryptu
Analizie literatury.

Jako pierwszy i korespondencyjny autor powyższej międzynarodowej publikacji, oceniam swój wkład procentowy w publikację na poziomie 45%, doktora Michała Lanckorońskiego na poziomie 35%, pozostałych współautorów 5%.

Wyrażam zgodę na przedłożenie powyższej publikacji przez doktora Michała Lanckorońskiego jako część Jego rozprawy doktorskiej w formie spójnego cyklu artykułów naukowych opublikowanych w recenzowanych czasopismach naukowych.

Jednocześnie oświadczam, że samodzielna i możliwa do wyodrębnienia część powyższej publikacji wykazuje indywidualny wkład lek. Michała Lanckorońskiego przy zaprojektowaniu pracy, przygotowaniu manuskryptu, oraz analizie literatury na potrzeby tej pracy.

Z poważaniem,

Iwona Sudol-Szopińska

12. Piśmiennictwo

1. Greer, M.L.C. Whole-body magnetic resonance imaging: Techniques and nononcologic indications. *Pediatr. Radiol.* 2018, 48,1348–1363.
2. Schaefer, J.F.; Berthold, L.D.; Hahn, G.; von Kalle, T.; Moritz, J.D.; Schröder, C.; Stegmann, J.; Steinborn, M.; Weidemann, J.; Wunsch, R.; et al. Whole-Body MRI in Children and Adolescents—S1 Guidelines. *Fortschr. Röntgenstr.* 2019, 191, 618–625.
3. Giraud, C.; Lecouvet, F.E.; Cotton, A.; Eshed, I.; Jans, L.; Jurik, A.G.; Maas, M.; Weber, M.; Sudoł-Szopińska, I. Whole-body magnetic resonance imaging in inflammatory diseases: Where are we now? Results of an International Survey by the European Society of Musculoskeletal Radiology. *Eur. J. Radiol.* 2021, 136, 109533.
4. Spalkit, S.; Sinha, A.; Prakash, M.; Sandhu, M.S. Dermatomyositis: Patterns of MRI findings in muscles, fascia and skin of pelvis and thigh. *Eur. J. Radiol.* 2021, 141, 109812.
5. Sreelal, T.V.; Bhatia, A.; Suri, D.; Singh, S.; Saxena, A.K.; Tao, T.Y.; Sodhi, K.S. Whole-body MR imaging in evaluation of children with juvenile dermatomyositis. *Eur. J. Radiol.* 2022, 155, 110475.
6. Schaal, M.C.; Gendler, L.; Ammann, B.; Eberhardt, N.; Janda, A.; Morbach, H.; Darge, K.; Girschick, H.; Beer, M. Imaging in non-bacterial osteomyelitis in children and adolescents: Diagnosis, differential diagnosis and follow-up—An educational review based on a literature survey and own clinical experiences. *Insights Imaging* 2021, 12, 113.
7. Malievskiy, V. Arthralgia in children: The epidemiological study. *Pediatr. Rheumatol.* 2011, 9 (Suppl. S1), P144.
8. De Inocencio, J.; Carro, M.A.; Flores, M.; Carpio, C.; Mesa, S.; Marín, M. Epidemiology of musculoskeletal pain in a pediatric emergency department. *Rheumatol. Int.* 2016, 36, 83–89.
9. De Inocencio, J. Epidemiology of musculoskeletal pain in primary care. *Arch. Dis. Child.* 2004, 89, 431–434.
10. Remvig, L.; Jensen, D.V.; Ward, R.C. Epidemiology of General Joint Hypermobility and Basis for the Proposed Criteria for Benign Joint Hypermobility Syndrome: Review of the Literature. *J. Rheumatol.* 2007, 34, 804–809.
11. Mohanta, M.P. Growing pains: Practitioners' dilemma. *Indian Pediatr.* 2014, 51, 379–383. *J. Clin. Med.* 2024, 13, 998 15 of 16
12. Weiss, J.; Stinson, J.N. Pediatric pain syndromes and noninflammatory musculoskeletal pain. *Pediatr. Clin. N. Am.* 2018, 65,801–826. 2
13. Uziel, Y.; Hashkes, P.J. Growing pains in children. *Pediatrics* 2008, 147, 809–811.
14. Evans, A.; Scutter, S. Prevalence of “growing pains” in young children. *J. Pediatr.* 2004, 145, 255–258.
15. Lanckoroński, M.; Gietka, P.; Mańczak, M.; Sudoł-Szopińska, I. Whole-Body MRI at Initial Presentation of Chronic Recurrent Multifocal Osteomyelitis, Juvenile Idiopathic Arthritis, Their Overlapping Syndrome, and Non-Specific Arthropathy. *J Clin Med.* 2024,13, 998. doi.org/10.3390/jcm13040998
16. Chianca, V.; Lanckoroński, M.; Curti, M.; Chalian, M.; Sudoł-Szopińska, i.; Giraud, G.; Del Grande. F. Whole - Body Magnetic Resonance Imaging Imaging in

17. Sudoł-Szopińska, I.; Lanckoroński, M.; Diekhoff, T.; Ključevšek, D.; Del Grande, F.; Doria, A. Update on MRI in rheumatic diseases. *J North Clin Am.* 2024; <https://doi.org/10.1016/j.rcl.2024.03.003>0033-8389/24.
18. Malattia, C.; Tolend, M.; Mazzoni, M.; Panwar, J.; Zlotnik, M.; Otobo, T.; Vidarsson, L.; Doria, A.S. Current status of MR imaging of juvenile idiopathic arthritis. *Best Pract. Res. Clin. Rheumatol.* 2020, 34, 101629.
19. Koneru, S.; Magid, M.S.; Fritz, J. Case of the Season: Asymmetric Chronic Recurrent Multifocal Osteomyelitis. *Semin. Roentgenol.* 2021, 57, 184–190.
20. Zhao, Y.; Sato, T.S.; Nielsen, S.M.; Beer, M.; Huang, M.; Iyer, R.S.; McGuire, M.; Ngo, A.; Otjen, J.P.; Panwar, J.; et al. Development of a Scoring Tool. for Chronic Nonbacterial Osteomyelitis Magnetic Resonance Imaging and Evaluation of its Interrater Reliability. *J. Rheumatol.* 2020, 47, 739–747.
21. Panwar, J.; Tolend, M.; Lim, L.; Shirley, M.; Tse, S.M.; Doria, A.S.; Laxer, R.M.; Stimec, J. Whole-body MRI Quantification for Assessment of Bone Lesions in Chronic Nonbacterial Osteomyelitis Patients Treated with Pamidronate: A Prevalence, Reproducibility, and Responsiveness Study. *J. Rheumatol.* 2021, 48, 751–759.
22. Aquino, M.R.; Tse, S.M.L.; Gupta, S.; Rachlis, A.C.; Stimec, J. Whole-body MRI of juvenile spondyloarthritis: Protocols and pictorial review of characteristic patterns. *Pediatr. Radiol.* 2015, 45, 754–762.
23. Sato, T.S.; Watal, P.; Ferguson, P.J. Imaging mimics of chronic recurrent multifocal osteomyelitis: Avoiding pitfalls in a diagnosis of exclusion. *Pediatr. Radiol.* 2020, 50, 124–136.
24. Kieninger, A.; Sch.fer, J.F.; Tsiflikas, I.; Moll, M.; Kümmerle-Deschner, J.; Kraus, M.S.; Esser, M. Early diagnosis and response assessment in chronic recurrent multifocal osteomyelitis: Changes in lesion volume and signal intensity assessed by whole-body MRI. *Br. J. Radiol.* 2021, 95, 20211091.
25. Shah, A.; Rosenkranz, M.; Thapa, M. Review of spinal involvement in Chronic recurrent multifocal osteomyelitis (CRMO): What radiologists need to know about CRMO and its imitators. *Clin. Imaging* 2022, 81, 122–135.
26. Damasio, M.B.; Magnaguagno, F.; Stagnaro, G. Whole-body MRI: Non-oncological applications in paediatrics. *Radiol. Med.* 2016, 121, 454–461.
27. Koné-Paut, I.; Mannes, I.; Dusser, P. Chronic Recurrent Multifocal Osteomyelitis (CRMO) and Juvenile Spondyloarthritis (JSpA): To What Extent Are They Related? *J. Clin. Med.* 2023, 12, 453.
28. Pračoń, G.; Simoni, O.P.; Gietka, P.; Aparisi, P.; Sudoł-Szopińska, I. Conventional Radiography and Ultrasound Imaging of Rheumatic Diseases Affecting the Pediatric Population. *Semin. Musculoskelet. Radiol.* 2021, 25, 68–81.
29. Sudoł-Szopińska, I.; Herregods, N.; Doria, A.S.; Taljanovic, M.S.; Gietka, P.; Tzaribachev, N.; Klauser, A.S. Advances in Musculoskeletal Imaging in Juvenile Idiopathic Arthritis. *Biomedicines* 2022, 10, 2417.
30. Sudoł-Szopińska, I.; Giraud, C.; Oei, E.H.G.; Jans, L. Imaging update in inflammatory arthritis. *J. Clin. Orthop. Trauma* 2021, 20, 101491.
31. Roderick, M.R.; Shah, R.; Rogers, V.; Finn, A.; Ramanan, A.V. Chronic recurrent multifocal osteomyelitis (CRMO)—Advancing the diagnosis. *Pediatr. Rheumatol. Online J.* 2016, 14, 47.
32. Petty, R.E.; TR Southwood, T.R.; Baum, J.; Betay, E.; Glass, D.N.; Manners, P.; Maldonado-Cocco, J.; Suarez-Almazor, M.; Orozco-Alcala, J.; Prieur, A.M.; et al.

- Revision of the proposed classification criteria for juvenile idiopathic arthritis: Durban, 1997. *J. Rheumatol.* 1998, 25, 1991–1994.
33. Cebecauerová, D.; Malcová, H.; Koukolská, V.; Kvíčalová, Z.; Souček, O.; Wagenknecht, L.; Bronský, J.; Šumník, Z.; Kynčl, M.; Cebecauer, M.; et al. Two phenotypes of chronic recurrent multifocal osteomyelitis with different patterns of bone involvement. *J. Pediatr. Rheumatol.* 2022, 20, 108.
34. Hofmann, S.R.; Kapplush, F.; Girchick, H.J.; Morbach, H.; Pablik, J.; Ferguson, P.J.; Hedrich, C.H.M. Chronic Recurrent Multifocal Osteomyelitis (CRMO): Presentation, Pathogenesis and treatment. *Curr. Osteoporos. Rep.* 2017, 15, 542–554.
35. Martini, A.; Ravelli, A.; Avcin, T.; Beresford, M.W.; Burgos-Vargas, R.; Cuttica, R.; Ilowite, N.T.; Khubchandani, R.; Laxer, R.M.; Lovell, D.J.; et al. Toward New Classification Criteria for Juvenile Idiopathic Arthritis: First Steps, Pediatric Rheumatology International Trials Organization International Consensus. *J. Rheumatol.* 2019, 46, 190–197.
36. Barnes, M.G.; Grom, A.A.; Thompson, S.D.; Griffin, T.A.; Luyrink, L.K.; Colbert, R.A.; Glass, D.N. Biologic similarities based on age at onset in oligoarticular and polyarticular subtypes of juvenile idiopathic arthritis. *Arthritis Rheum.* 2010, 62, 3249.
37. Weiss, P.F.; Colbert, R.A. Juvenile Spondyloarthritis: A Distinct Form of Juvenile Arthritis. *Pediatr. Clin. N. Am.* 2018, 65, 675–690.
38. Yıldız, M.; Ha.slak, F.; Adrovi., A.; .Sahin, S.; Barut, K.; Kasap.opur, .. Juvenile spondyloarthropathies. *Eur. J. Rheumatol.* 2022, 9, 42–49.
39. Sudoł-Szopińska I, Jurik AG, Eshed I, Lennart, J.; Grainger, A.; Østergaard, M.; et al. Recommendations of the ESSR Arthritis Subcommittee for the Use of Magnetic Resonance Imaging in Musculoskeletal Rheumatic Diseases. *Semin. Musculoskelet .Radiol.* 2015,19(4):396-411. doi:10.1055/s-0035-1564696
40. Costelloe, C.M.; Madewell, J.E.; Kundra, V.; Harrell, R.K.; Bassett, R.L.; Ma, J. Conspicuity of bone metastases on fast Dixon-based multisequence whole-body MRI: Clinical utility per sequence. *Magn. Reson. Imaging.* 2013,31(5):669-675. doi:10.1016/j.mri.2012.10.017
41. Del Grande, F.; Santini, F.; Herzka, D.A.Aro, M.R.; Dean, C.W.; Gold, G.E.; Carrino, J.A. Fat-suppression techniques for 3-T MR imaging of the musculoskeletal system. *Radiographics.* 2014,34(1):217-233. doi:10.1148/rg.341135130.
42. Robba, T.; Chianca, V.; Albano, D.; Clementi, V.; Piana, R.; Linari, A.; Comandone, A.; Regis, G.; Stratta, M.; Faletti, C.; Borre, A. Diffusion-weighted imaging for the cellularity assessment and matrix characterization of soft tissue tumour. *Radiol Medica.* 2017,122(11). doi:10.1007/s11547-017-0787-x.
43. Doniselli, F.M.; Albano, D.; Chianca, V.; Cimmino, M.A.; Sconfienza, L.M. Gadolinium accumulation after contrast-enhanced magnetic resonance imaging: what rheumatologists should know. *Clin. Rheumatol.* 2017,36(5):977-980. doi:10.1007/s10067-017-3604-y
44. Doniselli, F.M.; Albano, D.; Chianca, V.; Cimmino, M.A.; Scofienza, L.M. Gadolinium accumulation after contrast-enhanced magnetic resonance imaging: what rheumatologists should know. *Clin. Rheumatol.* 2017, 36(5):977-980. doi: 10.1007/s10067-017-3604-y.
45. Aquino, M.R.; Tse, S.M.L.; Gupta, S.; Rachlis, A.C.; Stimec, J. Whole-body MRI of juvenile spondyloarthritis: protocols and pictorial review of characteristic patterns. *Pediatr .Radiol.* 2015;45(5):754-762. doi:10.1007/s00247-015-3319-7.
46. Pagnini, I.; Savelli, S.; Matucci-Cerinic ,M.; Fonda, C.; Cimaz, R.; Simonini, G. Early predictors of juvenile sacroiliitis in enthesitis-related arthritis. *J. Rheumatol.* 2010,37(11):2395-2401. doi:10.3899/jrheum.100090

47. Elhai, M.; Meune, C.; Boubaya, M.; Avouac, J.; Hachulla, E.; Balbir-Gurman, A.; et al. Mapping and predicting mortality from systemic sclerosis. *Ann Rheum. Dis.* 2017,76(11):1897-1905. doi:10.1136/annrheumdis-2017-211448.
48. Schanz, S.; Henes, J.; Ulmer, A.; Kotter, I.; Fierlbeck, G.; Claussen, C.D.; Horger, M. Magnetic resonance imaging findings in patients with systemic scleroderma and musculoskeletal symptoms. *Eur. Radiol.* 2013,23(1):212-221. doi:10.1007/s00330-012-2584-1.
49. Schanz, S.; Henes, J.; Ulmer, A.; Kotter, I.; Fierlbeck, G.; Claussen, C.D.; Horger, M. Response evaluation of musculoskeletal involvement in patients with deep morphea treated with methotrexate and prednisolone: A combined MRI and clinical approach. *Am. J. Roentgenol.* 2013,200(4). doi:10.2214/AJR.12.9335.
50. Leão, R.V.; Calich, A.L.G.; Calich, I.; Calich, I.; Rodrigues, M.B.; Partezani Helito, P.V.; Amarai, D.T.; Bstista Pereira, R.F.; De Paula Correa, M.F. Magnetic resonance imaging findings in patients with polymyalgia rheumatica. *Radiol. Bras.* 2022,55(6):346-352. doi:10.1590/0100-3984.2021.0151.
51. Barakat, E.; Kirchgessner, T.; Triqueneaux, P.; Galant, C.; Stoenoiu, M.; Lecouvet, F.E. Whole-Body Magnetic Resonance Imaging in Rheumatic and Systemic Diseases: From Emerging to Validated Indications. *Magn. Reson. Imaging Clin. N. Am.* 2018,26(4):581-597. doi:10.1016/j.mric.2018.06.005.
52. Dimachkie, M.M.; Barohn, R.J.; Amato, A.A. Idiopathic inflammatory myopathies. *Neurol. Clin.* 2014,32(3):595-628. doi:10.1016/j.ncl.2014.04.007.
53. Cantwell, C.; Ryan, M.; O'Connell, M.; Cunningham, P.; Brennan, D.; Costigan, D.; Lynch, T.; Eustace, S. A comparison of inflammatory myopathies at whole-body turbo STIR MRI. *Clin. Radiol.* 2005,60(2):261-267. doi:10.1016/j.crad.2004.06.027.
54. Falip, C.; Alison, M.; Boutry, N.; Job-Deslandre, C.; Cotton, A.; Azoulau, R.; Adamsbaum, C. Chronic recurrent multifocal osteomyelitis (CRMO): A longitudinal case series review. *Pediatr Radiol.* 2013,43(3):355-375. doi:10.1007/s00247-012-2544-6.
55. Fordyce, M.J.F.; Solomon, L. Early detection of avascular necrosis of the femoral head by MRI. *J. Bone Joint Surg. Br* 1993,75(3),365-367. doi:10.1302/0301-620x.75b3.8496201.
56. Zadig, P.K.; von Brandis, E.; Flatø, B.; Ording Muller, L-S.; Narsal, E.B.; Tanturri de Horario, L.; Rosendahl, K.; Avenarius, D.F.; et al. Whole body magnetic resonance imaging in healthy children and adolescents: Bone marrow appearances of the appendicular skeleton. *Eur. J. Radiol.* 2022;153:110365. doi: 10.1016/j.ejrad.2022.110365.
57. von Brandis, E.; Zadig, P.K.; Avenarius, D.F.M.; Flato, B.; Knudsen, P.K.; Lilleby, V.; Nguyen, B.; Rosendahl, K.; Ording Muller, L-S. Whole body magnetic resonance imaging in healthy children and adolescents. Bone marrow appearances of the axial skeleton. *Eur. J. Radiol.* 2022,154,110425. doi: 10.1016/j.ejrad.2022.110425.
58. Panwar, J.; Tolend, M.; Redd, B.; Srinivasalu, H.; Colbert, R.A.; Akikusa, J.; et al. Consensus-driven conceptual development of a standardized whole body-MRI scoring system for assessment of disease activity in juvenile idiopathic arthritis: MRI in JIA OMERACT working group. *Semin Arthritis Rheum* 2021,51,1350–1359. <https://doi.org/10.1016/j.semarthrit.2021.07.017>.
59. Li, J.; Zhu, Y.; Guo, G. Enthesitis-related arthritis: The clinical characteristics and factors related to MRI remission of sacroiliitis. *BMC Musculoskelet. Disord.* 2022, 23, 1054.

60. Burgos-Vargas, R.; Pacheco-Tena, C.; Vazquez-Mellado, J. A short-term follow-up of enthesitis and arthritis in the active phase of juvenile onset spondyloarthropathies. *Clin. Exp. Rheumatol.* 2002, 20, 727–731.
61. Aden, S.; Won, S.; Yang, C.; Bui, T.; Higa, T.; Scheck, J.; Iyer, R.S.; Egbert, M.; Lindberg, A.; Zhao, Y. Increasing Cases of Chronic Nonbacterial Osteomyelitis in Children: A Series of 215 Cases from a Single Tertiary Referral Center. *J. Rheumatol.* 2022, 49, 929–934.
62. Menashe, S.J.; Iyer, R.S.; Ngo, A.; Rosenwasser, N.L.; Zhao, Y.; Maloney, E. Whole-body MRI at initial presentation of pediatric chronic recurrent multifocal osteomyelitis and correlation with clinical assessment. *Pediatr. Radiol.* 2022, 52, 2377–2387.
63. Papakonstantinou, P.; Prountzos, S.; Karavasilis, E.; Atsali, E.; Bizimi, V.; Alexopoulou, E.; Fotis, L. Whole-body magnetic resonance imaging findings and patterns of chronic nonbacterial osteomyelitis in a series of Greek pediatric Patients. *Acta Radiol. Open* 2022, 11, 1–10.
64. Tasar, S.; S.zeri, B. Whole-body MRI in Pediatric Patients with Chronic Recurrent Multifocal Osteomyelitis. *Med. J. Bakirkoy* 2023, 19, 78–85.
65. Gunz, A.C.; Canizares, M.; MacKay, C.; Badley, A.M. Magnitude of impact and healthcare use for musculoskeletal disorders in the paediatric: A population-based study. *BMC Musculoskelet. Disord.* 2012, 13, 98.